1971

Study of gamma rays emitted following 250 meV negative pion scattering on onoxygen-16

Bernard Joseph Lieb Jr.
College of William & Mary - Arts & Sciences

STUDY OF GAMMA RAYS EMITTED FOLLOWING 250 MeV NEGATIVE PION SCATTERING ON O^{16}

A Thesis
Presented to
The Faculty of the Department of Physics
The College of William and Mary in Virginia

In Partial Fulfillment
Of the Requirements for the Degree of
Doctor of Philosophy

---

by

Bernard Joseph Lieb

August 1971

APPROVAL SHEET

This thesis is submitted in partial fulfillment of

the requirements for the degree of

Doctor of Philosophy

Bernard J. Lieb Jr.

Bernard J. Lieb

Approved, August 1971

Herbert O. Funsten

John R. Kane (by Herbert Funsten)

John R. Kane

Richard L. Kiefer

Richard L. Kiefer

William J. Kossler

William J. Kossler

Robert T. Siegel

Robert T. Siegel

Rolf G. Winter

Rolf G. Winter

STUDY OF GAMMA RAYS EMITTED FOLLOWING 250 MeV NEGATIVE PION SCATTERING ON O^{16}

ABSTRACT

The spectrum of gamma rays emitted following 250 MeV negative pion scattering on O^{16} has been studied using a Ge(Li) detector. The gamma rays were detected in coincidence with an incident pion signature in three scintillation counters. Cross sections were measured for pion interactions resulting in excited states of O^{16}, N^{16}, O^{15}, N^{15}, N^{14}, C^{14}, C^{13}, and C^{12}.

The cross section for pion induced neutron knockout leading to the first $3/2^-$ state of O^{15} is 15.6 ± 3.8 mb. This can be compared to a recent cross section measurement for the same reaction at 180 MeV for all bound states of O^{15} which is 42 mb. The ratio of the cross section for the O^{15} $3/2^-$ state to that of its mirror state in N^{15} is 1.7 ± .4 compared to the quasi-free prediction of 3. The relative cross sections for reactions leading to excited states of N^{15} and O^{15} are compatable with a quasi-free interpretation but the excitation of the $5/2^+$ levels relative to the $3/2^-$ levels are a factor of ~3 greater than expected. Comparison with the decay schemes of the giant dipole states indicates that significant excitation of these states would result in greater relative excitation of the $5/2^+$ levels and would help to explain the observed neutron to proton knockout ratio.

Cross sections for two nucleon knockout resulting in excited states of N^{14} are found to be comparable to those for single nucleon knockout. The ratio of the first $0^+(T=1)$ excited state to that of the $1^+(T=0)$ state at 3.945 MeV is .39 ± .22 which can be understood in terms of a pion-nucleon pair interaction with the isospins coupled to T=1.

TABLE OF CONTENTS

I. INTRODUCTION

There have been several recent experiments[1,2,3,4,5] which used the pion as a nuclear probe, but their number has been limited by the low intensity and poor energy resolution of existing pion beams. It is to be expected that the opening of several meson factories[6] in the next few years will lead to an increase of work in this field.

The pion has several advantages over the conventional nuclear probes such as the proton, deuteron, or electron. The pion's spin of zero simplifies the interpretation of experimental results. Because the pion is an isotopic spin (T) = 1 particle, it can excite $\Delta T = 2$ states in nuclei. Certain processes, such as double charge exchange, make the pion unique as a nuclear probe. Because of the dominance of the $J = 3/2$, $T = 3/2$, π-N resonance in the 200 MeV region, the "off-energy-shell" amplitudes for π-N scattering may be computed with greater confidence than in the N-N case.[7,8]

The poor quality of existing pion beams has placed severe limitations on the types of experiments that can be performed. An exception to this can be found in the work of Stroot et al.[2,9] who measured differential and total cross sections for elastic and inelastic scattering of negative pions on C^{12} in the energy range from 120 MeV to 280 MeV.

Tanner et al.[1,10,11,12] surveyed pion scattering on low Z nuclei in the region of the (3,3) resonance by detecting the residual

radioactivity of targets bombarded by positive and negative pion beams. Targets of B^{10}, B^{11}, C^{13}, N^{14}, O^{18}, C^{12}, and O^{16} were used. Cross sections for single and double charge exchange were measured (Table I). Tanner also measured the cross sections for neutron knockout from C^{12} following bombardment by π^+ and π^- beams resulting in residual C^{11} radioactivity. The cross section for this reaction (Fig. 1), as a function of the incident pion energy, mirrors the π-N cross section, that is, exhibiting the (3,3) resonance, broadened somewhat by the Fermi motion of the struck nucleons in C^{12}. In fact, the results strongly suggest the experimental π-N cross sections folded into the nucleon momentum distribution of a 1p-neutron bound into an optical-model potential appropriate to C^{12}. A quasi-free (or impulse) approximation calculation by Kolybasov[13] and also one by Chivers et al.[1] predict the form of the energy dependence of the reaction over the (3,3) resonance. The quasi-free approximation, however, predicts that the ratio of π^- knockout reactions to π^+ should be

$$\frac{\sigma(C^{12}+\pi^-\rightarrow C^{11}+\pi^-+n)}{\sigma(C^{12}+\pi^+\rightarrow C^{11}+\pi^++n) + \sigma(C^{12}+\pi^+\rightarrow C^{11}+\pi^o+p)} = 3/1 \qquad (1)$$

and the experiment yielded the result .97±.09. Similar results were found for neutron knockout reactions from ^{14}N and ^{16}O targets. The 3 to 1 ratio is due to the isospin dependence of the π-N interaction at the (3,3) resonance. Since the cross section computed in the quasi-free approximation is proportional to the free π-N cross section, one would expect this ratio to hold for pion induced knockout reactions. Several theoretical mechanisms have been proposed to reduce the expected ratio of 3, and these are discussed in Chapter IV of this paper.

The work described in this thesis was undertaken in order to achieve two goals. It was, first of all, felt desirable to make a general survey of pion inelastic interactions in the region of the (3,3) resonance. A second consideration was the belief that such a survey would contribute to an understanding of the mechanism which reduces the $\sigma(\pi^-):\sigma(\pi^+)$ knockout ratio to unity. The technique which was adapted was the study of the prompt de-excitation gamma rays following π^- scattering on low-Z nuclei using a high resolution Ge(Li) detector. This method permits one to measure the final nuclear states following a variety of reactions such as inelastic scattering leading to an excited state of the target nucleus, single and multiple nucleon knockout reactions, and charge exchange.

Just as with the activation experiments of Tanner, the results are not always unambiguous. It was necessary to interpret a complex gamma spectrum with occasionally overlapping peaks in terms of the known gamma branches of the nuclear levels. Because of the low count rate, runs of 3 to 4 days were necessary, thus limiting measurements to one value of incident pion energy instead of spanning the (3,3) resonance.

The work reported in this paper involves scattering by negative pions on O^{16}. The quasi-free approximation predicts the cross section ratio

$$\frac{\sigma(O^{16}+\pi^- \rightarrow O^{15}+\pi^-+n)}{\sigma(O^{16}+\pi^- \rightarrow N^{15}+\pi^-+p) + \sigma(O^{16}+\pi^- \rightarrow N^{15}+\pi^o+n)} = 3/1 \qquad (2)$$

leading to excited states of the mirror nuclei O^{15} and N^{15}. A preliminary experiment using a C^{12} target and a NaI gamma spectrometer has been reported elsewhere.[14,15]

II. EXPERIMENT

A. General Technique

The experiment was performed at the N.A.S.A. Space Radiation Effects Laboratory 600 MeV Synchrocyclotron using the 250 MeV pion beam. The data for the O^{16} target was accumulated during a four day run from July 21, to July 24, 1970.

The beam of negative pions was focused by a pair of quadrupole magnets and momentum selected using a bending magnet. A beam study conducted prior to our run by another group[16] indicates that the beam was 85.3±7.% pions with the remainder being muons and electrons. During the data accumulation, a total of 6.2×10^{10} pions passed through the target. H_2O was used for the O^{16} target, and it was held in a 10.4 cm x 10.4 cm x 15.7 cm container constructed of .01 cm thick brass.

Figure 2 shows a diagram of the experimental apparatus. The beam passed through a lead collimator, through scintillation counters 1, 2, and 3 and was then incident on the target. Gamma rays induced by pion interactions in the target were detected by the Ge(Li) detector which was surrounded by an anti-coincidence scintillation cup Anti in order to veto events caused by charged particles. A good event was a $123\overline{\text{Anti}}$ γ. This signature gated on a Kicksort 8192 channel analogue to digital converter (ADC) in the Yale IBM Interface to the IBM 360 computer at SREL. The gamma ray energy was digitized and then transferred to the

computer where it was written on magnetic tape and also stored in core by the softwave.

There were five 12" x 12" x 1/4" scintillation counters labeled A to E surrounding the target which were used to detect the outgoing pion. If one of these counters received a pulse in coincidence with a 123$\overline{\text{Anti}}$ γ, then that information was transferred along with the ADC reading to the computer, and separate spectra were accumulated for each of the different scattering counters.

After the data for the O^{16} target had been accumulated, a run without a target was taken in order to aid in the elimination of background contamination. Where necessary, the areas of the peaks in the "target out" spectrum were normalized with respect to the number of 123's in each run and compared with the "target in" spectrum. A gamma peak appearing in both spectra was treated as background and was not considered when nuclear level assignments were made. The first excited state of C^{12} is an exception to this, and the normalization procedure used to compute a cross section for this state is described in Section IIIG.

B. Counters and Counter Geometry

The scintillation counter geometry is shown in Fig. 2. Counters 1 and 2 formed the beam telescope. Counter 1 was 8" x 8" x 1/4", and counter 2 was 6" x 6" x 1/4". Counter 3 was 4" x 4" x 1/8" and served as a target-defining counter. All of the scintillation counters were made of Pilot-B scintillant.

The anti-coincidence counter Anti had the shape of a cup and fitted over the Ge(Li) detector. It was used to detect charged

particles from the target or beam direction. Its purpose was to make it possible to gate out events caused by charged particles which would tie up the ADC and increase the background.

Counters A, B, C, D, and E, which were all 12" x 12" x 1/4", formed a five-sided box which surrounded the target. The average angle at the target subtended by counters A, C, D, and E was 1.38 steradians, and counter B subtended .86 steradians. If a $123\overline{\text{Anti}}$ γ was in coincidence with one of these counters, then the gamma event was stored in a separate spectrum corresponding to that particular counter.

Counters A-E were placed surrounding the target in order to distinguish an event resulting in a charged pion from one resulting in a π^o or a pion absorption process. The possibility of contamination resulting from knocked out protons or electrons from π^o decay limited the usefulness of this data. A proton knocked out of a nucleus with sufficient energy to escape the target could be detected in the counters. A calculation making use of proton dE/dx tables indicates that a 100 MeV proton would be stopped in 1/2 of the target length, so this energy will be used for comparison. If the proton is initially at rest and the kinematic effect of the other nucleons in the nucleus is ignored, then the knocked out proton would have 140 MeV for 180^o pion scattering. A 3-body final state phase space calculation[17] indicates that the phase space available to the proton reaches a maximum at ~100 MeV, and thus kinematically there is a high probability for emission of protons with E > 100 MeV. Most treatments of (π, πN) reaction mechanisms assume that the nucleon is emitted with a lower energy. Robson[18] assumed that the energy of the knocked out nucleon would be less than 50 MeV, and

Hewson[19] computes a maximum energy of 88 MeV. In order to insure against proton counting, 1/4" thick Cu degraders were placed in front of counters A, D, and E. This selection of degrader was based on an incorrect estimate of the probability that the high energy gammas resulting from π^o decay could produce an electron-positron pair in the degrader. This estimate was recalculated using the correct photon cross sections, and it was found that the degrader could lead to the detection of as many as 35% of all π^o's in counters A, D, and E. An attempt was made to sort our the contributors to each coincidence spectra by comparing the spectra corresponding to those counters with Cu degraders (A, D, and E) to the spectra corresponding to counters without degraders (B and C). This proved to be impossible due to poor statistics, and only spectra corresponding to counters B and C were used in the analysis.

C. Logic Circuitry

A block diagram of the logic circuitry used in this experiment is shown in Fig. 3. All of the scintillation counters were first put in coincidence forming a $123\overline{\text{Anti}}$ with each coincidence having a resolution of 15 nsec. The 1-2 coincidence unit was gated off for 1 millisecond during the prompt portion of the beam's macrostructure during which time the probability for random coincidences was greatest.

A timing signal from the Ge(Li) detector was obtained by placing a BNC tee on the input of the linear amplifier (Ortec 450), amplifying the resulting signal and using a constant fraction timing discriminator in the leading edge mode to obtain a fast timing output. This signal was put in coincidence with the $123\overline{\text{Anti}}$ in the following manner. A Ge(Li) timing signal formed a start signal for a time to

amplitude converter (TAC), and an output of the 123$\overline{\text{Anti}}$ was delayed and used as a stop signal. The TAC output was put into a 512 channel analyzer which was routed by the 123$\overline{\text{Anti}}$-γ coincidence unit. The resulting spectrum consisted of a peak corresponding to the time correlated 123$\overline{\text{Anti}}$ γ events and a flat background caused by randoms. Those pulses routed into the second half of the analyzer by the 123$\overline{\text{Anti}}$ γ router signal formed a window covering a range of channels which could be moved by varying the delays in the inputs to the 123$\overline{\text{Anti}}$ γ coincidence unit. When this window was centered on the peak corresponding to the time correlated events, then the coincidence between the 123$\overline{\text{Anti}}$ and the γ signal had been properly timed. The constant fraction timing discriminator was set so that gamma rays from .4 MeV to 8.5 MeV were selected. The timing peak from the O^{16} target was 50 nsec FWHM. It had a shoulder on the side of the peak corresponding to "late" gamma rays (attributed to slow rising pulses in the Ge(Li) detector) and a 4.1 to 1. peak to valley ratio. The resolving time of the 123$\overline{\text{Anti}}$ γ coincidence unit was 90 nsec.

If there was a charged particle coincidence in one of the scattering counters (A-E), then the identity of the counter was transferred to the IBM-YALE Interface. Signals from the scintillation counters were put into a strobe coincidence unit which was strobed by the 123$\overline{\text{Anti}}$. The signals were then given a long width (300 nsec) and then entered a second strobe unit which was strobed if there had been a 123$\overline{\text{Anti}}$ γ coincidence, and the resultant outputs were reshaped and fed into a Monitor Register on the IBM-YALE Interface.

D. On Line Data Processing

All data were processed and recorded by the IBM-YALE Data Acquisition Interface which has been described by Gelernter *et al.*[20] The Ge(Li) signal was digitized by a Kicksort 8192 channel ADC plugged into one of the component bins of the Interface. If one of the scattering counters (A-E) was in coincidence with the $123\overline{\text{Anti}}$ γ signature, then a signal was put into the corresponding input line of a Monitor Register which was capable of transferring up to 15 bits of information when it was interrogated by the Interface.

The ADC and the Monitor Register were successively "read" and their data transferred to the computer where it was written on magnetic tape and processed by the software. The ADC data was reduced to 1024 channels, and the following spectra were stored in memory:

1. a total spectrum including all events
2. five coincidence spectra, each one corresponding to an event in which there was a signal in one of counters A, B, C, D, or E in coincidence with $123\overline{\text{Anti}}$ γ
3. a non-coincidence spectrum which included all events in the total spectrum which were not in coincidence with a signal from one of the scattering counters (A-E)
4. a spectrum for accumulating radioactive sources for calibration purposes without erasing the other spectra.

Access of these spectra for monitoring purposes was obtained by line printer, CRT display, and plotter.

The full 8192 channel ADC readings were recorded on magnetic tapes, which were reread after the experiment. For the purpose of

analysis, these spectra were combined into 1024, 2048, and 4096 channels. Generally the 4096 channel spectrum with 2.5 keV per channel was used in the analysis.

E. Ge(Li) Spectrometer

The Ge(Li) Spectrometer consisted of a 40 cm^3 Lithium-Drifted Germanium detector with a Canberra Model 1408C Preamplifier and an Ortec Model 450 Research Amplifier. The Ge(Li) detector was five-sided coaxial with the front end closed. The preamp output signal was amplified by an Ortec 450 Research Amplifier with pole-zero cancellation and base line restoration. The unipolar output with integral and differential time constants of 2 microseconds was used. This signal was digitized by a Kicksort 8192 channel ADC which was interfaced to the IBM-YALE Data Acquisition System at SREL. The ADC was gain stabilized using a Kicksort digital stabilizer centered on a pulser peak in the 8 MeV energy region.

F. Calibration

The Ge(Li) spectrometer was calibrated using a combination of calibrated sources, peaks of known energy from the spectra, and a spectrum taken with a precision pulser. Periodically, source spectra were accumulated using Co^{60}, Y^{88}, Na^{22}, and Th^{228} radioactive sources. In addition to these, several peaks in the experimental spectra whose identification and energy were well-known were used to extend the energy range to above 6 MeV. These included the .511 MeV positron annihilation radiation, the second escape peak of the N^{15} $5/2^+$ to ground state transition, and the photopeak and escape peaks of the O^{16} 3^- transition to the ground state. The energies of the various gammas used in the calibration are listed in Table II.

Two different precision pulsers were used to measure deviations from linearity in the energy regions between sources. A precision 60 Hz. pulser (integral linearity of the attenuator = .02%) designed by J. A. Biggerstaff of Oak Ridge National Laboratory was used for the region below 3.5 MeV and a Tennelec TC 800 Pulser (integral linearity = .1%) for the region above 3.5 MeV. Pulses were applied to the .5 pf capacitor of the test input of the preamp to simulate a detector charge input, and a list of pulser setting versus channel centroid was obtained. These data were fitted to the second order polynomial

$$\text{ATTENUATOR SETTING} = C1 * \text{CHANNEL} + C2 * (\text{CHANNEL})^2 + C3 \qquad (3)$$

where C1, C2, and C3 were allowed to vary. Their values for each pulser are listed in Table III.

A calibration was then obtained by fitting the sources and the gammas of known energy to the function

$$\text{ENERGY} = D1 * (C1 * \text{CHANNEL} + C2 * (\text{CHANNEL})^2 + C3) + D2 \qquad (4)$$

where D1 and D2 were allowed to vary, and C1, C2, and C3 had the values determined by the two pulser fits. This process, in effect, takes the linearity curve from the pulser and normalizes it to the best fit through the radioactive source points. The values of D1 and D2 are listed in Table III. The system showed a .5% integral nonlinearity and a .9% differential nonlinearity, but the fitting procedure gave reasonable agreement with the gamma rays of known energy, (Table II).

A plot of Ge(Li) resolution versus energy is seen in Fig. 4. The points used were peaks from the experimental spectra which appeared

to have long lifetimes and, thus, represent the system resolution and any degradation of resolution due to drift or neutron damage to the detector.

G. Efficiency

The relative and absolute photopeak efficiencies of the Ge(Li) detector over the energy range of interest were determined by computations involving two different sets of efficiency data for the Ge(Li) detector supplied by Mr. Peter Martin.[21] This efficiency information is listed in Tables IV and V. One set of data was obtained from the π mesic X-ray yields from Pb^{208}, Sn^{120}, and Ce^{140} targets by assuming that the relative intensities of the X-ray transitions follow the predictions of the Hüfner Model.[22] The other set of efficiency data was obtained using a Co^{56} source, which contains several gamma transitions whose relative intensities are well-known.

Relative efficiency curves were obtained by least squares fitting both the mesic X-ray data and the Co^{56} data to the following function:

$$\text{RELATIVE EFFICIENCY} = C1 * (\text{ENERGY})^{C2} \qquad (5)$$

where C1 and C2 were allowed to vary. This function was determined by inspection of the data and a consideration of the theoretical shape.[23] The energy dependence of the efficiency is contained in the C2 term, and the values of this parameter determined from the two sets of data are in good agreement (Table VI). Because the mesic X-ray efficiency data covers the full energy range of interest from 300 keV to 6.5 MeV, the

value of C2 determined from this data was used to compute the energy dependence of the relative efficiency.

During the run several calibrated sources of known activity were placed in the target position and a spectrum accumulated for a fixed "live" time. The sources used and information concerning their activities are listed in Table VII. The relative efficiency data from the mesic X-ray studies was normalized to the absolute efficiency by fitting the points derived from the calibrated sources to the function of Eqn. 5, but with the energy dependent parameter C2 held constant at the value determined in the relative efficiency fits. In this manner, the absolute efficiency which was known only in the low energy region was extrapolated to 6.5 MeV. The parameters derived from this fit are listed in Table VI.

A Monte Carlo calculation was used to compute a correction factor for self-absorption of gammas in the O^{16} target. This calculation involved the selection of a site in the target for an event using a random number generator and then computing the attenuation a photon would experience in passing through the O^{16} target to the Ge(Li) detector. The photon cross sections of Storm and Israel[24] were used to compute the attenuation. The relative efficiency, the absolute efficiency, and the absolute efficiency corrected for self-absorption in the O^{16} target are plotted in Fig. 5.

The errors on the relative efficiency numbers listed in Table IV result from several considerations. The predictions of the Hüfner model are generally found to agree with experiment to within 5%. This error was combined with the error resulting from uncertainties in the fitting of the gamma peaks to produce the errors listed in Table IV.

The average error on these points was 6.2%. An estimate of the error in the least squares determination of the relative efficiency was obtained by computing the change in relative efficiency caused by changing the value of the energy dependent parameter C2 by two standard deviations. This procedure produces a 6.7% error over the energy range from 1 to 6 MeV. The error in the Monte Carlo self-absorption claculation was taken to be 5.%, the estimated error in the photon cross sections.[24] The average error in the efficiency data points (6.2%), the error involved in the fitting proecdure, and the error in the self-absorption correction were added in quadrature to produce a total error which was used to compare the relative efficiency of the Ge(Li) spectrometer between two points in the spectrum.

In cases where the error in the absolute efficiency was required, an additional error was combined with the relative efficiency error. This was taken to be the deviation of the Y^{88} 1.836 MeV point in the absolute efficiency fit. This point was chosen because it had the poorest agreement (13.9%) with the results of the absolute efficiency fit. This error (13.9%) was combined with the relative efficiency error to produce the total absolute efficiency error.

Figure 6 is a plot of the energy dependence of the ratio of the double escape peak intensity to the photopeak intensity (Curve A) and the double escape peak intensity to the single escape peak intensity, (Curve B), which is, as expected,[25] constant. The points in this graph were taken using a Th^{228} source (2.614 MeV), a PuBe source (4.439 MeV), the prominent O^{16} (6.135 MeV) line in the experimental spectra, and a radioactive peak in the experimental spectra at 7.65 MeV. In most

cases, photopeaks were used to determine the intensity of a gamma transition in the experimental spectra, however, wherever possible this information was verified by fitting the escape peaks.

III. DATA ANALYSIS

A. Analysis of Spectra

The gamma peaks in the spectra were analyzed using a Gauss-Seidel[26] least squares fitting procedure. The peaks, which were assumed to be Gaussian with an exponential background, were fit to the function

$$f(x) = A \exp\left[\frac{-2.773\ (X-XO)^2}{(FWHM)^2}\right] + AB \exp\left[S(X-XORIG)\right] \qquad (6)$$

where: A is the amplitude of the peak

XO is the center channel of the peak

FWHM is the full width at half maximum of the peak

XORIG is the original estimate of the center channel which remains fixed and is used as a convenient center for the exponential background

AB is the fitted amplitude of the background at XORIG

S is the parameter which determines the slope of the exponential background.

The fitting procedure varied the values of the parameters A, XO, FWHM, AB, and S so as to minimize the value of χ^2 which is defined

$$\chi^2 = \sum_{i=1}^{N} \left[\frac{Y_i - f(X_i)}{\sqrt{Y_i}}\right]^2 \qquad (7)$$

where Y_i is the number of counts in channel X_i, and N is the number of channels included in the fit. The parameters were varied in such a way as to minimize χ^2 until the change in each parameter was less than .001%.

The Variance of Fit is defined as the value of χ^2 divided by the number of points fitted minus the number of parameters. It is a measure of the "goodness of fit", and it has an expectation value of 1. if the gamma peak is well represented by a Gaussian. It was, however, necessary in certain cases, especially for two Gaussian fits, to accept the results of fits with a Variance of Fit as high as 2.3. In these cases, the fit was always performed several times over various ranges to check for consistency, and the most representative fit was selected.

Depending on the characteristics of the peak in question, spectra of 1024 channels (10. keV/channel), 2048 channels (5. keV/channel), or 4096 channels (2.5 keV/channel) were used for the analysis. In most cases, the 4096 channel spectrum was used. Generally the fit covered a range of channels from two to four times the FWHM, thus allowing a reasonable fit to the background. When adjacent peaks made it difficult to fit over an adequate range of channels, it was necessary to hold the background parameters constant at values determined by inspection.

When the parameters in Eqn. 6 had been determined, the area of the peak was computed by the expression for the area of a Gaussian:

$$\text{AREA} = 1.064 * A * \text{FWHM} \qquad (8)$$

From this, the cross section was calculated using the detector efficiency, beam composition, and the total number of $123\overline{\text{Anti}}$'s which were discussed in Chapter II. The energy was computed using Eqn. 4 making use of the value of the center channel X0 computed in the least squares analysis.

The fitting procedure provides an estimate of the uncertainty in the value of each parameter which is multiplied by the ratio of the computed value of the Variance of Fit to that of its expected value of 1. In addition to this, the uncertainties for some of the peaks were increased following visual inspection and considering circumstances such as neighboring peaks and background shape.

B. Determination of Gamma Peak Assignments

Tables VIII thru XIV list the cross sections for exciting various nuclear levels found in this experiment. Sections IIID, IIIE, IIIF, IIIG, and IIIH discuss in detail each assignment and the considerations involved in making it. Important criteria were the branching ratios for the decay of a level and its lifetime. If a level had two detectable branches, both transitions were considered in the assignment, but generally the branch with the best statistics was used for computing the cross sections. One criterion used in making assignments was that a peak which was believed to be due to a transition with a lifetime of less than 5×10^{-13} sec was required to be Doppler broadened.

In addition to the transitions that were detected, upper limits on the cross sections for a number of levels were determined. These were obtained by holding the center channel XO fixed at the proper energy and the FWHM fixed at a reasonable value considering the lifetime. The fitted value of the area was compared with an upper level estimate made by visual inspection, and the cross section was computed from the larger of these two numbers. In many cases, it was impossible to make an estimate because of overlapping peaks, and these

levels are indicated by asterisks. Generally in these cases, there was no indication of excitation greater than ~2 mb for these levels.

If there were no measurements of the lifetime of a particular state available, an estimate was made using the extreme single particle model of Weisskopf[27] multiplied by the average enhancement factors of Skorka et al.[28] This procedure was used to obtain lifetime estimates for the C^{14} state at 7.341 MeV and the N^{15} states at 8.576 MeV, 9.053 MeV, 9.762 MeV, 9.929 MeV, 10.070 MeV, and 10.800 MeV. None of these states was found to have a measurable cross section; however, the lifetime estimates were considered in setting upper limits on the cross sections for excitation of these states.

C. Discussion of Errors

The principle uncertainties involved in the cross sections discussed in Sections IIID to IIIH are the statistical uncertainties in the area of the peak and the errors in the absolute efficiency which were discussed in Section IIG. All of the uncertainties listed below were added in quadrature, and the results for the individual peaks are listed in Tables VIII to XIV. If it was necessary to subtract counts from a peak in order to correct for gamma branches from a higher energy state, then the errors which entered the calculation were the uncertainty in the relative efficiency and the statistical uncertainty of the peaks involved.

The uncertainty factors which were included in the calculations were:

(1) the errors in the numbers used for the relative efficiency calculation (Table IV). These are due to the uncertainties

in the predictions of the Hüfner model (5%) and the statistical uncertainty in the fitting of the peaks.

(2) the error resulting from the calculation of the relative efficiency discussed in Section IIG.

(3) the Monte Carlo self-absorption correction. This introduced a 5% uncertainty in the efficiency.

(4) the estimated error in normalizing the relative efficiency to the absolute efficiency discussed in Section IIG.

(5) the statistical uncertainty resulting from the least squares fitting procedure.

(6) the uncertainty in the target size estimated at 3.%.

(7) the uncertainty in the beam composition (±7.%).

(8) the effect of particles other than pions.

Muons and electrons, which comprise about 15% of the beam, do not interact strongly, and thus their cross sections would be low. Protons originating outside of the target are unlikely because of the selection of the bending magnet, and neutrons would not cause a 123$\overline{\text{Anti}}$ signature and thus would not be seen. The problem of secondary neutron effects produced in the target was studied in a previous run[14,15] with a C^{12} target. The target length was doubled and it was found that the rate of single nucleon knockout doubled. This indicates that secondary nucleon effects on the cross section are negligible to about 5%. An estimate of the expected magnitude of this effect for the O^{16} target was made by computing the probability of a 14.5 MeV neutron produced in the target undergoing an inelastic interaction. The cross section for a 14.5 MeV neutron[29] was used because it is near the maximum for neutron inelastic reactions. This calculation resulted in a 17%

probability for the neutron after being produced by a knockout reaction undergoing any form of inelastic scattering. Neutron reactions on O^{16} leading to excited states of N^{15}, O^{15}, N^{14}, C^{14}, and C^{12} would contribute less than 5% of the cross section measured for these reactions in the pion induced knockout results. The neutron contamination resulting in excited states of O^{16}, N^{16}, and C^{13} is more significant. This will be discussed in Sections VH and VI.

D. N^{15} and O^{15} Energy Levels

Tables VIII and IX list the cross sections measured for single nucleon knockout leading to excited states in N^{15} and O^{15} respectively. The factors which were considered for each level are discussed in this section. The principle sources of information on the various transitions were the papers of Warburton et al.[30], Phillips et al.[31], Skorka et al.[28], and Ajzenberg-Selove[32].

N^{15} Energy Levels

5.270 MeV: Data were determined by a two Gaussian fit (both widths constrained equal) to the second escape peak of the N^{15} and O^{15} $5/2^+$ levels. The cross section is corrected for the branch from the 7.155 MeV level. The 5.270 MeV state has branches from the 7.566 MeV (100% branch and $\sigma < .8$ mb), the 8.576 MeV (63% branch), and the 9.829 MeV (100% branch) levels, so a significant fraction of the cross section measured for this state could be due to branches from higher energy states.

5.299 MeV: Warburton et al.[33] discuss the problems involved in measuring this peak in a gamma spectrum. It is impossible to estimate an upper limit because this peak would be broad, and its second escape lies on the Compton edge of the C^{12} 4.439 MeV gamma.

6.323 MeV: Data were determined by a least squares fit to the photopeak.

7.155 MeV: Level has a 100% branch to the 5.270 MeV level. The number quoted represents an eye-fit to a narrow peak at 1.885 MeV.

7.566 MeV: This state has a 100% branch to the 5.270 MeV level and this transition overlaps the broad N^{14} 2.313 MeV peak. The number quoted was obtained by an estimate of the maximum contribution of decays from the 7.566 MeV level to this peak.

8.313 MeV: Upper limit represents a fit to the 78% ground state branch.

9.053 MeV: Upper limit represents a fit to the second escape of the ground state transition which has a 92% branch.

9.155 MeV: Steerman and Young[34] suggest that this level may be a doublet due to the variations in measured branching ratios. The decays from Steerman's STATE 1 cannot be determined due to overlapping peaks. STATE 2's upper limit was obtained by a least squares fit.

9.225 MeV: Reference (30) and Ref. (31) differ on branching ratios, possibly indicating the presence of a doublet. Reference (30) measured a 100% branch to the 5.299 MeV level which would have a second escape peak at 2.904 MeV. Reference (31) measured 31% for this branch and 25% for a branch at 6.323 MeV with a 2.902 MeV gamma. These two peaks would overlap, and this fact was used in setting an upper limit on the cross section.

9.762 MeV: Upper limit on cross section was determined by a fit to the second escape of the ground state transition.

9.929 MeV: Upper limit is based on a fit to the second escape of the ground state transition which has an 80% branch.

10.070 MeV: Estimate is based on a fit to the ground state transition (96% branch).

10.451 MeV: Warburton[33] measured a 70% branch from this level to the first two excited states of N^{15}. The first and second escapes of a transition to the second excited state of N^{15} (5.299 MeV) were detected, and the cross section is based on this.

O^{15} Energy Levels

5.181 MeV: It is impossible to estimate the contribution from this level. See the discussion of the N^{15} 5.299 MeV level.

5.242 MeV: Data was determined by a two Gaussian fit (with both widths constrained equal to the second escape of the N^{15} and O^{15} $5/2^+$ levels (see N^{15} 5.270 MeV level). The cross section is corrected for the 100% branch from the 7.276 MeV level.

6.177 MeV: Data was obtained by a two Gaussian fit to the O^{16} 6.135 MeV and the O^{15} 6.177 MeV gammas. This combination of a broad peak and a narrow peak proved difficult to fit. Thus, the Variance of Fit (2.1) and the energy agreement are poor. These peaks were fitted over several different channel ranges with good agreement.

6.788 MeV: Upper limit is based on a fit to the photopeak of the ground state transition (100% branch).

7.276 MeV: Cross section is based on the gamma from the 100% branch to the 5.242 MeV level.

8.283 MeV: Upper level estimate is based on a fit to the second escape of the ground state transition.

E. N^{14} and C^{14} Excited States

Tables X and XI list the cross sections for the production of excited states of N^{14} and C^{14} following two nucleon knockout reactions from the O^{16} target. The principle sources of information on these nuclei are the papers of Carlson[35], Allen et al.[36], Gorodetzky et al.[37], Alburger et al.[38], Skorka et al.[28], and Ajzenberg-Selove[32]. The N^{14} levels higher than 7.028 MeV are above the threshold for proton emission. The cross section upper limits listed assume that the proton channel is negligible although there is no experimental verification. These levels were included so that it would be possible to estimate the effect of branches from higher states on the other cross sections listed. If there were a significant proton branch, it would affect the total cross section of the states above 7.028 MeV, but would not invalidate any corrections for branches from higher states. There are no excited bound states of O^{14}, so no transitions from this nucleus could be detected.

N^{14} Energy Levels

2.313 MeV: Cross section was determined by a least squares fit and corrected for branches from the 3.945 MeV and 5.106 MeV levels. The large error quoted is due to the subtraction of the large branch from the 3.945 MeV level.

3.945 MeV: This level has a 96.4%[37] branch to the first excited state, and the gamma peak from this transition was fitted.

5.106 MeV: This level branches 74%[37] to the ground state and 26% to the 2.313 MeV state. Both branches are seen, but the branch to the 2.313 MeV level was used for the cross section. It was necessary to correct for a 73% branch[36] from the 5.833 MeV level.

5.833 MeV: Cross section was based on an eye-fit to the gamma ray peak from the transition to the 5.106 MeV level (73% branch)[36], but the 27% branch to the ground state was also detected.

6.444 MeV: This level branches 69%[37] to the ground state, and the cross section is based on a fit to this transition.

7.028 MeV: Upper limit to cross section is based on a fit to the photopeak of the ground state transition (97% branch).

7.966 MeV: The upper limit is based on an eye-fit to the ground state transition (55% branch)[32].

8.061 MeV: The upper limit is based on an eye-fit to the second escape of the ground state transition (82% branch)[32].

8.489 MeV: The upper limit is based on an eye-fit to the 100% branch[32] to the 5.106 MeV level. A gamma peak corresponding to this transition was detected; however, this assignment is doubtful because the proton branch is expected to be large.

8.617 MeV: The upper limit is based on an eye-fit to the 40% branch[32] to the 6.198 Mev level.

C^{14} Energy Levels

6.728 MeV: Cross section is based on an eye-fit to the photopeak of the ground state transition (93% branch)[38].

6.901 MeV: Cross section was determined by an eye-fit to the 100% branch[38] to the 6.093 MeV level.

7.012 MeV: This level has a 100% branch to the ground state. The cross section upper limit is based on a fit to the photopeak of this transition.

F. C^{13} ENERGY LEVELS

Table XII lists the cross sections for 3 nucleon knockout leading to excited states of C^{13}. The papers of Riess et al.[39] and Skorka et al.[28] were the principle sources of information on this nucleus. The possibility of contamination of the C^{13} cross sections by the (n, α) reaction is discussed in Section VH. N^{13} has no bound excited states and would not be seen in this experiment.

3.086 MeV: Upper limit is based on a fit to the ground state transition.

3.684 MeV: This level has a 99% branch to the ground state.[39] This experiment detected a cross section for excitation of this state of 2.9±.8 mb, but ~85% of this is due to the 37% gamma branch to this level from the 3.854 MeV level. (See below)

3.854 MeV: Cross section was based on a fit to the photopeak of the ground state transition (62% branch)[39], but the escape peaks were also detected. This level branches 37% to the 3.684 MeV level.

G. The First Excited State of C^{12}

The first excited state of C^{12} at 4.439 MeV is very prominent in the spectra (Fig. 8), but a significant contribution to this peak

would be due to inelastic scattering of pions on C^{12} atoms in the scintillation counters which surrounded the target (Fig. 2). The 4.439 MeV peak also appears in the "target out" spectrum discussed in Section IIA, and this fact was used to estimate the background contamination in the "target in" spectrum. The 4.439 MeV photopeak in the "target out" spectrum was least squares fitted, normalized to the O^{16} spectrum, and then subtracted. The proper normalization factor is ambiguous because removing the target alters the distribution of pions in the counters surrounding the target, and thus would alter the background contribution. Because of the solid angle it subtends, inelastic scattering in counter C would be the main contributor to the background. It is expected that the anti-coincidence counter would not contribute significantly because a pion interaction in this counter would generally be accompanied by an $\overline{\text{Anti}}$ signal which would gate out the event. Taking the number of counts in the "target out" 4.439 MeV photopeak and normalizing this number by the number of "target in" $123\overline{\text{Anti}}$ C's divided by the number of "target out" $123\overline{\text{Anti}}$ C's, one finds that 49% of the C^{12} 4.439 MeV events in the O^{16} "target in" spectra may originate outside of the target. Similar normalizations using the number of singles in the anti-coincidence counter yields a background contamination of 40.5%, and using the singles rate for counter C, results in 34.%. A background contamination of 49% was chosen because it is the most reasonable from considerations of geometry and because it would allow the most conservative estimate of the C^{12} 4.439 MeV cross section. The error computed for this number was increased so as to overlap the three different normalizations discussed above. The resulting cross section is 16.8 ± 6.4 mb.

In order to confirm this number, an estimate of the expected background contamination was made taking into account the size and location of the scintillation counters and their rates. A calculation using the cross sections for π^- inelastic excitation of the 4.439 MeV level of C^{12} measured by Binon et al.[2] suggested a contamination percentage less than the 49% value which has been adapted.

H. O^{16} and N^{16} Excited States

Table XIII lists the cross sections measured for O^{16} states excited by inelastic scattering of pions. The principle sources of information on these states were Wilkinson et al.[40] and Bromley et al.[41].

Table XIV lists the cross sections measured for pion charge exchange leading to excited states of N^{16}. Because these states occur in the very low energy portion of the spectra where there are a high number of background contamination peaks, the assignments placed on these peaks cannot be considered completely unambiguous. The possibility of contamination of these cross sections by (n, n') and (n, p) reactions is discussed in Section VI.

O^{16} Levels

6.056 MeV: This level decays by Internal Conversion and would not be seen.

6.135 MeV: The cross section was obtained by a two Gaussian fit to the O^{16} 6.135 MeV and the O^{15} 6.177 MeV gamma peaks. (See the discussion of the O^{15} 6.177 MeV level.)

8.88 MeV: Upper limit is based on an eye-fit to the 76% branch to the 6.135 MeV level.

N^{16} Levels

.120 MeV: This level would not be seen because the analyzer lower level was set above this energy.

.298 MeV: The cross section is based on an eye-fit to the 100% branch[42] to the ground state which has a lifetime greater than .7 psec.[43]

.398 MeV: This level has a 75% branch[42] to the .120 MeV level with a lifetime greater than .9 psec. The cross section is based on an eye-fit to a peak at .278 MeV.

I. Data from the Scattering Counters

The difficulties involved in the interpretation of the spectra of gammas in coincidence with a charged particle event in one of the scattering counters is discussed in Section IIB. It was concluded that only counters B and C would be relatively free of events triggered by electron-positron pairs resulting from the two high energy gammas from π^o decay. The peaks of the O^{15} - N^{15} $3/2^-$ mirror states are very weak in the spectrum for counter B, making it impossible to obtain a fit. The $3/2^-$ peaks in the counter C spectrum were fitted successfully, and they are compared in Table XV. There is a 15% probability of a pair production event in the target itself. This would affect the ratio of the excitation of the two $3/2^-$ states.

A comparison between the spectra corresponding to gammas in coincidence with a charged particle in any of scattering counters and gammas not in coincidence is contained in Table XV. If the mechanism for 2 nucleon emission resulting in excited states of N^{14} where π^-

absorption in flight, then two neutrons would be emitted, and the scattering counters would have a very low probability of detecting either neutron. This is discussed in Section VG.

J. Analysis of 600 MeV Proton Data

The interaction of a high energy proton with a nucleus is believed to be quasi-free, and thus it was desirable to compare the spectroscopy of proton-knockout reactions with the $(\pi^-, \pi X\gamma)$ reactions reported in this thesis. Pickup reactions such as (p,d) generally involve a two body final state and require that the resulting particle emerge from the nucleus primarily in a relative S state, thus requiring greater restrictions on the final states than reactions such as (p,pn), (p,2p), (p,pd), etc. There are no published results for this type of experiment which have measured the excitation of the residual nucleus.

Lankford and Funsten[44] performed an experiment in which the gamma rays produced in an O^{16} target following 600 MeV proton scattering were detected using a Ge(Li) detector. A preliminary analysis of this data was performed with their assistance, and the results are listed in Table XVI. The areas of the peaks in their spectra were estimated by eye using the same considerations as those discussed in Sections IIID to IIIH. There was no relative efficiency curve available for the Ge(Li) detector used in accumulating this data; however, the transition strengths listed in Table XVI were corrected for the energy dependence of the efficiency by making use of an efficiency curve for a detector of similar size and shape.[45] The results of this analysis should be considered as preliminary. No attempt was made to estimate

the uncertainties in these numbers because of the limitations discussed above.

IV. THEORY

This chapter will discuss some theoretical aspects of π-nucleus scattering. Since most experimental and theoretical work has concentrated on C^{12}, most of this discussion will be concerned with this target nucleus. In Chapter V, the theories developed in Chapter IV will be applied to the cross sections reported in Chapter III.

A. Pion-Nucleon Scattering

Since most theoretical treatments of pion nucleus scattering are based on the interaction of a pion with a free nucleon, some aspects of this interaction will be considered first. It is necessary to formulate a theory which takes into account the existence of the three charge states of the pion yet is also in agreement with the charge independence of nuclear forces. The nucleon has an isospin $T_N = 1/2$, and the pion's isospin is $T_\pi = 1$. Kemmer[46,47] proposed that the interaction of a pion and a nucleon with a certain parity and total angular momentum J depends on the total isotopic spin T which can have the values $T = 3/2$ (with $T_3 = \pm 1/2, \pm 3/2$) or $T = 1/2$ (with $T_3 = \pm 1/2$). The isotopic spin state vectors $|T, T_3\rangle$ for a state with different combinations of a pion and a nucleon can be obtained using the formalism for the addition of angular momentum developed for ordinary spin. Taking

linear combinations of these isotopic spin state vectors, the isotopic part of the pion-nucleon wave function may be expressed as follows:[47]

$$
\begin{aligned}
|\pi^+,p\rangle &= |3/2,\ 3/2\rangle \\
|\pi^o,p\rangle &= \sqrt{2/3}\ |3/2,\ 1/2\rangle - \sqrt{1/3}\ |1/2,\ 1/2\rangle \\
|\pi^-,p\rangle &= \sqrt{1/3}\ |3/2,-1/2\rangle - \sqrt{2/3}\ |1/2,-1/2\rangle \\
|\pi^+,n\rangle &= \sqrt{1/3}\ |3/2,\ 1/2\rangle + \sqrt{2/3}\ |1/2,\ 1/2\rangle \\
|\pi^o,n\rangle &= \sqrt{2/3}\ |3/2,-1/2\rangle + \sqrt{1/3}\ |1/2,-1/2\rangle \\
|\pi^-,n\rangle &= |3/2,\ -3/2\rangle
\end{aligned}
\tag{9}
$$

If the isotopic spin is a good quantum number, there will be no matrix elements connecting states with different values of isotopic spin. The scattering matrix is invariant under rotations in isotopic spin space and, thus, is independent of T_3.[48] With these assumptions, one can derive the isotopic spin part of the total cross sections[49]

$$
\begin{aligned}
\sigma(\pi^-n \to \pi^-n) &\propto |\langle \pi^-n|M|\pi^-n\rangle|^2 \\
&\propto |\langle 3/2,-3/2|M(3/2)|3/2,-3/2\rangle|^2 \\
&\propto |A(3/2)|^2
\end{aligned}
\tag{10a}
$$

where A(T) is a scattering amplitude associated with the matrix element M(T). In the same way:

$$\sigma(\pi^-p \to \pi^-p) \propto 1/9|A(3/2) + 2A(1/2)|^2 \tag{10b}$$

$$\sigma(\pi^-p \to \pi^on) \propto 2/9|A(3/2) - A(1/2)|^2 \tag{10c}$$

Cross sections for free pion-nucleon scattering, which were summarized by Bareyre,[50] indicate a striking dependence on energy which is indicative of resonance behavior. A comparison of the resonance peaks in $\pi^{\pm}N$ scattering with relations such as Eqns. 9 and 10 made it possible to determine that each peak represents a resonance with a particular value of isotopic spin (T = 3/2 or T = 1/2). The low energy cross section is dominated by a large peak at ~195 MeV which has been determined to be a resonance in the T = 3/2 channel. In this energy region, the A(1/2) amplitude may be neglected, and from Eqns. 9 and 10, one would expect that

$$\sigma(\pi^- n \to \pi^- n) : \sigma(\pi^- p \to \pi^- p) : \sigma(\pi^- p \to \pi^o n) = 9 : 1 : 2 \qquad (11)$$

which is found to be the case. If a resonance has a particular value of total angular momentum J and orbital angular momentum l, the cross section at the peak is given by

$$\sigma(J) = 2\pi \lambda\!\!\!^{-2}(2J+1) \qquad (12)$$

where $\lambda\!\!\!^{-}$ is the wavelength of the incident pion in the center of mass. This formula predicts the correct experimental cross section if the resonance is assumed to be J = 3/2, l = 1, a fact that is supported by the p-wave character of the differential cross sections. The peak in the cross section at ~195 MeV thus corresponds to a pion-nucleon resonance with T = 3/2 and J = 3/2. This resonance which is referred to as the N^* or (3,3) resonance has a lifetime of $\sim 10^{-22}$ seconds and occurs in four charge states from -1 ($\pi^- n$) to +2 ($\pi^+ p$).

B. Pion-Nucleus Scattering Using the Impulse Approximation

In the impulse approximation, the scattering operator for pion-nucleus scattering T_A (which should not be confused with the T referring to isospin in other sections) may be expressed in terms of two-body scattering operators t(j) which act only on the pion and the j-th nucleon in the target. The single scattering approximation consists of taking

$$T_A = \sum_{j=1}^{A} t(j) \tag{13}$$

where A is the number of nucleons in the target nucleus.[51]

If one further assumes that the structure of the target nucleus has no dynamical effect on the pion-nucleus scattering process, then the free pion-nucleon scattering amplitude $T_{\pi N}$ can be substituted for the two body scattering amplitude t(j):

$$\left\langle \vec{K}', \vec{P}_j' \middle| t(j) \middle| \vec{K}, \vec{P}_j \right\rangle \approx \left\langle \vec{K}', \vec{P}_j' \middle| T_{\pi N} \middle| \vec{K}, \vec{P}_j \right\rangle \tag{14}$$

This is the impulse approximation.[51] $\vec{K}$ and $\vec{K}'$ refer to the initial and final pion momentum, and $\vec{P}_j$ and $\vec{P}_j'$ refer to the initial and final nucleon momentum. In order to make use of this approximation, one must know the off-energy shell $T_{\pi N}$ matrix. In practice, this is often extrapolated from the on-energy shell $T_{\pi N}$ matrix for similar kinematics. Nuclear structure has no dynamical effect on the scattering process; but it does affect the kinematics because one must have the probability amplitude that a nucleon has momentum $\vec{P}$ in the initial state and $\vec{P}'$ in the final state.

C. Knockout Reactions

If the scattered nucleon receives sufficient momentum to knock it out of the nucleus, it may be possible to apply the impulse approximation if the pion nucleus kinematics are similar to that of free pion-nucleon scattering. This is referred to as quasi-free scattering. If the outgoing nucleon does not interact further in the nucleus, it can be represented by a plane wave. Using the single scattering (Eqn. 13) and the impulse approximation (Eqn. 14), one can derive an expression for the cross section:

$$\sigma(\pi,\pi N;E) = \sum_f \int d^3P\, \sigma_{\pi N} \left| g_{fi}(\vec{P}) \right|^2 \qquad (15)$$

where $\sigma_{\pi N}$ is the free pion-nucleon cross section and:[51]

$$g_{fi}(\vec{P}) = (2\pi)^{-3/2} \int d^3P_2 \ldots d^3P_A \left\langle \phi_f^*(\vec{P}_2 \ldots \vec{P}_A)\psi_i(\vec{P},\vec{P}_2 \ldots \vec{P}_A) \right\rangle \qquad (16)$$

where $\psi_i(\vec{P},\vec{P}_2 \ldots \vec{P}_A)$ is the wave function of the initial nucleus with A nucleons and $\phi_f^*(\vec{P}_2 \ldots \vec{P}_A)$ is the wave function of the final nucleus with (A - 1) nucleons.

The free π-N cross section in the region of the (3,3) resonance is dependent on the relative momentum difference between the pion and nucleon $\vec{K} - \vec{P}$. The average nucleon momentum in the 1p shell is ~150 MeV/C. This momentum distribution spreads the initial pion energy relative to the nucleon[52] by ~20%. If $\sigma_{\pi N}$ is averaged over the nucleon momentum distribution $\overline{\sigma_{\pi N}(E)}$, then the cross section can be written[52]

$$\sigma(\pi,\pi N;E) = \overline{\sigma_{\pi N}(E)} \sum_f \int d^3P |g_{fi}(\vec{P})|^2 \tag{17}$$

or

$$\sigma(\pi,\pi N;E) = \overline{\sigma_{\pi N}(E)} \sum_f S_{fi} \tag{18}$$

where[52]

$$S_{fi} = \int d^3P |g_{fi}(\vec{P})|^2 \tag{19}$$

The quasi-free approximation predicts the absolute value of the cross section, the relative cross sections for the different charge states of the pion, and also the relative excitation of the states of the residual nucleus. $\overline{\sigma_{\pi N}(E)}$ is the free πN cross section, somewhat broader, but with the isospin dependence of Eqn. 11. S_{fi} is the spectroscopic factor[53] commonly measured in pickup reactions. The spectroscopic factor for 1p nucleon removal may be derived by expanding the initial wave function of N 1p nucleons as a product of the wave function of (N - 1) 1p nucleons and the wave function of a single nucleon in the 1p shell.[54]

$$\psi^{IT\alpha}(1\ldots N) = \sum_{I_0T_0\alpha_0 j} \left\langle IT\alpha\{|I_0T_0\alpha_0,j\right\rangle \left[\phi^{I_0T_0\alpha_0}(1\ldots N-1)\phi^j(N)\right]^{IT} \tag{20}$$

where I is spin, T is isospin, α represents the other quantum numbers, j is the angular momentum of the transferred nucleon, and $\left\langle IT\alpha\{|I_0T_0\alpha_0,j\right\rangle$ is a coefficient of fractional parentage (CFP). With this definition, the spectroscopic factor (Eqn. 19) becomes

$$S_{fi} = N \left\langle IT\alpha\{|I_0T_0\alpha_0,j\right\rangle^2 \tag{21}$$

In the simplest shell model, the spectroscopic factor for neutron (or proton) removal would be the number of neutrons (or protons) in the outermost shell. There is a more detailed discussion of O^{16} wave functions and spectroscopic factors in Section VB.

There is no generally accepted theoretical framework for treating pion-nucleus scattering in the region of the (3,3) resonance. A proton of 190 MeV is known to exhibit quasi-free scattering (p,2p), but a pion of the same energy has less momentum available. The pion interacts more strongly with nucleons in this energy region. The average of π^+p and π^-p cross sections are four times as strong as the average of pp and pn cross sections. Quasi-free scattering assumes that the pion interacts with a single nucleon while the other nucleons act as spectators, but the wavelength of the pion at the (3,3) resonance is 4.1 fm which is ~3 times the internucleon distance in C^{12}.

Except for the π^-/π^+ cross section ratio, the existing data can be explained by the quasi-free approximation (Eqn. 18). Several groups[5,10,11,12,1] have studied the reaction $C^{12}(\pi^{\pm},\pi n)C^{11}$ by activation techniques. The energy dependence of this reaction (Fig. 1) shows a broad resonance which is reproduced by the $\overline{\sigma_{\pi N}(E)}$ term of the expression for quasi-free scattering (Eqn. 18). Since at the resonance $\overline{\sigma_{\pi^-n}(E)}$ ~ 100 mb and the measured cross section is 68 mb one finds $\sum S_{fi}$ ~ .7, in disagreement with the simple shell model prediction $\sum S_{fi}$ ~ 4.[51] This discrepancy may be partially due to the averaging of $\overline{\sigma_{\pi^-n}(E)}$; however, it is believed that the Pauli exclusion principle, which forbids final nucleon momentum states less than the Fermi momentum, and also distortion of the incoming pion and outgoing pion and nucleon plane waves have a major role in reducing $\sum S_{fi}$.

The Charpak[8] group at CERN found evidence of quasi-free scattering in their investigation of the $C^{12}(\pi^+,\pi^+p)B^{11}$ reaction for 200 MeV pions at such angles where the outgoing proton and pion have about equal energies. It was found that the ratio of the cross section for this reaction to that of the free π^+p reaction was about the same as the ratio of the cross section for 160 MeV protons on C^{12} to the cross section for free protons. That is:

$$\frac{\sigma(C^{12}+\pi^+\rightarrow B^{11}+\pi^++p)}{\sigma(\pi^++p\rightarrow\pi^++p)_{free}} \sim \frac{\sigma(C^{12}+p\rightarrow B^{11}+p+p)}{\sigma(p+p\rightarrow p+p)_{free}} \qquad (22)$$

In both pion induced and proton induced nucleon knockout, the cross sections were an order of magnitude lower than the quasi-free prediction. In the pion case, at the (3,3) resonance $\overline{\sigma_{\pi n}(E)}$ ~ 100 mb and $\sum S_{fi} \sim 4$; the quasi-free prediction exceeds both the measured total inelastic cross section (~350 mb) and the geometric cross section (~320 mb).

The center of the (3,3) resonance peak in pion-nucleus knock-out reactions is ~25 MeV lower than the resonance in πN scattering (Fig. 1). Bertini[55] suggested that this downward shift may be an indication of the real part of the pion nucleus optical potential which Fujii[56] calculated to be ~-40 MeV in his analysis of elastic pion scattering on C^{12}. Thus the pion would gain energy when it enters the nucleus, causing a downward shift in the apparent resonance energy.

Several quasi-free calculations have been performed to explain the activation data. Reeder and Markowitz[5] developed expressions for the probability of a pion entering C^{12}, scattering on a nucleon, and escaping, based on the mean free path of pions and neutrons in nuclear

matter. In one calculation, they assumed that the scattered nucleon shares its energy with the other nucleons, and the resultant nuclear excitation eventually leads to the evaporation of one neutron. This calculation failed to produce the broad peak at the (3,3) resonance energy found in the experimental data. A quasi-free calculation assumed that the scattered neutron escaped without exciting the nucleus, and this successfully produced the energy dependence of the data. Additionally, because of the short mean free path of the pion in nuclear matter, their calculation predicted that the reaction occurs predominately on the upstream surface and pole tips of the C^{12} nucleus and that 180^{o} pion scattering dominates.

Bertini[55,57] performed a Monte Carlo type quasi-free calculation of the $C^{12}(\pi^{-},\pi^{-}n)C^{11}$ cross section which yielded excellent agreement with experiment. Kolybasov[13] calculated the cross section using the pole approximation which treats the process as a virtual decay of C^{12} emitting a neutron which is then scattered by the pion. This results in a good fit to the data except in the low energy region (Fig. 1) and yields $\sum S_{fi} \sim .33$[51] (Eqn. 18). Dalkarov[58] was able to improve the agreement for low energies by assuming that the N^{*} re-scatters on the residual C^{11} nucleus with a cross section of 3 mb.

A serious problem for the quasi-free treatment of these reactions is found in the work of Tanner et al.[1,10,11,12] who measured the ratio of cross sections at 180 MeV:

$$\frac{\sigma(\pi^{-},\pi^{-}n)}{\sigma(\pi^{+},\pi^{+}n) + \sigma(\pi^{+},\pi^{o}p)} \sim 1.\pm.1 \qquad (23)$$

for C^{12}, N^{14}, and O^{16} targets using activation techniques. The results of this experiment are summarized in Table I. Since the expression for quasi-free scattering (Eqn. 18) contains $\overline{\sigma_{\pi N}(E)}$, one would expect the ratio of the cross sections of Eqn. 23 to have the value 3 (Section IVA). A calculation by Kolybasov and Smorodinskaya[59], taking into account the isospin T = 1/2 state and the effect of the nuclear motion of nucleons, yielded a value of 2.4 - 2.6 for this ratio at 180 MeV. A Monte Carlo cascade-plus-evaporation calculation by Bertini[55] also yielded a ratio ~3. The value of unity of Eqn. 23 casts serious doubt on the validity of the quasi-free approximation for the π nucleus reaction. But, compounding the problem, it has been observed[60] that the reaction $He^4(\pi^-,\pi^-n)He^3$ has 4.8 ± 1.3 times the cross section of $He^4(\pi^-,\pi^-p)H^3$ in fair agreement with the quasi-free estimate of 9. Various mechanisms such as a pion interaction with nucleon pairs,[1] excitation of C^{12} to an excited state with a definite value of isospin T,[1] and several final state interactions[18,19,61] have been proposed to explain the experimental value of Eqn. 23. These will be discussed in greater detail in Sections IVD to IVG.

Data presented in Chapter III indicated the result

$$\frac{\sigma(O^{16}+\pi^-\rightarrow O^{15*}+\pi^-+n)}{\sigma(O^{16}+\pi^-\rightarrow N^{15*}+\pi^-+p) + \sigma(O^{16}+\pi^-\rightarrow N^{15*}+\pi^o+n)} = 1.7 \pm .4 \qquad (24)$$

for excitation of the $3/2^-$ mirror states in O^{15} and N^{15} in disagreement with the quasi-free assumption. This and other considerations resulting from the $(\pi^-,\pi N\gamma)$ data will be discussed in Chapter V. Consideration of this data has been postponed because the theories to be discussed in

the remainder of this chapter were proposed to explain the Tanner activation experiment and generally involve a C^{12} target and a summation over all bound states of the residual nucleus.

D. Initial State Interactions

Wilkinson[62] suggested that some form of coherent inelastic scattering such as $C^{12}(\pi,\pi)C^{12*}(n)C^{11}$ may be a significant contributor to the single nucleon knockout cross section. If such inelastic scattering were to excite a virtual state of C^{12} with well-defined isotopic spin, such as the giant dipole resonance with $J^{\pi} = 1^{-}$, T = 1, then the cross section would be independent of the charge state of the incident pion. Tanner[1] estimated the relative cross sections using the relations of Eqn. 11:

Relative Probability for Initial Excitation		Relative Probability for Decay Products	
.45	$\pi^{-}+C^{12}\rightarrow\pi^{-}+C^{12*}\rightarrow C^{11}+n$	.225	(25)
	$\pi^{-}+C^{12}\rightarrow\pi^{-}+C^{12*}\rightarrow B^{11}+p$	.225	
.45	$\pi^{+}+C^{12}\rightarrow\pi^{+}+C^{12*}\rightarrow C^{11}+n$	.225	
	$\pi^{+}+C^{12}\rightarrow\pi^{+}+C^{12*}\rightarrow B^{11}+p$	.225	
.10	$\pi^{+}+C^{12}\rightarrow\pi^{o}+N^{12*}\rightarrow C^{11}+p$	.100	(26)

This assumes equal probability for π^{-} or π^{+} excitation of giant dipole states in C^{12} and that π^{+} would excite N^{12} dipole states by charge

exchange with a probability of 2/9 that of its excitation of C^{12} states. Excitation of giant dipole states of B^{12} by π^- charge exchange would not contribute to Tanner's cross section ratio because it decays to B^{11}. Combinations of Eqns. 25 and 26 yield a π^-/π^+ ratio for C^{11} activity of ~.7.

Kolybasov[59] performed a calculation in which it was assumed that the quasi-elastic mechanism and the coherent inelastic scattering contributed equally to the $C^{12}(\pi^{\pm},\pi n)C^{11}$ cross section. No details of this calculation are given, but they report that the energy dependence of the cross section is in better agreement with experiment than the quasi-free calculation alone. Wilkinson[62] argues that significant giant dipole excitation by pion scattering is unlikely because giant dipole excitation is only a small fraction of the cross section for inelastic scattering of high energy protons. Aganyants,[4] however, proposed this mechanism to explain the anisotropy in the angular distribution of the recoil protons from the reaction $C^{12}(\pi^-,\pi^-p)B^{11}$ at incident pion momentum of 1.04 GeV/C. If the contribution from coherent inelastic scattering at small momentum transfer is 17% of the total cross section, a significant improvement between theory and his experimental results for this reaction is obtained.

Chatwin and Richter[63] take the view that Tanner's results (Eqn. 23) arise from a different attenuation of the π^+ and π^- inside the nucleus. Using a distorted wave impulse approximation, they compute a reduction factor which is found to be approximately equal for both π^- and π^+. They argue, however, that the assumption of absorption processes and four nucleon correlations would favor the π^+ induced knockout by a factor of ~3, thus producing the results of Eqn. 23.

E. Pair Interaction

If pion-nucleus scattering were to involve an interaction with more than one nucleon either as a quasi-deuteron or as a re-scattering of the N^* on another nucleon (Section IVF), then the charge dependence of the reaction would not follow the quasi-free prediction. Tanner[64] proposed that it may be necessary to treat the pion-nucleus interaction as a quasi-free scattering of a pion with a nucleon pair (πNN) instead of with a single nucleon. The Pauli principle makes the contribution from np pairs more important than nn or pp pairs, and thus the interaction would tend to be charge independent. Tanner detected the reactions $C^{12} \xrightarrow{\pi^+} C^{10}$ and $O^{18} \xrightarrow{\pi^+} N^{16}$ so some pair interactions do occur, either directly or indirectly. Since, however, the reaction $C^{12} \xrightarrow{\pi^-} C^{10}$ was not detected, Tanner concludes that if there is a specific πNN interaction, the πNN states of T = 2 do not contribute because $\pi^- nn$ can only couple to T = 2. Furthermore, contributions from the T = 0 states are likely to be small because they could not involve the (3,3) resonance. Multiplying Clebsch-Gordon coefficients for a pure T = 1 πNN interaction with all pairs in C^{12}, Tanner computed a ratio of .64 for the π^-/π^+ ratio of Eqn. 23.[1]

F. N^* Re-scattering

Another possible interaction which might reduce the π^-/π^+ neutron knockout ratio is some form of interaction between the N^* and the residual nucleus. Dalkarov[58] improved the agreement of Kolybasov's pole diagram calculation of pion knockout reactions by adding a triangle graph which treated the elastic scattering of the N^* on the C^{11} nucleus. The triangle graph was found to contribute only below 200 MeV

incident pion energy. The expression for the cross section contained one free parameter which was varied so as to give a good fit to the data at 160 MeV and with this determined, an excellent fit to the data over the range of the (3,3) resonance was obtained.

An N^* which scatters on another nucleon could decay without emitting a pion. This is essentially π absorption in flight. The probability of such an interaction is increased in nuclear matter because the lifetime of the N^* is lengthened at low energies by the Pauli principle which forbids final nucleon states of momentum less than the Fermi momentum.

This process ($N^* + N \rightarrow N + N$) would be the inverse reaction to the inelastic N-N collision which results in $N^* + N$, that is ($N + N \rightarrow N^* + N$). This assumes that the properties of the N^* would not be affected by the high density of nuclear matter, which was also assumed in the quasi-free approximation. Applying the principle of microscopic reversibility to the reaction ($N + N \rightarrow N^* + N$) Fraenkel[65] calculated the cross section for N^* decay by inelastic scattering on a nucleon. This calculation made use of the one pion exchange model for N^* production, which assumes that the N^* is created by the resonant scattering of a virtual pion on the incoming nucleon. The first approximation to the scattering matrix element for this process is taken to be identical with the matrix element for the scattering of a real pion. Fraenkel calculated the total cross section for the reaction $N^*(T_z = 3/2) + n \rightarrow p + p$ as a function of the kinetic energy of the N^*. This calculation[65] indicated that about 40% of the N^*'s created in nuclear matter would decay in this manner.

Since the pion's rest mass energy would be absorbed by the two nucleons, the probability of one of the nucleons remaining in the nucleus is low, and the effect on the single nucleon knockout cross sections would be minimal. This process can proceed only in the T = 1 state and thus could be the mechanism of the T = 1, πNN pair interaction which Tanner discussed (Section IVE).

G. Final State Interactions

Several authors attempt to explain the ratio of (π^-/π^+)-neutron knockout cross sections (Eqn. 23) in terms of a final state interaction between the emerging nucleon and the residual nucleus. An optical model calculation by Hewson[19] includes the effect of charge exchange between the struck nucleon and the residual nucleus. A spin independent, complex optical potential of form $V(r) + W(r)(t\cdot T)$ is used where t is the nucleon isospin operator and T is the nucleus isospin operator. The (π^-/π^+)-neutron knockout ratio resulting from Hewson's calculation ranges from 1.57 to 2.03 depending on the values chosen for the potential. It is not possible to obtain the experimental value of 1. using reasonable parameters for the potential.

Robson[18,61] has treated the problem of final state interactions between the outgoing nucleon and the nucleus in a general isospin formalism. He introduces a final state interaction $V_{N'B'}$ between the outgoing nucleon N' and the residual nucleus B'

$$T_{fi} = \left\langle f\left|(V_\pi+V_{N'B'})(1+G^+V_\pi)\right|i\right\rangle \qquad (27)$$

where V_π is the total pion-nucleus interaction and $G^{(+)}$ is the propagator

for the three body-final states. The $V_{N'B'}$ interaction is considered to be dependent on the isospin coupling $T_{A'}$ of the outgoing nucleon $T_{N'}$, and the residual nucleus $T_{B'}$, ($T_{A'} = T_{N'} + T_{B'}$, where primed quantities refer to final values). Robson assumes the impulse approximation (Eqn. 14) and also that $T_{B'}$ is single valued, which would be the case for self conjugate target nuclei with T = 0. The resulting expression is

$$T_{fi} = \sum_{T_{A'},T_{N*}} \alpha_{T_{N*}T_{A'}} \Omega_{N'B'}^{T_{A'},T_{B'}} \top_{\pi}^{T_{N*}} \Theta_{T_{B'}}^{T_A} \tag{28}$$

where $\top_{\pi}^{T_{N*}}$ is the πN scattering amplitude at the (3,3) resonance,

$\Theta_{T_{B'}}^{T_A}$ is a generalized coefficient of fractional parentage, and

$\Omega_{N'B'}^{T_{A'},T_{B'}}$ is a function of the final state interaction.

$\alpha_{T_{N*}T_{A'}}$ carries the charge dependence of the interaction and is defined by:

$$\begin{aligned}\alpha_{T_{N*}T_{A'}} = \sum_{T} & C(T_A T_\pi T, T_{ZA} T_{Z\pi} T_Z) C(T_{B'}, T_N, T_{A'}, T_{ZB'}, T_{ZN}, T_{ZA'}) \\ & \times C(T_{A'}, T_\pi, T, T_{ZA'}, T_{Z\pi}, T_Z) U(T_{B'} T_N T T_\pi; T_{A'} T_{N*}) \\ & \times U(T_{B'} T_N T T_\pi; T_{A'} T_{N*})\end{aligned} \tag{29}$$

where the $C(T_A T_\pi T, T_{ZA} T_{Z\pi} T_Z)$'s are Clebsch Gordan coefficients, and the $U(T_{B'} T_N T T_\pi; T_{A'} T_{N*})$'s are Racah coefficients.

Robson does not attempt to evaluate $\Omega_{N'B'}^{T_{A'},T_{B'}}$ but consideres the charge dependence of the interaction introduced by the dependence on $T_{A'}$, the total isospin of the emerging nucleon and the nucleus. The isospin of the residual nucleus $T_{B'}$, is assumed to be single valued and $T_{A'} = T_{B'} \pm 1/2$. With the definitions

$$\sigma{+}{+} = \sum_f \left| T^{T_{B'},+1/2} \right|^2$$
$$\sigma{-}{-} = \sum_f \left| T^{T_{B'},-1/2} \right|^2 \tag{30}$$

where $T^{T_{A'}}$ is the scattering amplitude for a particular value of $T_{A'}$ and

$$\sigma{+}{-} = \sum_f \mathrm{Re}\left(T^{T_{B'},+1/2} T^{T_{B'},-1/2*} \right) \tag{31}$$

the cross section for $C^{12}(\pi^-,\pi^-n)C^{11}$ is written (suppressing the $T_{N*}(= 3/2)$ subscript on $\alpha_{T_{N*}T_{A'}}$)

$$\sum \sigma_{fi} \propto \alpha_1^2\, \sigma{+}{+} + \alpha_0^2\, \sigma{-}{-} + 2\alpha_1\alpha_0\, \sigma{+}{-} \tag{32}$$

Robson argues that in a radiochemical cross section measurement, the energy averaging in Σ is over tens of MeV and the isospin splitting of the final state is ~10 MeV, and thus he assumes $\sigma{+}{+} \sim \sigma{-}{-}$. If a coherence parameter is defined

$$\chi = \sigma{+}{-}/\sigma{+}{+} \tag{33}$$

then

$$\sum_f \sigma_{fi} = [\alpha_1^2 + \alpha_0^2 + 2\alpha_1\alpha_0\ \chi]\sigma_{++} \qquad (34)$$

Evaluating this using Eqn. 29 and calculating a similar expression for $C^{12}(\pi^+,\pi N)C^{11}$, one finds a value for the π^-/π^+ induced neutron knockout ratio of

$$R(\pi^-/\pi^+) = \frac{5 + 4\chi}{7 - 4\chi} \qquad (35)$$

which yields the experimental results of Tanner (Eqn. 23) for $\chi = .25$. A similar expression can be derived to describe the π^--O^{16} (O^{15}/N^{15}) knockout ratios. For $\chi = 1.$, this expression yields the quasi-free prediction of 3. If random interference occurs between the $T_{A'} = 0$ and the $T_{A'} = 1$ components, then $\chi = 0.$,and the expression for a pure compound nucleus results. Robson does not attempt to evaluate χ, but uses it as a fitting parameter. He finds[61] that χ ranges from .18 to .33 for C^{12}, N^{14}, and O^{16}; from .7 to .9 for He^4 [60], and from .28 to .82 for Be^9.

V. DISCUSSION OF RESULTS

A. General Considerations

The cross sections for excitation of various nuclear states by pion inelastic scattering and pion induced knockout reactions are listed in Tables VIII to XIV. A direct comparison of these numbers with the results of the $\pi^{\pm}$ activation work of Tanner (Table I) is difficult because of the different nature of the two experiments. At 180 MeV incident π energy, they measured a cross section of 42 mb for excitation of all bound states of O^{15} in the $O^{16}(\pi^-,\pi^-n)O^{15}$ reaction. If it is assumed that the energy dependence of the $O^{16}(\pi^-,\pi^-n)O^{15}$ cross section is similar to that for C^{12}, one can extrapolate this to a cross section of 38 mb at 233 MeV. At this energy, the $(\pi^-,\pi n\gamma)$ experiment (Table IX) measured 2.1 mb for excitation of the $5/2^+$ state in O^{15}, 15.6 mb for excitation of the $3/2^-$ state, and .8 mb for excitation of the $7/2^+$ state for a total of 18.5 mb. If one assumes a simple shell model, the probability of neutron knockout from a shell is proportional to the number of neutrons N in that shell. Thus, the probability for removal of a $p_{1/2}$ neutron (N = 2) leading to the O^{15} ground state would be ~1/2 the probability for removal of a $p_{3/2}$ neutron (N = 4) leading to the first $3/2^-$ state or other higher $3/2^-$ states. Kashy[66] estimates that the first $3/2^-$ state has 70% of the total $p_{3/2}$ strength. Using this number, the total $p_{3/2}$ strength can be set at 22.3 mb (10./7. x 15.6 mb) and the $p_{1/2}$ strength at 11.1 mb (1/2 of the $p_{3/2}$

strength). If these are added to the cross sections for the O^{15} $5/2^+$ and $7/2^+$ levels, the result is ~36 mb in good agreement with the extrapolation of Tanner's results to 233 MeV (38 mb).

Generally the relative excitation of states of O^{15} and N^{15} resulting from pion induced knockout reactions support the quasi-free interpretation. The exception to this is the relatively strong excitation of the $5/2^+$ levels in O^{15} and N^{15}. The $5/2^+$ levels have a $((P_{1/2})^{-2}\ d_{5/2})$ configuration,[67] and their presence in the spectra can be understood in terms of the known (2p, 2h) admixtures to the ground state of O^{16} (Section VB) but not in the strength measured. If the O^{16} and N^{16} giant dipole states are strongly excited, then one would expect to have a larger cross section for the $5/2^+$ levels relative to the $3/2^-$ (Section VE) than the quasi-free prediction.

The cross section ratios of π^--neutron knockout to π^--proton knockout leading to excited mirror states of O^{15} and N^{15} disagree with the quasi-free prediction of 3. The $\pi^-(O^{15}/N^{15})$ ratio is 1.7 ± .4 for excitation of the first $3/2^-$ mirror states in O^{15} and N^{15} and .58 ± .29 for excitation of the $5/2^+$ mirror states. Figure 14 is a histogram which shows the relative excitation of the states of O^{15} and N^{15}. The arrows indicate the location of states not seen in this experiment.

Tanner detected two cases which involved removal of two nucleons, the $C^{12} \xrightarrow{\pi^+} C^{10}$ reaction and the $O^{18} \xrightarrow{\pi^\pm} N^{16}$ reaction. Tables X and XI indicate a significant cross section for neutron-proton removal leading to excited states of N^{14} and a limited indication of two proton removal leading to excited states of C^{14}. The 2 neutron removal process could not be detected in this experiment because there are no bound

excited states of O^{14}. The spectroscopy of the two nucleon removal process is discussed in Section VG.

A cross section of 6.6 ± 1.6 mb was measured for the removal of two protons and a neutron (or they may be emitted as He^3 or d + p) leading to the third excited state of C^{13}. There are no bound excited states of N^{13} so the 2 neutron and 1 proton (or triton or d + n) knock-out process could not be detected. In addition to this, there is a large cross section (16.8 ± 5.8 mb) for removal of 2 protons and 2 neutrons leading to the first excited state of C^{12}, although the problems discussed in Section IIIG throw some doubt on these results.

Inelastic π scattering led to the population of the 3^- excited state of O^{16}, but no other states were detected. Charge exchange scattering leading to excited states of N^{16} was also measured (Table XIII) with cross sections comparable to those of Tanner (Table I).

B. Discussion of the O^{16} Wave Functions

The description of the O^{16} ground state in terms of double closed nuclear shells is not adequate, and deformed components play an important role. These deformations can be understood in terms of two particle, two hole (2p, 2h) and four particle, four hole (4p, 4h) admixtures to the ground state. Brown and Green[68] write the O^{16} ground state wave function as

$$|O^{16}_{g.s.}\rangle = .874|0p\text{-}0h\rangle + .469|2p\text{-}2h\rangle + .130|4p\text{-}4h\rangle \qquad (36)$$

The (2p, 2h) admixtures are treated by coupling the particles and holes so that the force is attractive, and thus the energy difference

between the ground state and excited states is reduced. Zamick[69] assumed that since the T = 0 states in O^{16} lie lower than the T = 1 states, the T = 0 particle-hole force is strongly attractive, and the T = 1 force is repulsive. Thus, couplings which put a maximum number of particle-hole pairs in relative T = 0 states are favored. The lowest particle-hole energy is obtained by, first, coupling particles and holes separately to maximum isospins T_p and T_h and, then, coupling these to minimum total isospin T.[70]

Nilsson[71] introduced a Hamiltonian formalism for single particles in a distorted oscillator potential in which the axes are oriented so that j_z and $\Omega = \Sigma j_z$ are good quantum numbers, but l^2, l_z, s, and j are not. He obtained a series of diagrams in which the single particle level energy with a particular value of Ω is plotted as a function of a deformation parameter $\beta = \Delta R/R$. The Nilsson diagrams for O^{16} indicate that for $\beta \sim .3$, it requires very little energy to excite two particles from the No. 4 Nilsson orbital ($p_{1/2}$ with $\Omega = 1/2^-$) to the No. 6 Nilsson orbital ($d_{5/2}$ with $\Omega = 1/2^+$). Brown and Green[70] write the wave function for the (2p, 2h) state in O^{16} as:

$$(2p,2h)^{J=0,T=0} = \left\{[\alpha^+_{1/2}(6)\alpha^+_{1/2}(6)]^{J_p=0}_{T_p=1}[a(p_{1/2})a(p_{1/2})]^{J_h=0}_{T_h=1}\right\}^{T=0} \left|O^{16}_{g.s.}\right\rangle \qquad (37)$$

where the $a(p_{1/2})$'s are annihilation operators for the $p_{1/2}$ shell and the $\alpha^+_{1/2}(6)$'s are creation operators for particles in the No. 6 Nilsson orbital:

$$\alpha^{+}_{1/2}(6) = .828\ a^{+}_{1/2}(1d_{5/2}) + .573\ a^{+}_{1/2}(2s_{1/2}) - .16\ a^{+}_{1/2}(1d_{3/2}) \qquad (38)$$

where the $a^{+}_{1/2}(1_j)$ are creation operators for the #6 orbital with $\Omega = 1/2$. The coefficients in this expression correspond to $\beta = .3$ and were obtained by Brown and Green[70] from the results of Rost who calculated Nilsson orbitals in a Saxon-Woods potential.

The effect of the admixtures to the O^{16} ground state is to alter the spectroscopic factors (Eqn. 21) predicted by the simple shell model. The spectroscopic factor for removal of a neutron from the $p_{1/2}$ or $p_{3/2}$ shell of O^{16} would be (from Eqns. 21 and 36)

$$S(p_{1/2}) = 2.(.874)^2 + 1.(.469)^2 + 0.(.130)^2 = 1.748 \qquad (39)$$

$$S(p_{3/2}) = 4.(.874)^2 + 4.(.469)^2 + 4.(.130)^2 = 4.000 \qquad (40)$$

The effect of admixtures between the $p_{3/2}$ and $p_{1/2}$ states is small[72] and has been neglected.

Zamick[69] assumes that the Coulomb contribution is only ~10% of the total particle-hole energy, and thus (2p, 2h) excitations of protons and neutrons are equally probable. Thus in the average, for (2p, 2h) excitations, one of the particles is a proton, and the other a neutron (i.e. N = 1), and thus the spectroscopic factors for removal of a neutron from a $d_{5/2}$ or $s_{1/2}$ admixture to the ground state of O^{16} would be:

$$S(d_{5/2}) = 1.(.469)^2\ (.828)^2 = .151 \qquad (41)$$

$$S(s_{1/2}) = 1.(.469)^2\ (.573)^2 = .072 \qquad (42)$$

In a simple shell model, removal of a neutron from the $p_{1/2}$ or $p_{3/2}$ shell would leave the resultant O^{15} nucleus in the ground state or 6.177 MeV state respectively; however, some of the $p_{1/2}$ or $p_{3/2}$ strength may lie in a state of higher excitation, reducing the spectroscopic factors for the ground state and 6.177 MeV state. Snelgrove and Kashy[66] estimate that as much as 30% of the $p_{3/2}$ strength could be in states greater than 6.177 MeV.

C. Single Nucleon Knockout Reactions

Figure 14 is a comparison of the states excited in O^{15} and N^{15} following pion induced knockout reactions. The most prominent states detected are the mirror $3/2^-$ states at 6.177 MeV in O^{15} and 6.323 MeV in N^{15}. The configuration of these states[67] is $(p_{3/2})^{-1}$ corresponding to the removal of a $p_{3/2}$ neutron (or proton for N^{15}) from the O^{16} ground state. The shell model predicts a spectroscopic factor of 4.0 (Section VB) for nucleon removal leading to this state. In gamma decay experiments, it is necessary to determine if the cross section for excitation of a particular state may be augmented by branches from higher states. All cross sections reported in this paper have been corrected for branches from higher states which are known to be excited, but it is difficult to correct for all possible branches. There are several known bound states of O^{15} which branch to the 6.177 MeV level for which no upper limit could be determined. They are the 7.552 MeV $1/2^+$ state (57% branch), the 8.739 MeV $1/2^+$ state (33% branch), and the 8.918 MeV 3/2 state (30% branch). Although it was not possible to determine upper limits for the cross section of these levels, one can assume in most

cases that the cross sections were less than ~2 mb, or the transition would have been detectable in the spectra. With these assumptions, it can be estimated that, at most, ~15% of the O^{15} $3/2^-$ level could be due to branches from higher states. The cross section of the first N^{15} $3/2^-$ state has been corrected for the 12% branch from the 10.451 MeV level, and no other state has a branch to it greater than 10%.

The configuration of the $5/2^+$ mirror states in O^{15} and N^{15} corresponds to two holes in the $p_{1/2}$ shell and a nucleon in the $d_{5/2}$ shell. The O^{16} ground state is believed to have a 20% admixture of (2p, 2h) states (Section VB), but this is not adequate to explain the observed cross sections for $5/2^+$ excitation. The O^{15} $5/2^+$ state has a 100% branch from the 7.276 MeV state for which a correction has been made and a 40% branch from the 8.283 MeV level (σ <.5 mb) which could contribute at most 10% to the measured $5/2^+$ cross section. Thus, the O^{15} $5/2^+$ cross section is almost certainly due to actual excitation of the $5/2^+$ state and not branches from higher states. This cannot be verified for the N^{15} $5/2^+$ state with large branches from the 7.566 MeV, 8.576 MeV, and 9.829 MeV levels which could be significant contributors to the N^{15} $5/2^+$ cross section.

The O^{15} $7/2^+$ level at 7.276 MeV was detected, but its mirror level at 7.566 MeV in N^{15} was not observed. The O^{15} $7/2^+$ level has no branches from higher states. Gamma rays from the N^{15} $5/2^+$ level at 7.155 MeV were also detected, but the O^{15} $5/2^+$ mirror state at 6.859 MeV was obscured by neighboring peaks. The N^{15} $5/2^+$ state has a 23% branch from the 9.155 MeV state (σ <.5 mb), and therefore less than 20% of the 7.155 MeV cross section could be due to branches from higher levels.

Gamma rays from a branch of the N^{15} 10.451 MeV state were detected with a cross section of 1.0 mb but this level's mirror state in O^{15} is unbound.

D. Discussion of the Cross Sections for Single Nucleon Knockout

The absolute cross sections for the pion induced knockout reactions, which are in reasonable agreement with the activation work of Tanner (Section VA), may be compared with the quasi-free prediction of Eqn. 18 for neutron knockout by π^-. At the (3,3) resonance $\overline{\sigma_{\pi^- n}(E)} \sim 100$ mb and $\sigma = 15.6$ mb was measured for excitation of the first $3/2^-$ state in O^{15}. Thus, one finds $S(p_{3/2}) \sim .16$ which can be compared with the shell model prediction of $S(p_{3/2}) \sim 4$. (Section VB). This discrepancy is not serious because absorption and other effects generally reduce the absolute value of the summed spectroscopic factors for other direct reactions such as (p, 2p) (Eqn. 22).

The relative cross sections for neutron knockout compared with those for proton knockout (Fig. 14) do not support a quasi-free interpretation of the data. The quasi-free prediction of 3 for the $\pi^-(O^{15}/N^{15})$ ratio can be compared with a ratio of $1.7 \pm .4$ for excitation of the first $3/2^-$ mirror states, $.58 \pm .24$ for excitation of the $5/2^+$ mirror states and $1.29 \pm .37$ for all states of O^{15} and N^{15}. The $\pi^-(O^{15}/N^{15})$ cross section ratios indicate that the value of unity measured by Tanner for the ratio of the π^-/π^+ cross sections may hold no special significance.

The $\pi^-(O^{15}/N^{15})$ knockout ratio for the spectrum in coincidence with a charged particle in counter C (Section IIB) was 2.1 ± 1.0 for

excitation of the $3/2^-$ mirror states. Requiring a charged particle coincidence should eliminate the (π^-, π^o) charge exchange reaction and the quasi-free prediction of the ratio of neutron knockout to proton knockout should be 9 to 1 instead of 3 to 1. A value of 2.1 is in greater disagreement with the quasi-free interpretation than the results quoted above, but the large error associated with this number makes it difficult to reach any conclusions regarding the contribution of the charge exchange to the reaction.

The final state interaction theory of Robson (Section IVG) yields the experimental $\pi^-(O^{15}/N^{15})$ ratio of 1.29 ± .37 if the value of the coherence parameter is $\chi = .44 \pm .21$. This is in fair agreement with the coherence parameters ($\chi = .18$ to $.33$) computed for the C^{12}, N^{14}, and O^{16} results of Tanner.[61] Robson's expression (Eqn. 35), however, has great flexibility through the fitting parameter χ and could predict any reasonable ratio. The experimental verification of this theory must await a measurement of the (π^-/π^+)-nucleon knockout ratio from two targets with the same residual nucleus, in which case the χ dependence cancels out and the predictions of the theory are unique.

The charge dependence of the π-nucleus interaction disagrees with a quasi-free interpretation, but the spectroscopy of the reaction appears to support it. The limited number of transitions detected and also their relative intensity support a quasi-free interpretation. Figure 14 is a histogram which shows the relative excitation of the various states of O^{15} and N^{15} by the pion induced nucleon knockout reaction. The first $3/2^-$ state is prominent in each residual nucleus, a result compatible with a spectroscopic factor of 4 (Section VB). Reactions leading to the ground state could not be detected; however,

the calculation of Section VA which compares the π^--gamma ray results with the activation results of Tanner indicate a ground state cross section not incompatible with a $S(p_{1/2}) = 1.75$. For quasi-free scattering, the $5/2^+$ mirror states should have a spectroscopic factor which is 4% that of the $3/2^-$ state (Section VB). The experimental results indicated that $\sigma(O^{15}\ 5/2^+)/\sigma(O^{15}\ 3/2^-) = .13 \pm .04$ and $\sigma(N^{15}\ 5/2^+)/\sigma(N^{15}\ 3/2^-) = .39 \pm .11$. This ratio is reliable for O^{15}, but the N^{15} $5/2^+$ level has several states which branch to it (Section VC), and this could contribute significantly to the ratio. Nonetheless, the cross sections for the $5/2^+$ mirror states are larger than one would expect from the direct reaction spectroscopic factors. Excitation of the giant dipole states in O^{16} and N^{16} would be a factor in increasing the cross sections for these states. This is discussed in Section VE.

The N^{15} $5/2^+$ state is seen in π^- absorption where the process is thought to involve nucleon pairs. This is interpreted[73] as the result of an absorption on p shell particles leading to a final state with one nucleon free and the other in the $d_{5/2}$ state. Since the cross sections for pion interactions involving two nucleons are large (Tables X and XI), one can also interpret the relatively strong excitation of the $5/2^+$ levels as the result of a pion-nucleon pair interaction in which one of the nucleons remains in the $d_{5/2}$ shell, and the other escapes the nucleus.

In the remainder of this section, the π induced single nucleon knockout cross sections will be compared with the experimental spectroscopic factors deduced from several reactions involving single nucleon removal from O^{16} by a reaction thought to be direct. This comparison is facilitated by the use of histograms in which the abscissa identifies

the energy of a particular state, and the vertical height of each point is proportional to the cross section. The blocks representing the π-knockout data are black. The normalization of the comparison data is described in the caption for each figure.

Figure 15 is a histogram which compares the $(\pi^-, \pi N\gamma)$ results with the 600 MeV proton data (Table XVI) discussed in Section IIIJ. The cross sections show reasonable agreement for N^{15}, but there is some discrepancy with the O^{15} 6.177 MeV level. The good agreement of the $5/2^+$ levels in the two nuclei is noteworthy, perhaps indicating that gamma branching may be a significant contributor to this level.

The spectroscopic factors based on the results of an $O^{16}(p,d)O^{15}$ experiment by Snelgrove and Kashy[66] are compared with the $(\pi^-, \pi N\gamma)$ cross sections in Fig. 16. This comparison indicates that pion induced knockout yields considerably stronger excitation to the $5/2^+$ state than the (p,d) direct reaction.

Also shown in Fig. 16 is a histogram which compares the $(\pi^-,\pi N\gamma)$ cross sections with the spectroscopic factors resulting from the $O^{16}(He^3,\alpha)O^{15}$ reaction at 11 MeV studied by Bohne et al.[74] The O^{15} $5/2^+$ states at 5.242 MeV and 6.859 MeV were strongly excited in the (He^3,α) work. This may be significant; however, the initial energy of the He^3 was only 11 MeV, and there may be some energy dependence to the reaction at this energy.

Figure 16 also compares the $(\pi^-,\pi N\gamma)$ results with the spectroscopic factors of Hiebert et al.[75] for the $O^{16}(d,He^3)N^{15}$ reaction. The authors consider the computed spectroscopic factors for the $5/2^+$ and $1/2^+$

levels to be upper limits. They did not report excitations to any levels above the first $3/2^-$ level.

These comparisons indicate that the relative cross sections resulting from the $(\pi^-,\pi N\gamma)$ reaction are in reasonable agreement with other direct reactions. The negligible excitation of the numerous O^{15} and N^{15} states with zero spectroscopic factors is certainly compatible with a direct reaction interpretation of the data. Excitation of the $5/2^+$ levels relative to the $3/2^-$ is stronger than expected. This may be explained by significant excitation of the giant dipole states in O^{16} by pion scattering or by pion-nucleon pair interactions in which one nucleon remains in the $d_{5/2}$ shell.

E. Giant Dipole Excitation

The proposal (Section IVD) that pion scattering at the (3,3) resonance could excite the giant dipole states in O^{16} and N^{16}, which would then decay by emitting a neutron or a proton with equal probability, may be investigated by studying the decay schemes of the giant dipole states. Certain of the giant dipole states are excited in photonuclear reactions, μ^- capture, and radiative π^- capture. The photonuclear reaction populates giant dipole states of O^{16}, and the capture reactions populate analogue dipole states in N^{16}. The dipole states excited would have to be relatively pure T = 1 because a very small admixture of T = 0 greatly changes the neutron to proton decay ratio. If the different proton and neutron barrier penetrabilities are ignored, any admixture of T = 0 will favor proton emission over neutron emission.[76] This is due to the isospin coupling in the reduced width amplitudes for the break up of O^{16*} into O^{15} + n and N^{15} + p.

Caldwell et al.[77] studied the residual states of O^{15} and N^{15} following photoexcitation of the O^{16} giant dipole states from 16 to 29 MeV. Using the ratio of neutron emission to proton emission and the theory of Barker and Mann[76], Caldwell deduced the isospin purity of the states in this energy range. The average (T = 0)/(T = 1) amplitude ratio was found to be ~.08 over the range of states from 16 to 19 MeV with definite minima ~.02 in the region below 19 MeV and between 20.8 and 21.6 MeV.

In Fig. 17, Caldwell's cross sections[77] for photoexcitation of all O^{16} states between 16 and 29 MeV leading to residual states of O^{15} and N^{15} are compared with the $(\pi^-,\pi N\gamma)$ results. It should be noted that the threshold for neutron emission resulting in a state of O^{15} is ~3 MeV higher than the threshold for proton emission resulting in that state's mirror in N^{15}. This would be a major factor favoring proton emission if dipole states below ~21.5 MeV were preferentially excited by pion scattering. (The threshold for neutron emission resulting in the $5/2^+$ state of O^{15} is 21.5 MeV, for the $3/2^-$ state it is 21.8 MeV, and for the $3/2^+$ state is is 22.1 MeV.[77]) The $3/2^-$ mirror states in N^{15} and O^{15} have the largest cross sections which was also the case for the direct reaction mechanisms. This is to be expected from the one particle-one hole nature of the giant dipole excitation. The decay of the O^{16} giant dipole states also yields a high cross section (relative to the $3/2^-$ states) for excitation of the first $5/2^+$ and $1/2^+$ (unresolved) levels in the two nuclei, in agreement with the $(\pi^-,\pi N\gamma)$ results. The first $3/2^+$ level is seen with strength greater than the $5/2^+$ and $1/2^+$ levels, in disagreement with the pion induced knockout results. Caldwell,

however, published several graphs which indicate that the $3/2^+$ state is not seen significantly in the proton decay of giant dipole states below 22 MeV (this is below the threshold for neutron emission), but the $3/2^-$ and $(5/2^+, 1/2^+)$ states are detected. This is the region with the greatest isospin purity, and the pion may selectively excite these states. Also there are several dipole states in this energy region whose decay leads significantly to the $(5/2^+, 1/2^+)$ levels, a fact which would conform with the spectroscopy of the $(\pi^-,\pi N\gamma)$ reaction if there is a large cross section for giant dipole excitation by pion scattering. Proton emission is favored over neutron emission by the presence of any isospin impurity and also by the threshold effect mentioned above. The decay of the giant dipole states of O^{16} is more likely to populate the ground states of N^{15} and O^{15} than a quasi-free nucleon knockout. (The ground state transition strength for $O^{16*} \longrightarrow O^{15}+p$ is ~1.5 times the $3/2^-$ strength, and for $O^{16*} \longrightarrow O^{15}+n$ it is ~2.8 times the $3/2^-$ strength. This can be compared with the expected value of $S(p_{1/2})/S(p_{3/2}) = .44$ (Section VB) for quasi-free knockout.) One might expect that the same mechanism which gave Tanner a ratio of unity for the (π^-/π^+) neutron knockout ratio would also result in unity for the $\pi^-(O^{15}/N^{15})$ ratio. Tanner's cross sections, however, included knockout reactions resulting in the ground state, and the $(\pi^-,\pi N\gamma)$ cross sections do not. Reactions which populated the ground states with different strengths such as giant dipole excitation may be the origin of the differences in the knockout ratio for the two types of experiment.

A combination of quasi-free knockout and giant dipole excitation in pion scattering could produce the charge dependence of the

reactions reported by Tanner and those in Tables XIII and XIV and also yield relatively strong excitation of the $5/2^+$ levels.

The π^- charge exchange excitation of the analogue dipole states of N^{16}, which would have a probability of 2/9 (= 22%) of the total giant dipole excitation (Eqn. 26), would favor neutron emission. Some of the N^{16} giant dipole states are excited in μ^- capture, and the decay of these states could be similar to the decay of states excited by pion scattering. Figure 17 compares the residual states in N^{15} following μ^- capture with those resulting from the $O^{16}(\pi^-,\pi N\gamma)N^{15}$ reaction. The μ^- capture data was taken by Kaplan et al.[78] It should be noted that the $5/2^+$ excitation is 37% that of the $3/2^-$, but the authors did not correct for gamma branches from higher states. The authors conclude that the relatively stronger excitation of the first $5/2^+$ and $1/2^+$ states is the major difference between the residual states following analogue dipole excitation by μ^- capture and the photoexcitation results of Caldwell.[77]

F. Discussion of States Resulting from Two Nucleon Transfer

Several gamma ray transitions (Tables X and XI) were detected which corresponded to residual states in N^{14} and C^{14} and thus involved the removal of two nucleons from O^{16}. These large cross sections appear to support Tanner's hypothesis of some form of πNN pair interaction. O^{14} has only one bound level, and thus could not be detected by the gamma ray technique. This is unfortunate because it would provide a test of Tanner's assumption that the πNN pair interaction (Section IVE) couples to isospin T = 1 which was based on his failure to detect two neutron removal from C^{12} by π^- scattering (πnn can only couple to T = 2).

The first excited state of N^{14} at 2.313 MeV is an 0^+ state with isospin 1 and a $(p_{1/2})^2$ configuration.[67] The cross section for this level has been corrected for gamma branches from the 3.945 MeV level (96.4% branch) and the 5.106 MeV level (21% branch). It was not possible to correct for branches from the 5.691 MeV level (64% branch) and the 6.198 MeV level, but an inspection of the spectra indicates that transitions from these levels would be negligible contributions to the 2.313 MeV cross section.

The N^{14} 3.945 MeV state with spin and parity 1^+ and isospin 0 is predominately $(p_{3/2},p_{1/2})^{-1}$ [67] but has admixtures arising from the excitation of $p_{3/2}$ particles out of the C^{12} core into higher orbitals.[79] This state has branches for which a correction could not be made from the 7.966 MeV (45% branch), 8.061 MeV (11% branch), 8.617 MeV (24% branch) levels, but these would introduce only a 5% uncertainty in the cross section. The 3.945 MeV state has a 96.4% branch to the 2.313 MeV level, which introduces some uncertainty in the cross section of the 2.313 MeV state.

The cross section for the N^{14} 5.106 MeV level was measured to be 3.9 mb, however, 1.6 mb of this cross section appears to be due to a gamma branch from the 5.833 MeV level (79% branch). The 5.106 MeV level is a 2^- state with a $(p_{1/2},d_{5/2})$ configuration.[67]

Other N^{14} states detected were the 3^- state at 5.833 MeV (σ = 2.0 mb) and the 3^+ state at 6.444 MeV (σ = 1.0 mb). The 6.444 MeV state has no branches from higher levels, but the 5.833 MeV state has a 90% branch[32] from the 8.907 MeV level, for which no upper limit could be determined. The 8.907 MeV level is above the threshold for proton emission, and it is likely that the gamma branch is small.

Gamma rays from two excited states of C^{14} were detected. The 6.728 MeV 3^- state was found to have $\sigma = 1.3 \pm .5$ mb. This level has a 35% branch[38] from the 2^- state at 7.341 MeV so there is some uncertainty in this cross section. The 6.901 MeV 0^- state had a cross section of $2.1 \pm .9$ mb. This level has no gamma branches from higher states. The 6.728 MeV state and the 6.901 MeV state are the analogue states of the N^{14} 8.907 MeV and 8.80 MeV states respectively. The C^{14} ground state is the analogue of the N^{14} 2.313 MeV level which had a relatively high cross section.

G. Spectroscopy of Two Nucleon Removal

The discussion of Section VF indicated relatively large cross sections for pion induced two nucleon knockout. Tanner proposed that at the (3,3) resonance a pion might have a quasi-free interaction with a nucleon pair instead of with a single nucleon. Another mechanism for two nucleon removal would be N^* re-scattering resulting in absorption of the pion (Section IVF). A third possibility is that pion scattering may start an intranuclear cascade resulting in the evaporation of one or more nucleons from the nucleus.

If the pion induced two nucleon removal process occurs through a direct interaction, then one would expect the spectroscopy to be similar to other direct processes. Unfortunately the two nucleon transfer process is more complex than the single nucleon process, and theoretical treatments have met with less success. Towner and Hardy[80], in a recent review, discuss several factors which enter into the two nucleon transfer process for conventional nuclear probes.

The spectroscopic factor (the wave function overlap of nucleus A and nucleus A-2) is analogous to the single nucleon spectroscopic factors discussed in Section IVC. Cohen and Kurath[81] have computed theoretical two nucleon transfer spectroscopic factors which are computed in terms of two nucleon coefficients of fractional parentage (2 CFP) defined analogously to the single nucleon CFP (Section IVC)

$$\left\langle IT\ \alpha\{|I_0T_0\alpha_0, J\Delta\beta\right\rangle \tag{43}$$

where I is spin, T is isospin, α represents the remaining quantum numbers, and the transferred nucleons are coupled to angular momentum J, isospin Δ, and β refers to the nature $(n_1l_1j_1,\ n_2l_2j_2)$ of the transferred nucleons. The two nucleon spectroscopic factors are written

$$S_{fi} = 1/2N(N-1)\left\langle IT\alpha(N)\{|I_0T_0\alpha_0(N-2),\ J\Delta\beta\right\rangle^2 \tag{44}$$

The factor $1/2N(N-1)$ is the number of nucleon pairs in the shell.

Cohen and Kurath[81] have calculated the spectroscopic factors for two nucleon transfer from O^{16} using 2 CFP's computed making use of intermediate coupling wave functions. They compute S = 2.212 for excitation of the 0^+, T = 1, 2.313 MeV level and a total S = 2.756 for the 1^+, T = 0, 3.945 MeV level. The ratio of the two spectroscopic factors is $R(0^+/1^+) = .80$.

Another term which enters in the two particle transfer cross section is, in the notation of Towner[80], D(S,T) which is dependent on the strength of the spin and isospin exchange terms between the nucleons in the incoming particle and the two transferred nucleons. Its effect

would be to reduce the S = 1 (T = 0) term more than the S = 0 (T = 1) term. Generally this term is difficult to determine theoretically and must be deduced experimentally. For example, Hardy[82] found that the ratio D(1,0)/D(0,1)~.33 for the $O^{16}(p,He^3)N^{14}$ reaction. The pion is not identical with the nucleon, and there would be no exchange term equivalent to D(S,T) for the $(\pi^-,\pi NN)$ reaction. It will enter into the conventional two nucleon transfer reactions, and thus the magnitude of the cross sections from various two nucleon transfer reactions cannot be compared directly.

The light particle spectroscopic factor, which is essentially the overlap of the initial and final wave functions of the incoming and outgoing particles, will also be a factor in the two nucleon transfer cross sections. Towner and Hardy[80] give expressions for this term for the usual pickup reactions. For the pion-2 nucleon knockout case, the light particle spectroscopic factor would include a 6-j symbol for coupling the isospins of the two nucleons with the pion.

The factors which enter into the two nucleon transfer processes make comparison among various reactions difficult. There is some value in comparing different experimental results, however, because Cohen and Kurath[81] compute zero values for the spectroscopic factors for several states which are detected in the $O^{16}(a,b)N^{14*}$ reactions. The relative intensities resulting from two nuclear transfer reactions are compared in Fig. 18. Pehl et al.[83] have measured the relative cross sections for excitation of N^{14} states in the $O^{16}(d,\alpha)N^{14}$ process. The ground state of O^{16} is T = 0 and both the deuteron and the alpha particle have T = 0; thus, the isospin change in this reaction must be zero and

the 2.313 MeV state would not be excited. Both T = 0 and T = 1 states in N^{14} have large cross sections in the π-knockout results, indicating that there are no strong isospin selection rules for this process. The (p,He^3) reaction[83] proceeds through the singlet or triplet S states, and thus the isospin change is Δ = 0 or 1. The (p,pNNγ) results compared in Fig. 18 are from the 600 MeV proton experiment discussed in Section IIIJ. One can conclude that there is qualitative agreement between the particular states seen in both the $(\pi^-,\pi NN\gamma)$ reaction and the other reactions which are assumed to be direct. The relative intensities of the states excited vary greatly, but this would be expected due to the variation of the factors entering into the cross sections.

One can compare the ratio of the excitation of the 1^+ state at 3.945 MeV to that of the 0^+ at 2.313 MeV. For the (p,pNNγ) results $R(0^+/1^+)\sim 1.$ and for (p,He^3), $R(0^+/1^+)\sim .7$. (Excitation of the 2.313 MeV level is forbidden for (d,α) by the selection rules.) The theoretical spectroscopic factor[81] ratio is $S(0^+)/S(1^+)\sim .8$ which is in reasonable agreement with the above. The ratio of the $(\pi^-,\pi NN\gamma)$ cross sections is $R(0^+/1^+) = .39 \pm .22$, but the effect of the isospin coupling in the light particle spectroscopic factor has not been considered. Problems involving the coupling of three angular momenta (and by analogy, the coupling of three isospins) are treated using 6-j symbols. The isospins of the two nucleons are first coupled to $T_{NN} = 0$ or 1 and then coupled to the isospin of the pion resulting in a particular value of $T_{\pi NN}$. If two nucleons coupled to $T_{NN} = 0$ are knocked out, then the residual nucleus will be left in a T = 0 state such as the 1^+, T = 0 state at 3.945 MeV. Similarly, knockout of two nucleons coupled to $T_{NN} = 1$ could lead to

the 0^+, T = 1 state at 2.313 MeV. The cross section for each reaction will be proportional to the fourth power of the corresponding 6-j symbol. Thus, the ratio of the excitation of the 0^+ state to the 1^+ state should be equal to the product of the ratio of the spectroscopic factors[81] (~.8) and the fourth power of the ratio of the 6-j symbols. The assumption of a $T_{\pi NN}$ = 1 pair interaction yields a prediction of $R(0^+/1^+)\sim.45$ in good agreement with the experimental value of $R(0^+/1^+) = .39 \pm .22$. T = 0 coupling is not likely because it does not involve the (3,3) resonance. For a T = 2 reaction, the isospins could not couple to give the 0^+ state. Thus, a πNN pair interaction coupled solely to T = 2 can be ruled out. It can be concluded that the results are not incompatible with a pure T = 1 pair interaction.

The contribution of pion absorption to the neutron + proton transfer process may be investigated by comparing N^{14} states in the Coincidence spectra with those in the Non-coincidence spectra (Section III-I). If the pion is absorbed on a pn pair, then the two neutrons would be emitted with a low probability of being detected in the scattering counters. Thus the corresponding gamma event would not appear in the coincidence spectrum. The ratio of σ(Coincidence)/σ(Non-coincidence) is ~.46 ± .07 for the 3.945→2.313 MeV transition. This can be compared with an expected value of ~.43 based on the ratio of the $123\overline{\text{Anti}}$ + scattering counter rate to the rate of the $123\overline{\text{Anti}}$ + no scattering counter. The ratio of the total counts in the Coincidence spectrum to the total counts in the Non-coincidence spectrum was ~.52. This indicates that the pion absorption process does not appear to be a significant contributor to the πNN interaction.

H. Multiple Nucleon Knockout Reactions

The spectra contained several gamma peaks which corresponded to π-knockout of more than two nucleons from O^{16}. The C^{13} 3.854 MeV $5/2^+$ level was detected with a cross section of 6.6 mb. Transitions from the 3.684 MeV $3/2^-$ level were also detected, however, this appears to be due primarily to the 37% branch to this level from the 3.854 MeV state. All higher energy levels are unbound, so these cross sections are not ambiguous. There are no bound excited states of N^{13}, so the analogue to the C^{13} 3.854MeV state could not be detected.

Because of the high cross section for the (n,α) reaction, it is probable that contamination from secondary neutrons would contribute to the C^{13} cross sections. The cross section for a pion reaction resulting in one or more neutrons being emitted was estimated to be ~100 mb (the total inelastic π^- cross section on O^{16} is ~350 mb). From this, the neutron flux in the target was computed. An upper limit on the neutron induced contamination of the C^{13} 3.854 MeV cross section was then determined to be ~2.7 mb using the (n,α) cross sections of B. Leroux et al.[84]. Because this is an upper limit on the neutron contamination, no correction was made to the 3.854 MeV cross section.

Balashov et al.[85] has calculated spectroscopic factors for quasi-free knockout of He^3 and α particles from 1p shell nuclei. Their results for the $O^{16}(p,pHe^3)C^{13}$ reaction, which were published in the form of an excitation graph, indicate spectroscopic factors for the 3.684 and 3.854 MeV levels (they are not resolved) which are ~2.5 times the ground state strength. There is no indication of any strength for the 3.086 MeV level in their calculations, and this was found to be the case in the π-knockout results. ($\sigma < .8$ mb for the 3.086 MeV state)

Balashov[85] also calculated spectroscopic factors for quasi-elastic knockout of α particles by protons resulting in S = 1.031 for the first excited state of C^{12} (4.439 MeV). The π-knockout experiment measured $\sigma(C^{12}$ 4.439 MeV)~16.8 ± 6.4 mb although the reliability of this number is questionable due to background uncertainties (Section IIIG). Comparing the π-knockout results with Balashov's calculation is not a certain procedure because of the unknown factors such as the light particle spectroscopic factors which would be dependent on the isospin coupling. Despite this uncertainty, the high cross section for C^{12} and C^{13} levels appears to give support to the quasi-free treatment of the pion induced knockout reactions.

I. Inelastic Scattering and Charge Exchange

A cross section of 12.5 ± 2.8 mb was measured for inelastic excitation of the 6.135 MeV 3^- state in O^{16}. This level has a $(1p_{1/2})^{-1}$ $(d_{5/2})^1$ configuration. It has a 76% branch from the 8.88 MeV 2^- level which was found to have an upper limit of .9 mb. The branching ratio information on this nucleus is limited, and no other gamma assignments could be made. The cross section for neutron excitation of the 3^- state in O^{16} is large[86]. A calculation with the assumptions regarding the neutron flux of Section VH resulted in an upper limit of 3.0 mb for the neutron contamination of the cross section for this state.

Inelastic scattering data taken at the (3,3) resonance such as the $C^{12}(\pi^-,\pi^-)C^{12}$ results of Stroot[2] have been successfully analyzed using the Kisslinger[87] non-local potential (which should be valid for pions below 100 MeV) and the Glauber multiple scattering formalism[88,89,90]

(valid above 500 MeV). Ericson and Hüfner[91] have also treated pion inelastic scattering at this energy with a simple model characterizing the nucleus as a slab of material with a given refractive index.

It has been observed[92] that inelastic scattering exhibits qualitative similarity in the relative intensity of excitation of states of the target nucleus independent of the projectile scattered, provided it has sufficient energy for a direct interaction. Because the incident projectile tends to preferentially excite the collective modes of the target nucleus, the spectrum of states excited is more characteristic of the target nucleus than the projectile type. Crawley and Garvey[92] publish an expression for the differential cross section in the distorted-wave-Born approximation

$$\frac{d\sigma}{d\Omega} = \left(\frac{M}{2\pi h}\right)^2 \frac{k_f}{k_i} \frac{2J_f + 1}{2J_i + 1} \sum_{l,m} \frac{|\beta lm|^2}{2l + 1} \qquad (45)$$

where k_i and k_f refer to the relative momenta of the system in the initial and final states, M is the reduced mass and $\beta_{lm}{}^2$ may be related to the reduced electromagnetic transition probability for decay of the state excited. One can use Eqn. 45 to predict the cross section for $\pi^- - O^{16}$ inelastic scattering leading to the 3^- state relative to the cross section for $\pi^- C^{12}$ 2^+ excitation. Using experimental numbers for the reduced electromagnetic transition probability in Eqn. 45 results in the prediction $\sigma(O^{16}3^-) \sim 2.1\sigma(C^{12}2^+)$. Stroot[2] measured differential cross sections for π^- excitation of the 2^+ state in C^{12}. A crude integration over his cross sections yields $\sigma(C^{12}2^+) \sim 8.8$ mb. The cross section for the $O^{16}3^-$ state is reported in Table XIII to be 12.5 ± 2.8 mb so the

ratio of the two cross sections is in reasonable agreement with Eqn. 45. The observation of the insensitivity of the inelastic scattering mechanism to the type of projectile appears to be valid for pions also.

Several gamma transitions were detected which correspond to charge exchange reactions resulting in excited states of N^{16}. The N^{16} states seen were the .298 MeV 3^-(.33 ± .08 mb) and the .398 MeV 1^-(.60 ± .19 mb) levels. There are no higher energy bound states of N^{16}, so these cross sections would not be uncertain due to branches from other states. The probability of contamination of these cross sections by secondary neutron effects is large. There are no published $O^{16}(n,p)$ cross sections for excitation of particular states of N^{16} but using cross sections[93] for all states of N^{16} results in a contamination of ~1 mb. Without $O^{16}(n,p)N^{16}$ cross sections for specific states in N^{16}, the measured cross sections for the $O^{16}(\pi^-,\pi^o)N^{16}$ reaction must be treated as being very doubtful.

An $N^{15}(d,p)N^{16}$ experiment found "reduced widths" of $(2J + 1)\theta^2 = .33$ for the .298 MeV level and .58 for the .398 MeV level. This is compatible with the ratio of the cross sections for the two states in the pion charge exchange scattering. The analogue states to the N^{16} .298 MeV and .398 MeV levels in O^{16} could not be detected due to uncertainties in the decay schemes of the higher energy levels of O^{16}.

J. Conclusion

Generally the experimental results support a quasi-free treatment for π-nucleus interactions at the (3,3) resonance. The spectroscopic factors for single nucleon removal resulting from reactions

thought to be direct are in good agreement with the pion induced knockout cross sections leading to excited states in O^{15} and N^{15}, although the $5/2^+$ is excited considerably more strongly than expected. The $\pi^- O^{16} \rightarrow O^{15}/N^{15}$ knockout ratio is at variance with a quasi-free interpretation. Significant excitation of the O^{16} and N^{16} giant dipole states would explain this difference. The relatively large cross sections for excitation of the $5/2^+$ mirror states may be interpreted as evidence of strong giant dipole excitation. A pion-nucleon pair interaction in which one of the nucleons is raised to the $d_{5/2}$ shell and the other escapes the nucleus would also result in a relatively large cross section for the $5/2^+$ states.

There is a significant cross section for two nucleon knockout reactions leading to excited states of N^{14} and C^{14}. Tanner[12] had proposed that the pion at the (3,3) resonance may interact with nucleon pairs in order to explain the ratio of π^-/π^+-neutron knockout results. His data suggested that the reaction goes primarily through the T = 1 channel. This proposal was supported by the relative excitation of the first and second excited states of N^{14} following two nucleon knockout from O^{16}. The two nucleon knockout reactions were relatively strong, with cross sections comparable to the single nucleon knockout cross sections. The relative excitation of states in N^{14} agreed with other two nucleon transfer reactions. Cross sections were measured corresponding to He^3 and α particle knockout. Generally the spectroscopy of the states excited by multiparticle knockout was compatible with a direct reaction interpretation.

VI. TABLES

TABLE

XIV. Cross sections for π^- charge exchange scattering leading to excited states of N^{16}.

XV. Scattering counter data.

XVI. Relative cross sections for the (p,pN) reaction leading to excited states of N^{15} and O^{15}.

XVII. Relative cross sections for the (p,p2N) reaction leading to excited states of N^{14}.

Table I - Results of $\pi^{\pm}$ activation experiments of Tanner et al.[1]

Ratios of cross sections for pion reactions at 180 MeV.

Target	Product	Ratio $\sigma(\pi^-):\sigma(\pi^+)$
^{12}C	^{11}C	0.97±.09
^{14}N	^{13}N	0.96±.09
^{16}O	^{15}O	1.02±.09

Cross sections for pion reactions at 180 MeV.

Target	Product	Reaction	Cross section (mb)
^{12}C	^{11}C	$(\pi^+, \pi^+n + \pi^op)$	75. ±4.
^{14}N	^{13}N	$(\pi^+, \pi^+n + \pi^op)$	56. ±6.
^{16}O	^{15}O	$(\pi^+, \pi^+n + \pi^op)$	41. ±4.
^{10}B	^{10}C	(π^+, π^o)	1.3 ±0.2
^{11}B	^{11}C	(π^+, π^o)	5.3 ±0.9
^{13}C	^{13}N	(π^+, π^o)	3.3 ±1.0
^{14}N	^{14}O	(π^+, π^o)	≦0.05
^{18}O	^{18}F	(π^+, π^o)	3.5 ±0.7
^{11}B	^{11}Be	(π^-, π^o)	≦0.5
^{19}F	^{19}O	(π^-, π^o)	1.3 ±0.6
^{18}O	^{18}Ne	(π^+, π^-)	≦0.1
^{12}C	^{10}C	$(\pi^+, \ )$	4.9 ±0.5
^{12}C	^{10}C	$(\pi^-, \ )$	≦0.5
^{10}B	$^{8}B, ^{8}Li$	$(\pi^+, \ )$	5.8 ±1.6
^{10}B	$^{8}Li, ^{8}B$	$(\pi^-, \ )$	5.1 ±2.4
^{11}B	^{10}C	$(\pi^+, \ )$	0.85±0.3

Table II - Gamma rays of known energy used to calibrate the Ge(Li) spectrometer. The last column indicates the energy computed using the calibration procedure described in Section IIF.

SOURCE	ENERGY (MeV)	FITTED ENERGY (MeV)
Positron Annihilation	.511	.511
Co^{60}	1.173	1.173
Co^{60}	1.332	1.332
Th^{228} (Second Escape)	1.592	1.593
Th^{228} (First Escape)	2.103	2.104
Th^{228} (Photo)	2.614	2.615
N^{15} $(5/2^+)$ (Second Escape)	4.248	4.247
O^{16} (3^-) (Second Escape)	5.113	5.110
O^{16} (3^-) (First Escape)	5.624	5.623
O^{16} (3^-) (Photopeak)	6.135	6.137

Table III - The parameters listed below were used to calculate the energy calibration (Section IIF).

	BIGGERSTAFF CALIBRATION[a]	TENNELEC CALIBRATION[b]
C1	$.22509 \times 10^{-2}$	$.105774 \times 10^{-2}$
C2	$.15381 \times 10^{-7}$	$.636513 \times 10^{-8}$
C3	-.22039	$-.177905 \times 10^{0}$
D1	.54937	$.117432 \times 10^{-1}$
D2	$-.956218 \times 10^{-1}$	$-.132882 \times 10^{-1}$

[a] This set of parameters was determined using the data from the Biggerstaff pulser and was used to compute the energy calibration for the region below 3.5 MeV.

[b] This set of parameters was determined using the data from the Tennelec 800 pulser and was used to compute the energy calibration for the region above 3.5 MeV.

Table IV - Relative efficiency data for Ge(Li) spectrometer determined from π-mesic X-ray yields[21] in Pb^{208}, Sn^{120} and Ce^{140}.

ELEMENT	TRANSITION	ENERGY (MeV)	RELATIVE INTENSITY	% ERROR
Sn^{120}	$4f_{7/2} - 3d_{5/2}$	.345	2.366	5.7
Sn^{120}	$4f_{5/2} - 3d_{3/2}$	.350	2.42	6.2
Ce^{140}	$2p_{3/2} - 1s$	.474	2.07	6.8
Pb^{208}	$4f_{5/2} - 3d_{3/2}$	.937	.75	5.1
Pb^{208}	$4f_{7/2} - 3d_{5/2}$	.970	.758	5.1
Sn^{120}	$3d_{5/2} - 2p_{3/2}$	.980	.827	5.8
Sn^{120}	$3p_{3/2} - 2p_{1/2}$	1.022	.97	5.8
Ce^{140}	$3d_{3/2} - 2p_{1/2}$	1.303	.618	7.2
Ce^{140}	$3d_{5/2} - 2p_{3/2}$	1.313	.716	5.8
Pb^{208}	$3d_{5/2} - 2p_{3/2}$	2.5	.306	5.1
Pb^{208}	$3d_{3/2} - 2p_{1/2}$	2.641	.341	5.4
Sn^{120}	$2p_{1/2} - 1s$	3.41	.225	6.0
Sn^{120}	$2p_{3/2} - 1s$	3.45	.192	5.5
Ce^{140}	$2p_{1/2} - 1s$	4.172	.108	12.4
Pb^{208}	$2p_{1/2} - 1s$	5.778	.1	6.2
Pb^{208}	$2p_{3/2} - 1s$	5.963	.115	5.3

Table V - Relative efficiency data for Ge(Li) spectrometer determined using a Co^{56} source[21]

ENERGY (MeV)	INTENSITY
.847	1.
1.038	.82
1.238	.64
1.360	.68
1.771	.48
2.015	.44
2.035	.44
2.599	.29
3.202	.24
3.254	.22
3.273	.27

Table VI - Relative efficiency parameters

	π-MESIC X-RAY DATA[a]	Co^{56} DATA[b]	ABSOLUTE EFFICIENCY[c]
C1	.863±.031	.851±.018	$1.014 \times 10^{-4} \pm .00278 \times 10^{-4}$
C2	-1.036±.039	-1.019±.046	-1.036 (fixed)

[a] Results of a least squares fit to the π-mesic x-ray relative efficiency data.

[b] Results of a least squares fit to the Co^{56} relative efficiency data.

[c] Results of a least squares fit to the absolute efficiency data (Table VII) with the value of the C2 parameter fixed at the value determined in the π-mesic x-ray efficiency fit.

Table VII - Calibrated sources used for absolute efficiency determination

SOURCE	ENERGY (MeV)	ACTIVITY CORRECTED TO 7/26/70 (μ Ci)	% GAMMA EMITTED PER DISINTEGRATION	COMPUTED ABSOLUTE EFFICIENCY
Y^{88}	.898	2.52	91.4	1.245×10^{-4}
Co^{60}	1.173	9.76	99.74	$.815 \times 10^{-4}$
Na^{22}	1.274	7.82	99.95	$.780 \times 10^{-4}$
Co^{60}	1.332	9.77	99.85	$.732 \times 10^{-4}$
Y^{88}	1.836	2.75	99.4	$.627 \times 10^{-4}$

Table VIII - Cross sections for the $O^{16}(\pi^-,\pi N\gamma)$ reaction leading to excited states of N^{15}.

STATE (MeV)[32]	SPIN AND PARITY[32]	CONFIGURATION[67]	CROSS SECTION (mb)
.0	$1/2^-$	$(p_{1/2})^{-1}$	*
5.270	$5/2^+$	$(p_{1/2})_0{}^2d_{5/2}$	3.5 ± 1.1
5.299	$1/2^+$	$(p_{1/2})_0{}^2s_{1/2}$	*
6.323	$3/2^-$	$(p_{3/2})^{-1}$	9.1 ± 2.5
7.155	$5/2^+$	$(p_{1/2})_1{}^2d_{5/2}$	.7 ± .2
7.301	$3/2^+$	$(p_{1/2})_1{}^2s_{1/2}$	*
7.566	$7/2^+$	$(p_{1/2})_1{}^2d_{5/2}$	<.8
8.313	$1/2^+$	$(p_{1/2})_1{}^2s_{1/2}$	<.4
8.576	$3/2^+$	$(p_{1/2})_1{}^2d_{5/2}$	*
9.053	$1/2^+$		<.8
9.155 (State 2)[34]	(5/2)		<.5
9.225	≤5/2		<.4
9.762	$5/2^-$		<.6
9.829	7/2		*
9.929	$(1/2^+,3/2^+)$		<.6
10.070	$3/2^+$		<.5
10.451	3/2,5/2,7/2		1.0 ± .4
10.800	$3/2^{(-)}$		*

$$\sigma(5.270\ \text{MeV})/\sigma(6.323\ \text{MeV}) = .39 \pm .11$$

* indicates that no upper limit could be determined for the cross section for this state.

Table IX - Cross sections for the $O^{16}(\pi^-,\pi^-n\gamma)$ reaction leading to excited states of O^{15}.

STATE (MeV)[32]	SPIN AND PARITY[32]	CONFIGURATION[67]	CROSS SECTION (mb)
0.	$1/2^-$	$(p_{1/2})^{-1}$	*
5.181	$1/2^+$	$(p_{1/2})_0{}^2s_{1/2}$	*
5.242	$5/2^+$	$(p_{1/2})_0{}^2d_{5/2}$	2.1 ± .9
6.177	$3/2^-$	$(p_{3/2})^{-1}$	15.6 ± 3.8
6.788	$3/2^+$	$(p_{1/2})_1{}^2s_{1/2}$	<.6
6.859	$5/2^+$	$(p_{1/2})_1{}^2d_{5/2}$	*
7.276	$7/2^+$	$(p_{1/2})_1{}^2s_{1/2}$	.8 ± .3
7.552	$1/2^+$	$(p_{1/2})_1{}^2d_{5/2}$	*
8.283	$3/2^+$		<.5
8.739	$1/2^+$		*
8.918	3/2		*
8.978	$(1/2,3/2)^-$		<.6

$$\sigma(5/2^+)/\sigma(3/2^-) = .13 \pm .04$$

* indicates that no upper limit could be determined for the cross section for this state.

Table X - Cross sections for the $O^{16}(\pi^-,\pi NN\gamma)$ reaction leading to excited states of N^{14}.

STATE (MeV)[32]	SPIN AND PARITY[32]	CONFIGURATION[67]	CROSS SECTION (mb)
0.	1^+	$(p_{1/2})^2$	*
2.313	0^+, T=1	$(p_{1/2})^2$	6.3 ± 3.6
3.945	1^+	$(p_{3/2}, p_{1/2})^{-1}$	16.4 ± 3.5
4.913	$(0,1)^-$	$(p_{1/2}, s_{1/2})$	*
5.106	2^-	$(p_{1/2}, d_{5/2})$	2.3 ± 1.6
5.691	1^-	$(p_{1/2}, s_{1/2})$	*
5.833	3^-	$(p_{1/2}, d_{5/2})$	2.0 ± .7
6.198	1^+	$(s_{1/2})^2$	*
6.444	3^+	$(s_{1/2}, d_{5/2})$	1.0 ± .8
7.028	2^+	$(p_{3/2}, p_{1/2})^{-1}$	<.6
7.966	$2^{(-)}$		<.9
8.061	1^-, T=1		<.5
8.489	(4^-)		<1.2
8.617	0^+, T=1		<.1
8.80	0^-, T=1		*
8.907	3^-, T=1		*
8.963	5^+		*
9.129	2^-		*
9.172	2^+, T=1		*
9.508	2^-, T=1		*

$$\sigma(3.945 \text{ MeV})/\sigma(2.313 \text{ MeV}) = .39 \pm .22$$

* indicates that no upper limit could be determined for the cross section for this state.

Table XI - Cross sections for the $O^{16}(\pi^-,\pi NN\gamma)$ reaction leading to excited states of C^{14}.

STATE (MeV)[32]	SPIN AND PARITY[32]	CROSS SECTION (mb)
0.	0^+, T=1	*
6.093	1^-	*
6.589	0^+	*
6.728	3^-	1.3 ± .5
6.901	0^-	2.1 ± .9
7.012	2^+	<.6
7.341	2^-	*

Table XII - Cross sections for the $O^{16}(\pi^-,\pi X\gamma)$ reaction leading to excited states of C^{13} and C^{12}.

STATE (MeV)[32]	SPIN AND PARITY[32]	CROSS SECTION (mb)
C^{13} 3.086	$1/2^+$	<.8
C^{13} 3.684	$3/2^-$	.4 ± 1.0
C^{13} 3.854	$5/2^+$	6.6 ± 1.6
C^{12} 4.439	2^+	16.8 ± 6.4

* indicates that no upper limit could be determined for the cross section for this state.

Table XIII - Cross sections for π^- inelastic scattering leading to excited states of O^{16}.

STATE (MeV)[28]	SPIN AND PARITY[28]	CROSS SECTION (mb)
0.	0^+	*
6.056	0^+	*
6.135	3^-	12.5 ± 2.8
6.920	2^+	≤1.1
7.115	1^-	*
8.88	2^-	≤.9

Table XIV - Cross sections for π^- charge exchange scattering leading to excited states of N^{16}.

STATE (MeV)[43]	SPIN AND PARITY[43]	CONFIGURATION[94]	CROSS SECTION (mb)
0.	2^-	$(p_{1/2})^{-1}d_{5/2}$	*
.120	0^-	$(p_{1/2})^{-1}2s_{1/2}$	*
.298	3^-	$(p_{1/2})^{-1}d_{5/2}$	.33 ± .08
.398	1^-	$(p_{1/2})^{-1}2s_{1/2}$	.60 ± .19

* indicates that no upper limit could be determined for the cross section for this state.

Table XV - Scattering Counter Data

Relative cross sections for gamma transitions in coincidence with an event in the scattering counters.

	$\frac{\sigma(O^{15}\ 6.177\ MeV)}{\sigma(N^{15}\ 6.323\ MeV)}$
Counter C	2.1 ± 1.0
Coincidence Counters (Total)	2.0 ± .6
Non-Coincidence (Total)	1.8 ± .3
Total	1.8 ± .4

Comparison of the cross section for a particular gamma transition in the Coincidence spectrum with the cross section for the same transition in the Non-coincidence spectrum.

Transition	$\frac{\sigma(Coincidence)}{\sigma(Non\text{-}Coincidence)}$
N^{14}(3.945 MeV → 2.313 MeV)	.46 ± .07
C^{13}(3.854 MeV)	.54 ± .11

Table XVI - Relative cross sections for the (p,pN) reaction leading to excited states of N^{15} and O^{15}.

STATE (MeV)	RELATIVE CROSS SECTION[a]
N^{15} 5.270	3.7
N^{15} 6.323	11.5
N^{15} 7.155	.7
N^{15} 10.451	1.0
O^{15} 5.242	2.6
O^{15} 6.177	9.7
O^{15} 6.788	1.7
O^{15} 7.276	1.9

[a] The normalization of these relative cross sections is such that the sum of all cross sections in the proton work leading to excited states of N^{15} and O^{15} is equal to the sum of all the cross sections in the $(\pi^-,\pi N\gamma)$ work leading to excited states of N^{15} and O^{15} (Tables VIII and IX).

Table XVII - Relative cross sections for the (p,p2N) reaction leading to excited states of N^{14}.

STATE (MeV)	RELATIVE CROSS SECTION[a]
2.313	11.2
3.945	11.3
5.106	.4
5.833	3.4
6.444	1.6

[a] The normalization of these relative cross sections is such that the sum of all cross sections in the proton work leading to excited states of N^{14} is equal to the sum of all the cross sections in the $(\pi^-,\pi NN\gamma)$ experiment leading to excited states of N^{14} (Table X).

VII. ACKNOWLEDGMENTS

The author would like to acknowledge the following persons for their assistance:

Dr. Herbert O. Funsten, his advisor, for his interest and guidance during all phases of this research and his suggestions and encouragement in the preparation of the manuscript.

Drs. William J. Kossler and John R. Kane for helpful discussions and reading the manuscript.

Drs. Robert T. Siegel, Rolf G. Winter and Richard L. Kiefer for reading the manuscript and offering useful suggestions.

Mr. James G. Batterson for his help in the accumulation of the data and the preparation of the manuscript.

Dr. William F. Lankford for many useful discussions and for his assistance with the data accumulation.

Mr. Stanley G. Hummel and the Physics Department Machine Shop for construction of the scintillation counters and the experimental apparatus.

Mr. Donald S. Makowiecki for his assistance with the electronics.

The staff of the William and Mary Computer Center for their help during the analysis of the data.

The staff of the Space Radiation Effects Laboratory for their efficient operation of the synchrocyclotron.

Miss Dianne Britton for typing the manuscript.

Miss Frances Ware for typing preliminary drafts of the manuscript.

This work was supported in part by the National Aeronautics and Space Administration and the National Science Foundation.

VIII. FOOTNOTES AND REFERENCES

1. D. T. Chivers, E. M. Rimmer, B. W. Allardyce, R. C. Witcomb, J. J. Domingo, and N. W. Tanner, Nucl. Phys. A126, 129 (1969).
2. F. Binon, P. Duteil, J. P. Garron, J. Gorres, L. Hugon, J. P. Peigneux, C. Schmit, M. Spighel, and J. P. Stroot, Nucl. Phys. B17, 168 (1970).
3. C. Zupancic, Proc. Symposium on the Use of Nimrod for Nuclear Structure Physics, RHEL/R166, (1968) p. 67.
4. A. O. Aganyants, Yu. D. Bayukov, V. N. Deza, S. V. Donskov, V. B. Fedorov, N. A. Ivanova, V. D. Khovansky, V. M. Kolybasov, G. A. Leksin, V. L. Stolin, L. S. Vorobyev, Nucl. Phys. B11, 79 (1969).
5. Paul L. Reeder and Samuel S. Markowitz, Phys. Rev. 133, B639 (1964).
6. Los Alamos Meson Physics Facility (LAMPF), Tri-University Meson Facility at Vancouver (TRIUMF), Swiss Institute for Nuclear Research (SIN), and Joint Institute for Nuclear Research at Dubna, U.S.S.R.
7. D. H. Wilkinson, Comments Nuclear Particle Phys. 1, 169 (1967).
8. C. Zupancic, High Energy Physics and Nuclear Structure, edited by G. Alexander (North-Holland Publishing Co., Amsterdam, 1967) p. 171.
9. J. P. Stroot, Proc. Symposium on the Use of Nimrod for Nuclear Structure Physics, RHEL/R166, (1968) p. 81.
10. N. W. Tanner, High Energy Physics and Nuclear Structure, edited by S. Devons (Plenum Press, New York, 1970) p. 346.

11. N. W. Tanner, Proc. Symposium on the Use of Nimrod for Nuclear Structure Physics, RHEL/R166, (1968) p. 91.

12. D. T. Chivers, J. J. Domingo, E. M. Rimmer, R. C. Witcomb, B. W. Allardyce, and N. W. Tanner, Phys. Lett. 26B, 573 (1968).

13. V. M. Kolybasov, J. Nucl. Phys. (U.S.S.R.) 2, 144 (1965).

14. B. J. Lieb, H. O. Funsten, and W. F. Lankford, A.P.S. Bulletin, Series II, 15, 596 (1970).

15. J. Lieb and H. Funsten, High Energy Physics and Nuclear Structure, edited by S. Devons (Plenum Press, New York, 1970) p. 458.

16. C. B. Spence, private communication.

17. The 3 body final state phase space calculation made use of program ATHOS from the CERN Program Library (W 501) written by M. Horowitz.

18. D. Robson, "Final State Interactions and the Charge Dependence of (π,πN) Reactions from Nuclei", Florida State University (Tallahassee, Florida) preprint.

19. P. W. Hewson, Nucl. Phys. A133, 659 (1969).

20. H. L. Gelernter, J. Birnbaum, M. Mikelsons, J. D. Russell, F. Cochrane, D. Groff, J. F. Schofield, and D. A. Bromley, Nucl. Instr. and Meth. 54, 77 (1967).

21. P. Martin, private communication.

22. J. Hüfner, Z. Physik 190, 81 (1966).

23. J. L. Black and W. Gruhle, Nucl. Instr. and Meth. 46, 213 (1967).

24. E. Storm and H. Israel, Nuclear Data Tables A7, 565 (1970).

25. J.Kopecký, W. Ratyński, and E. Warming, Nucl. Instr. and Meth. 50, 333 (1967).

26. R. H. Moore and R. K. Zeigler, LA-2367, Los Alamos Scientific Laboratory, (1959).

27. D. H. Wilkinson, Nuclear Spectroscopy, edited by F. Ajzenberg-Selove Academic Press, New York, 1960) part B, p. 852.

28. S. J. Skorka, J. Hertel, and T. W. Retz-Schmidt, Nuclear Data, (Section A) 2, 347 (1966).

29. R. C. Allen, R. E. Carter, H. L. Taylor, Fast Neutron Physics, edited by J. B. Marion and J. L. Fowler (Interscience Publishers, New York, 1963) p. 1429.

30. E. K. Warburton, J. W. Olness, and D. E. Alburger, Phys. Rev. 140, B1202 (1965).

31. G. W. Phillips, F. C. Young, and J. B. Marion, Phys. Rev. 159, 891 (1967).

32. F. Ajzenberg-Selove, Nucl. Phys. A152, 1 (1970).

33. E. K. Warburton, K. W. Jones, D. E. Alburger, C. Chasman, and R. A. Ristinen, Phys. Rev. Lett. 14, 146 (1965).

34. C. E. Steerman and F. C. Young, Phys. Lett. 27B, 8 (1968).

35. R. R. Carlson, Phys. Rev. 148, 991 (1966).

36. K. W. Allen, T. K. Alexander, and D. C. Healey, Can. J. Phys. 46, 1575 (1968).

37. S. Gorodetzky, R. M. Freeman, A. Gallmann, and F. Haas, Phys. Rev. 149, 801 (1966).

38. D. E. Alburger, A. Gallmann, J. B. Nelson, J. T. Sample, and E. K. Warburton, Phys. Rev. 148, 1050 (1966).

39. F. Riess, P. Paul, J. B. Thomas, and S. S. Hanna, Phys. Rev. 176, 1140 (1968).

40. D. H. Wilkinson, D. E. Alburger, and J. Lowe, Phys. Rev. 173, 995 (1968).

41. D. A. Bromley, H. E. Gove, J. A. Kuehner, A. E. Litherland, and E. Almqvist, Phys. Rev. 114, 758 (1959).

42. F. Ajzenberg-Selove and T. Lauritsen, Nucl. Phys. 11, 1 (1959).

43. M. J. Throop, Phys. Rev. 179, 1011 (1969).

44. W. F. Lankford and H. O. Funsten, private communication.

45. G. H. Miller, private communication.

46. N. Kemmer, Proc. Roy. Soc. A166, 127 (1938).

47. W. O. Lock and D. F. Measday, Intermediate Energy Nuclear Physics, (Methuen and Co. Ltd., London, 1970) p. 55.

48. G. Källén, Elementary Particle Physics, (Addison-Wesley Publishing Company, Inc., Reading, Mass., (1965)) p. 71.

49. W. O. Lock and D. F. Measday, Intermediate Energy Nuclear Physics, (Methuen and Co. Ltd., London, 1970) p. 91.

50. P. Bareyre, C.Bricman, and G. Villet, Phys. Rev. 165, 1730 (1968).

51. D. S. Koltun, Advances in Nuclear Physics, edited by M. Baranger and E. Vogt (Plenum Press, New York, 1969) vol. 3, pp. 83-88.

52. D. S. Koltun, Advances in Nuclear Physics, edited by M. Baranger and E. Vogt (Plenum Press, New York, 1969) vol. 3, pp. 135-147.

53. M. H. Macfarlane and J. B. French, Rev. Mod. Phys. 32, 567 (1960).

54. S. Cohen and D. Kurath, Nucl. Phys. A101, 1 (1967).

55. H. W. Bertini, Phys. Rev. 171, 1261 (1968).

56. T. A. Fujii, Phys. Rev. 113, 695 (1959).

57. H. W. Bertini, Phys. Rev. 131, 1801 (1963).

58. O. D. Dalkarov, Phys. Lett. 26B, 610 (1968).

59. V. M. Kolybasov and N. Ya. Smorodinskaya, Phys. Lett. 30B, 11 (1969).

60. Yu. A. Budagov, P. F. Ermolov, E. A. Kushnirenko, and V. I. Moskalev, Sov. Phys. 15, 824 (1962).

61. D. Robson, Medium Energy Study Seminar, Space Radiation Effects Laboratory, Newport News, Virginia, July 28, 1970.

62. D. H. Wilkinson, Int. Conf. on Nuclear Structure, Tokoyo, 1967, p. 469.

63. R. A. Chatwin and A. Richter, "Comment on Recent Measurements of Pion-Induced Nucleon-Knockout Reactions on Light Nuclei", Florida State University (Tallahassee, Florida) preprint.

64. Tanner attributes the suggestion of a πNN pair interaction to M. Huber in Ref. 12.

65. Zeev Fraenkel, Phys. Rev. 130, 2407 (1963).

66. J. L. Snelgrove and E. Kashy, Phys. Rev. 187, 1246 (1969).

67. S. Raman and J. Miller, Data Summaries (Nuclear Structure Physics) ORNL-4317-2, Oak Ridge National Laboratory, August 1969.

68. G. E. Brown and A. M. Green, Nucl. Phys. 75, 401 (1966).

69. L. Zamick, Phys. Lett. 19, 580 (1965).

70. G. E. Brown and A. M. Green, Nucl. Phys. 85, 87 (1966).

71. S. DeBenedetti, Nuclear Interactions, (John Wiley and Sons, Inc., New York, 1964), p. 115.

72. B. E. Chi, Nucl. Phys. 83, 97 (1966).

73. W. J. Kossler, H. O. Funsten, B. A. MacDonald, and W. F. Lankford, "Nuclear De-Excitation γ-rays in ^{14}N, ^{14}C, and ^{15}N Following π^- Capture on ^{16}O", College of William and Mary (Williamsburg, Virginia) preprint (1971).

74. W. Bohne, H. Homeyer, H. Morgenstern, and J. Scheer, Nucl. Phys. A113, 97 (1968).

75. J. C. Hiebert, E. Newman, and R. H. Bassel, Phys. Rev. 154, 898 (1967).

76. F. C. Barker and A. K. Mann, Phil Mag. 2, 5 (1957).

77. J. T. Caldwell, S. C. Fultz, and R. L. Bramblett, Phys. Rev. Lett. 19, 447 (1967).

78. S. N. Kaplan, R. V. Pyle, L. E. Temple, and G. F. Valby, Phys. Rev. Lett. 22, 795 (1969).

79. W. W. True, Phys. Rev. 130, 1530 (1963).

80. I. S. Towner and J. C. Hardy, Advances in Phys. 18, 401 (1969).

81. S. Cohen and D. Kurath, Nucl. Phys. A141, 145 (1970).

82. J. C. Hardy and I. S. Towner, Phys. Lett. 25B, 98 (1967).

83. R. H. Pehl, J. Cerny, E. Rivet, and B. G. Harvey, Phys. Rev. 140, B605 (1965).

84. B. Leroux, K. El-Hammami, J. Dalmas, R. Chastel, G. Lamot, C. Fayard, and J. Hajj Boutros, Nucl. Phys. A116, 196 (1968).

85. V. V. Balashov, A. N. Boyarkina, and I. Rotter, Nucl. Phys. 59, 417 (1964).

86. J. Prud'homme, A. Sattar, N. Bostrom, I. Morgan, Bull. Am. Phys. Soc. 2, 308 (1957).

87. G. W. Edwards and E. Rost, Phys. Rev. Lett. 26, 785 (1971).

88. R. Guardiola, "Inelastic Scattering of Pions on Carbon", International Centre for Theoretical Physics (Trieste) preprint (1970).

89. C. Wilkin, Lettere al Nuovo 4, 491 (1970).

90. K. Bjornenak, J. Finjord, P. Osland, and A. Reitan, Nucl. Phys. B22, 179 (1970).

91. T. E. O. Ericson and J. Hüfner, Phys. Lett. 33B, 601 (1970).

92. G. M. Crawley and G. T. Garvey, Phys. Rev. 160, 981 (1967).

93. E. Paul and R. Clarke, Can. J. Phys. 31, 267 (1953).

94. P. V. Hewka, C. H. Holbrow, and R. Middleton, Nucl. Phys. 88, 561 (1966).

IX. FIGURE CAPTIONS

1. Energy dependence of the $C^{12}(\pi^{\pm},\pi n)C^{11}$ reaction as measured by Tanner[1] and Reeder and Markowitz.[5] The solid line represents a quasi-free calculation by Kolybasov.[13]
2. Diagram of the experimental geometry. Before entering counter 1, the π beam passed through an 8" x 8" lead beam slit. Counters D and E are not shown in Fig. 2. Counter D was located above the target, co-planer with the upper edges of counters A and C. Counter E was located below the target, co-planer with the lower edges of counters A and C.
3. Diagram of the electronics. D = discriminator, GDG = gate and delay generator, C = coincidence unit, LSD = logic shaper and delay, TFA = timing filter amplifier, CFTD = constant fraction timing discriminator, TAC = time to amplitude converter, ADC = analogue to digital converter, S = shaper which converts NIM logic level signals to the proper Interface signal levels, and SC = strobed coincidence (EGG C126/N). The strobed coincidence unit will have a signal at a particular output if there is a coincidence between the corresponding input and the strobe input. The RF trigger pulse from the cyclotron was used as a reference for gating off the 12 coincidence unit for the duration of the prompt portion of the beam.

4. Ge(Li) spectrometer resolution as a function of energy.
5. Relative and absolute efficiency of the Ge(Li) spectrometer as a function of energy (Section IIG).
6. Comparison of the relative intensity of the escape peaks of the Ge(Li) spectrometer vs. energy. Curve A = (double escape intensity/photopeak intensity), and Curve B = (double escape intensity/single escape intensity).
7. Experimental gamma spectrum from 1. to 3. MeV.
8. Experimental gamma spectrum from 3. to 5. MeV.
9. Experimental gamma spectrum from 5. to 6.5 MeV.
10. Energy levels of N^{15} and O^{15}. The arrows indicate transitions detected in this experiment.
11. Energy levels of C^{14} and N^{14}. The arrows indicate transitions detected in this experiment.
12. Energy levels of C^{13} and C^{12}. The arrows indicate transitions detected in this experiment.
13. Energy levels of N^{16} and O^{16}. The arrows indicate transitions detected in this experiment.
14. Histogram comparing pion induced single nucleon knockout cross sections for excited states of O^{15} and N^{15}.
15. Histogram comparing pion induced single nucleon knockout cross sections with proton induced single nucleon knockout cross sections. (Table XVI).
16. Histogram comparing pion induced single nucleon knockout cross sections with several direct single nucleon transfer reactions.

The normalization is such that the sum of the pion cross sections is equal to the sum of the cross sections of each comparison reaction.

17. Histogram comparing the pion induced single nucleon knockout cross sections with studies of the decay of giant dipole states excited by photoexcitation[77] and muon capture.[78] The normalization is such that the sum of the pion cross sections is equal to the sum of the cross sections of each comparison reaction.

18. Histogram comparing the pion induced 2-nucleon knockout cross sections with those of other 2-nucleon transfer reactions. The normalization is such that the sum of the pion cross sections is equal to the sum of the cross sections of each comparison reaction.

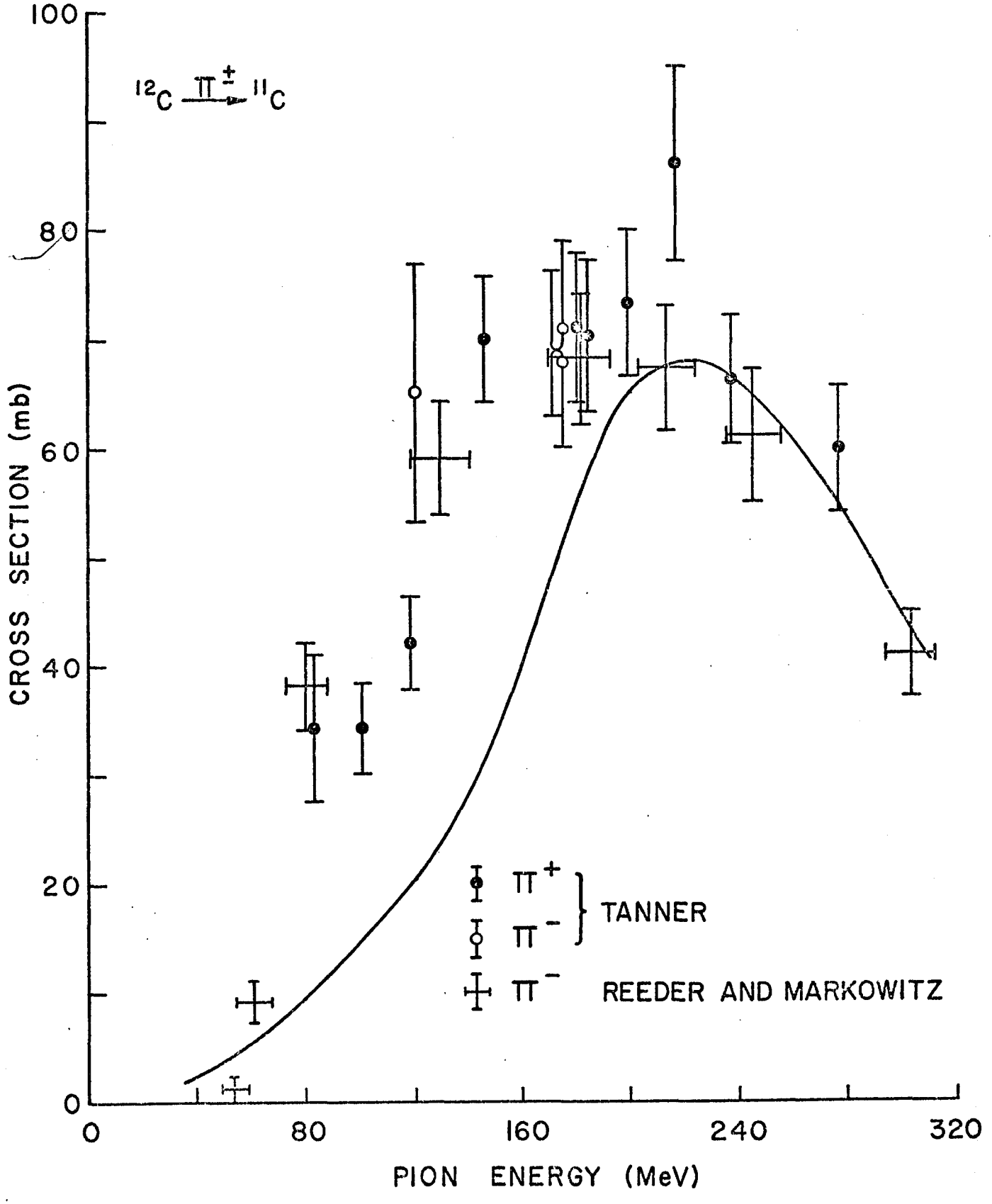
100
80
60
40
20
0
CROSS SECTION (mb)
$^{12}C \xrightarrow{\pi^{\pm}} {}^{11}C$
π^+
π^-
TANNER
π^-
REEDER AND MARKOWITZ
0
80
160
240
320
PION ENERGY (MeV)

FIG. 1

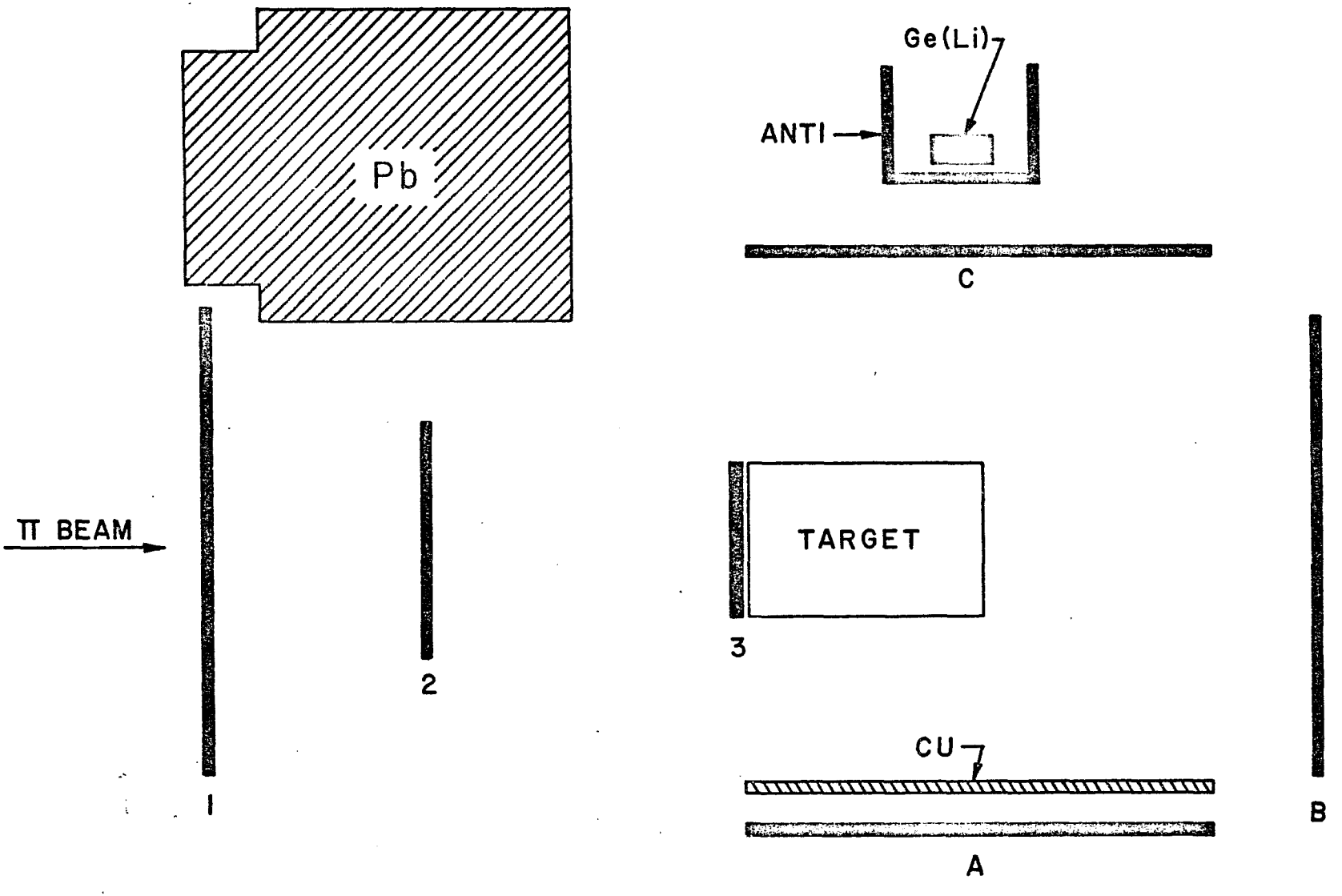

SCALE: 1/4" = 1'-0"

FIG. 2

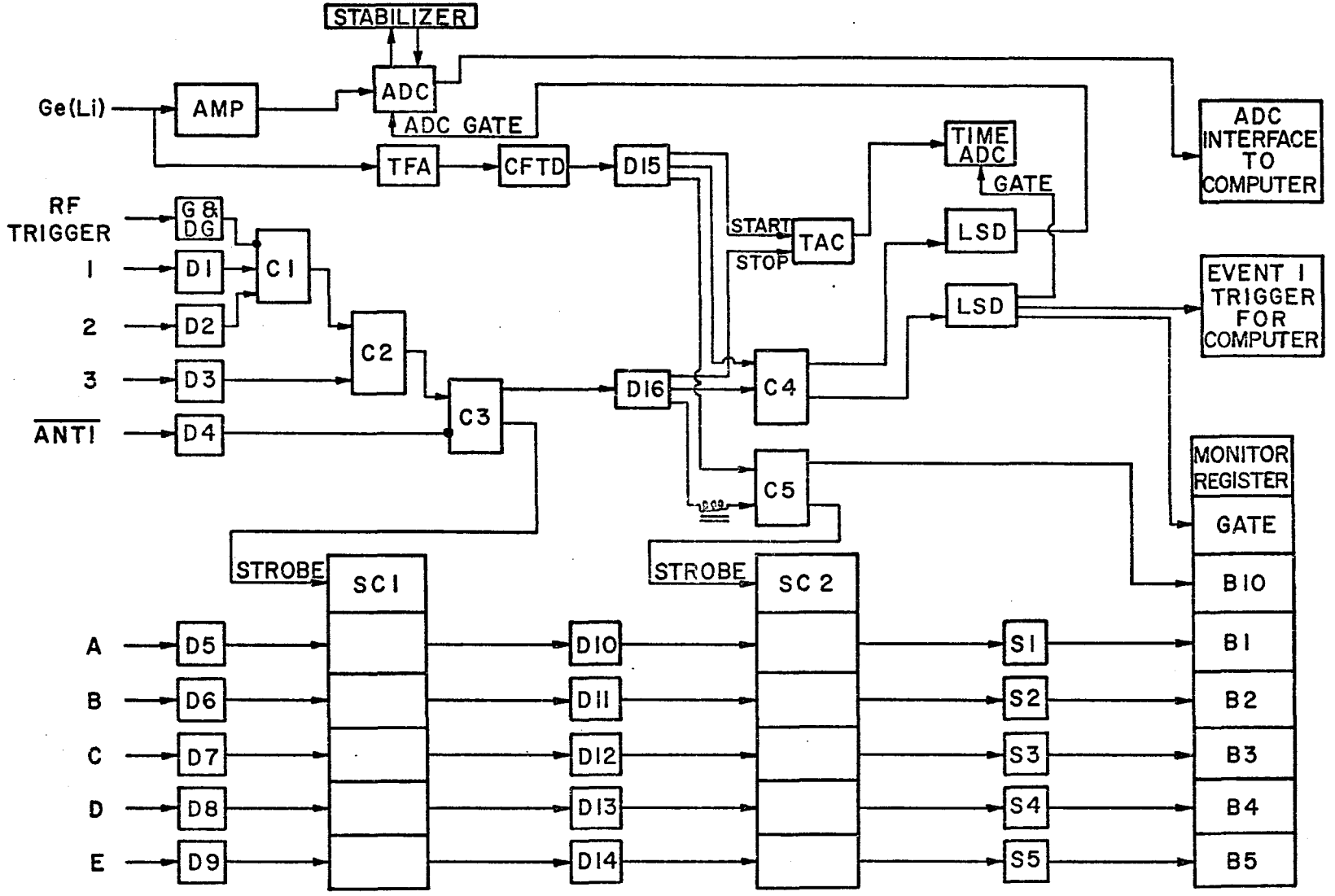
STABILIZER
ADC
ADC GATE
Ge(Li)
AMP
TFA
CFTD
D15
ADC INTERFACE TO COMPUTER
TIME ADC
GATE
START
STOP
TAC
LSD
LSD
EVENT I TRIGGER FOR COMPUTER
RF TRIGGER
G & DG
1
D1
2
D2
3
D3
ANTI
D4
C1
C2
C3
D16
C4
C5
MONITOR REGISTER
GATE
B10
STROBE
SC1
STROBE
SC 2
A
D5
B
D6
C
D7
D
D8
E
D9
D10
D11
D12
D13
D14
S1
S2
S3
S4
S5
B1
B2
B3
B4
B5

FIG. 3

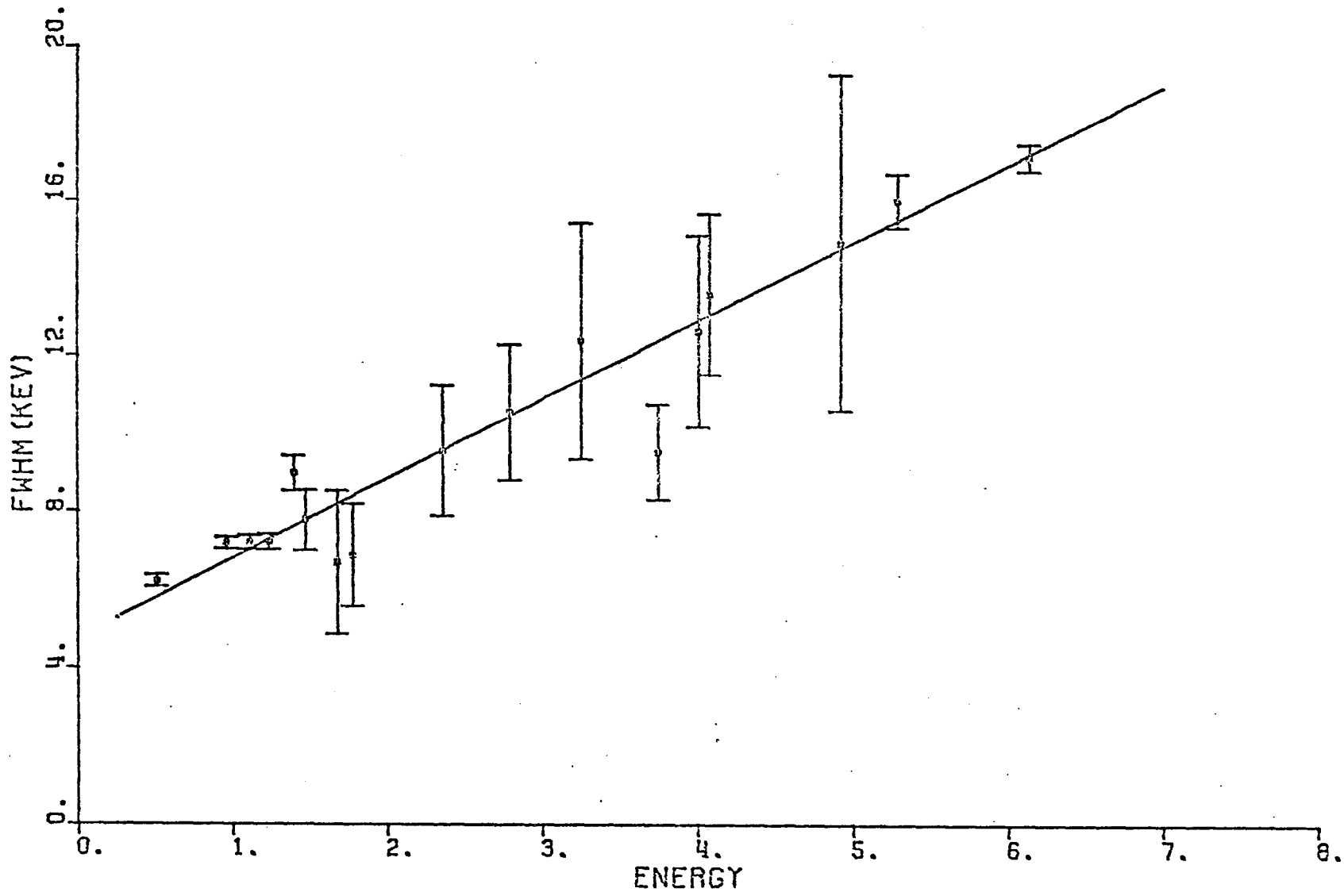

FIG. 4

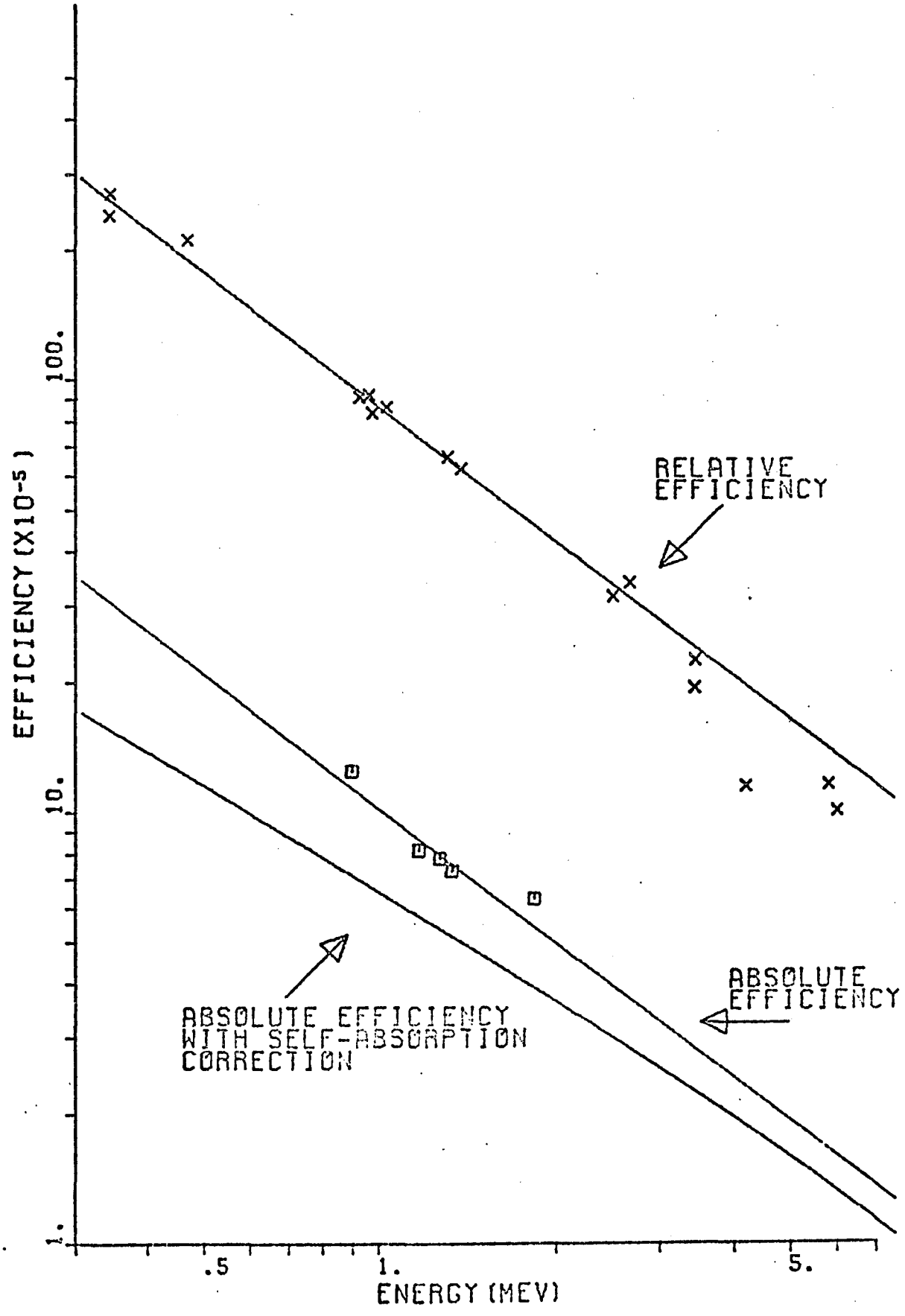
EFFICIENCY (X10-5)
100.
10.
1.
.5
1.
5.
ENERGY (MEV)
RELATIVE EFFICIENCY
ABSOLUTE EFFICIENCY
ABSOLUTE EFFICIENCY WITH SELF-ABSORPTION CORRECTION

FIG. 5

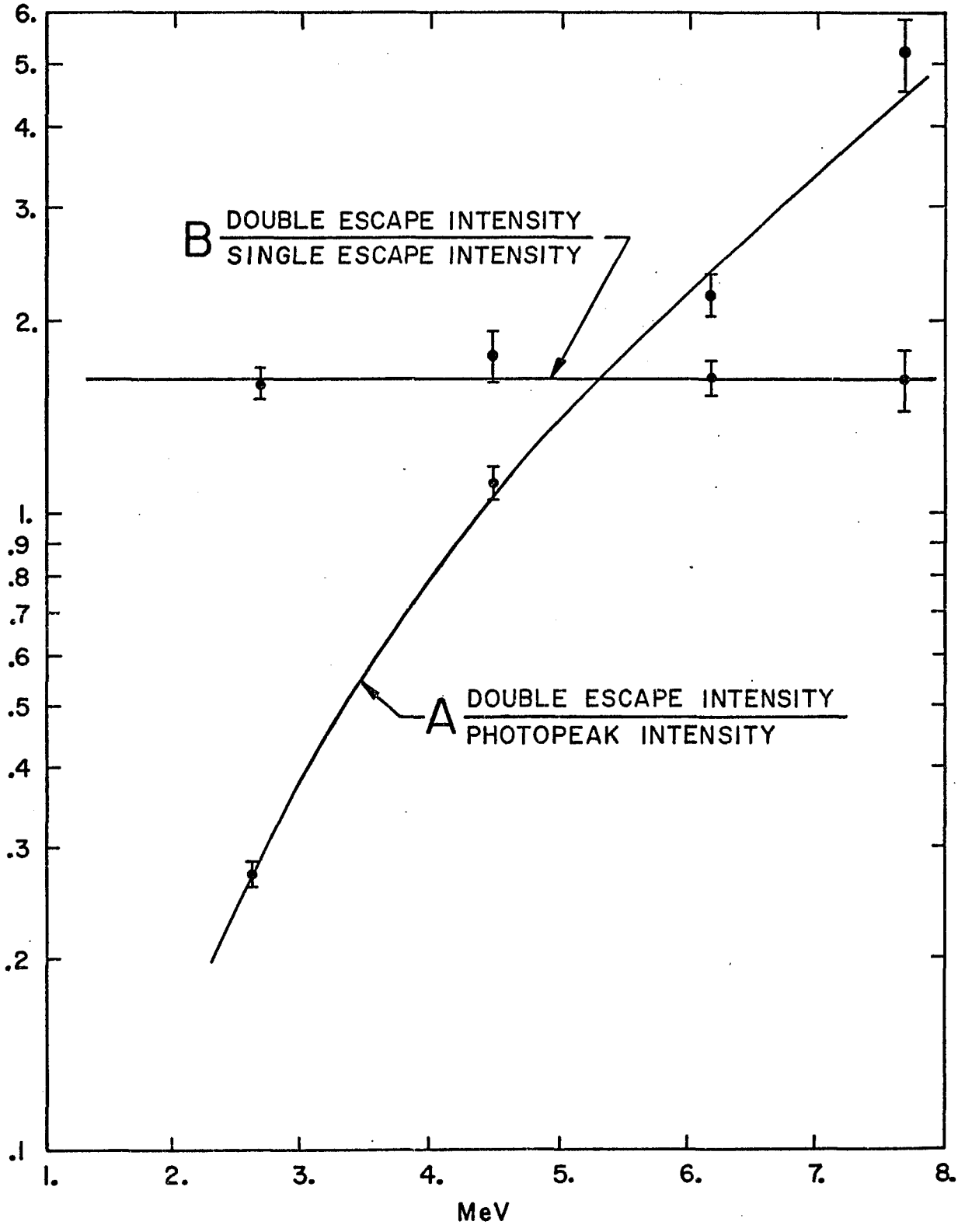
6.
5.
4.
3.
2.
1.
.9
.8
.7
.6
.5
.4
.3
.2
.1
B DOUBLE ESCAPE INTENSITY / SINGLE ESCAPE INTENSITY
A DOUBLE ESCAPE INTENSITY / PHOTOPEAK INTENSITY
1.
2.
3.
4.
5.
6.
7.
8.
MeV

FIG. 6

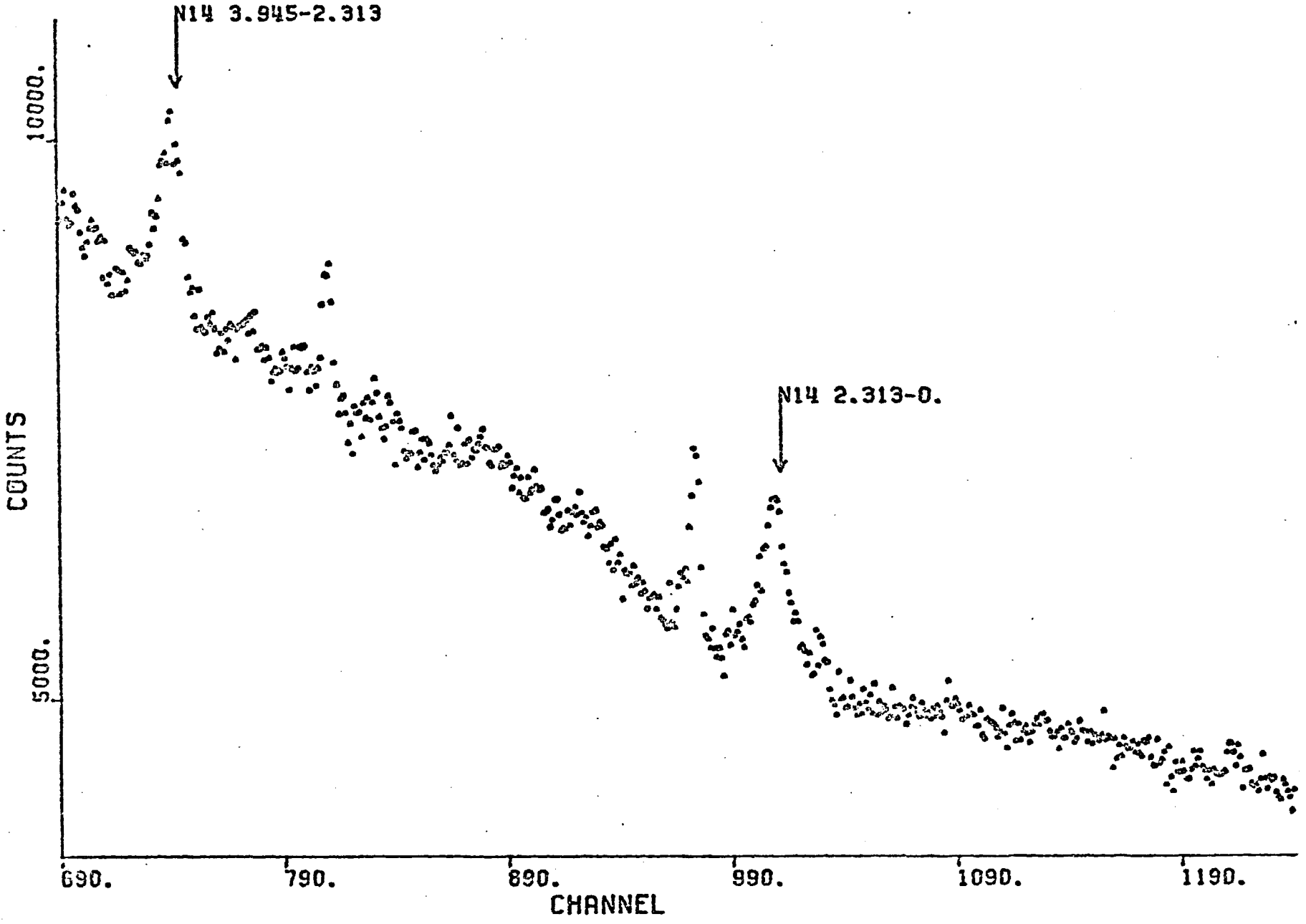
N14 3.945-2.313
N14 2.313-0.
10000.
5000.
COUNTS
690.
790.
890.
990.
1090.
1190.
CHANNEL

FIG. 7

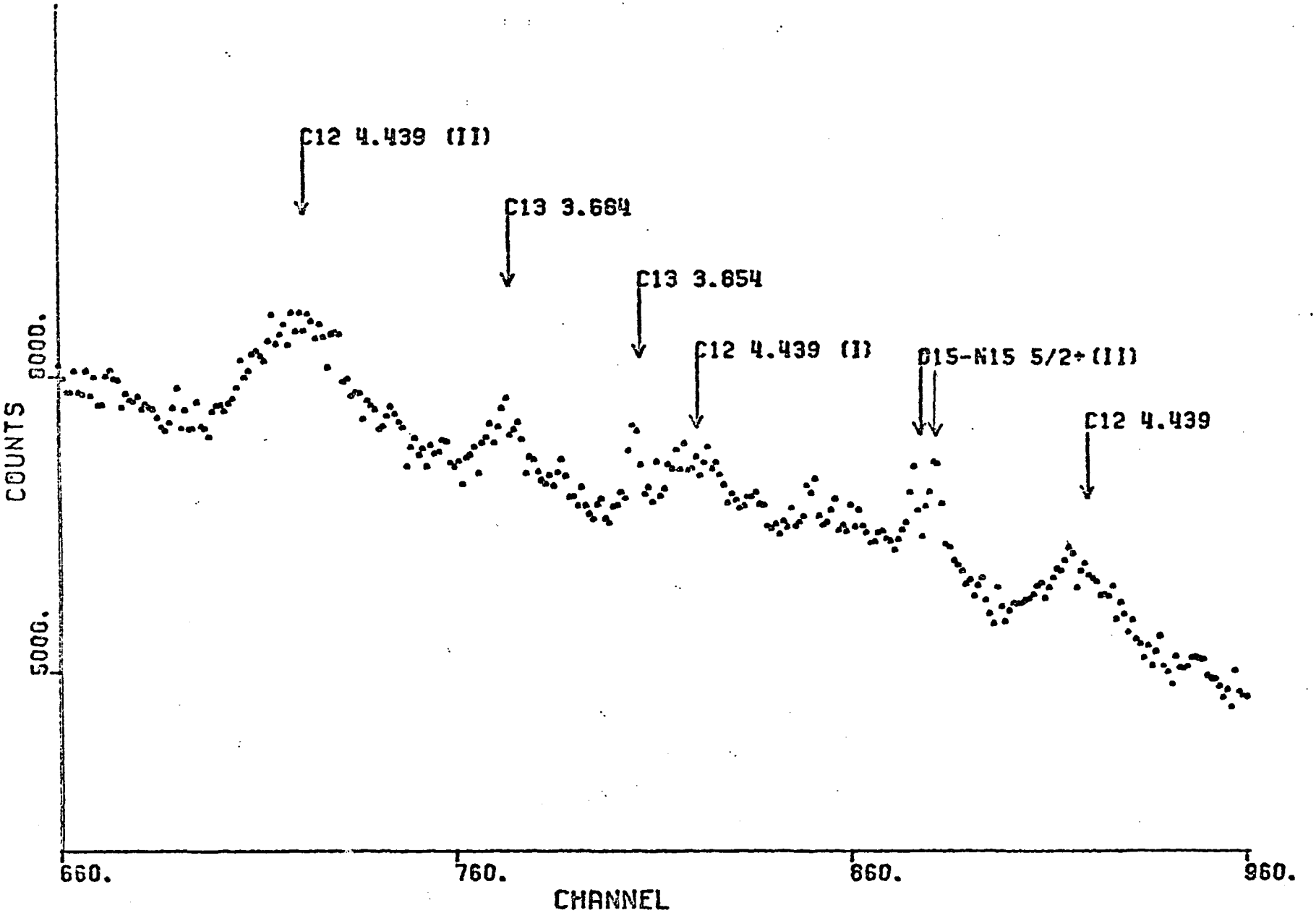
C12 4.439 (II)
C13 3.684
C13 3.654
C12 4.439 (I)
O15-N15 5/2+(II)
C12 4.439
8000.
5000.
COUNTS
660.
760.
860.
960.
CHANNEL

FIG. 8

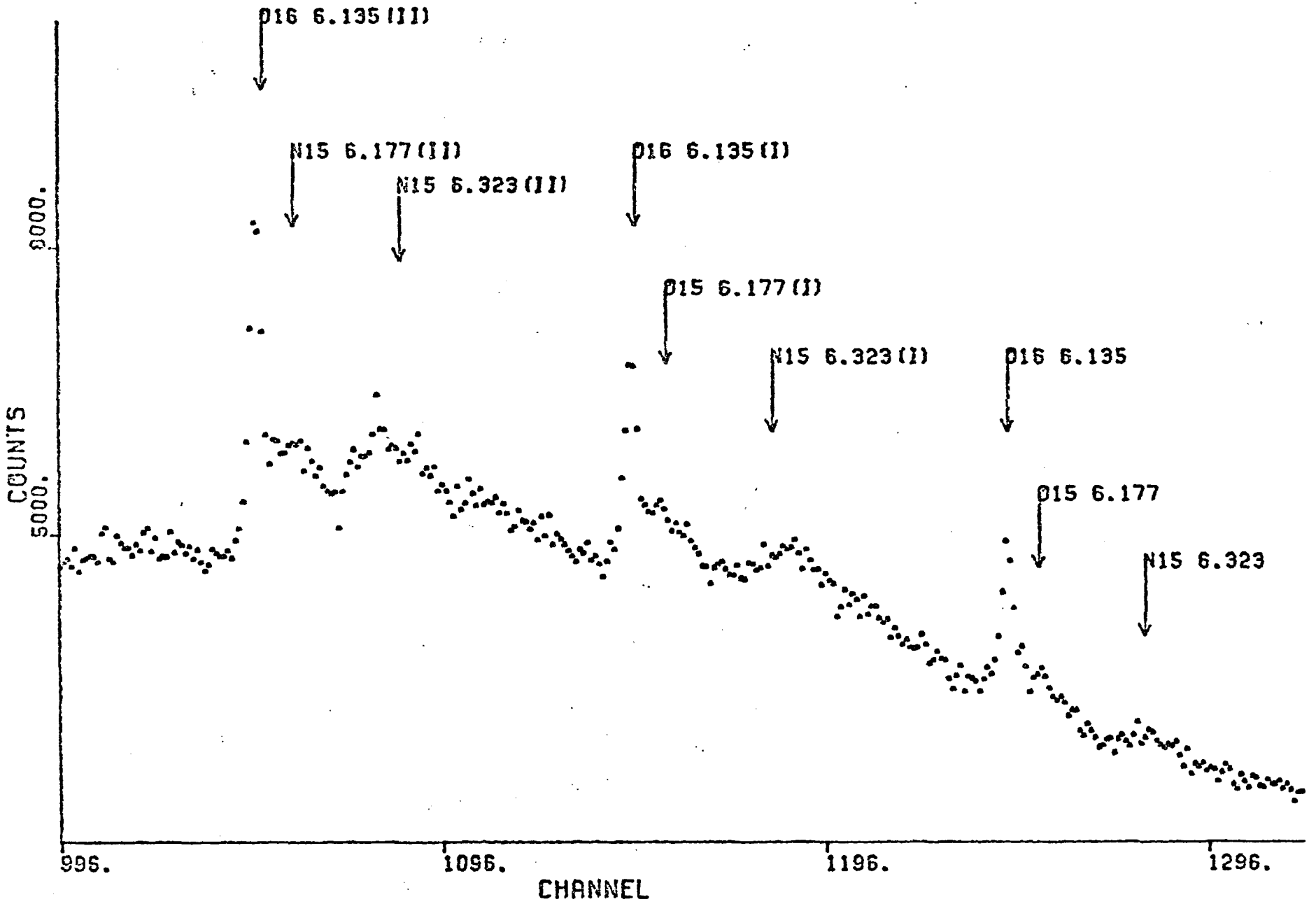
O16 6.135(II)
N15 6.177(II)
N15 6.323(II)
O16 6.135(I)
O15 6.177(I)
N15 6.323(I)
O16 6.135
O15 6.177
N15 6.323
COUNTS
8000.
5000.
995.
1095.
1195.
1295.
CHANNEL

FIG. 9

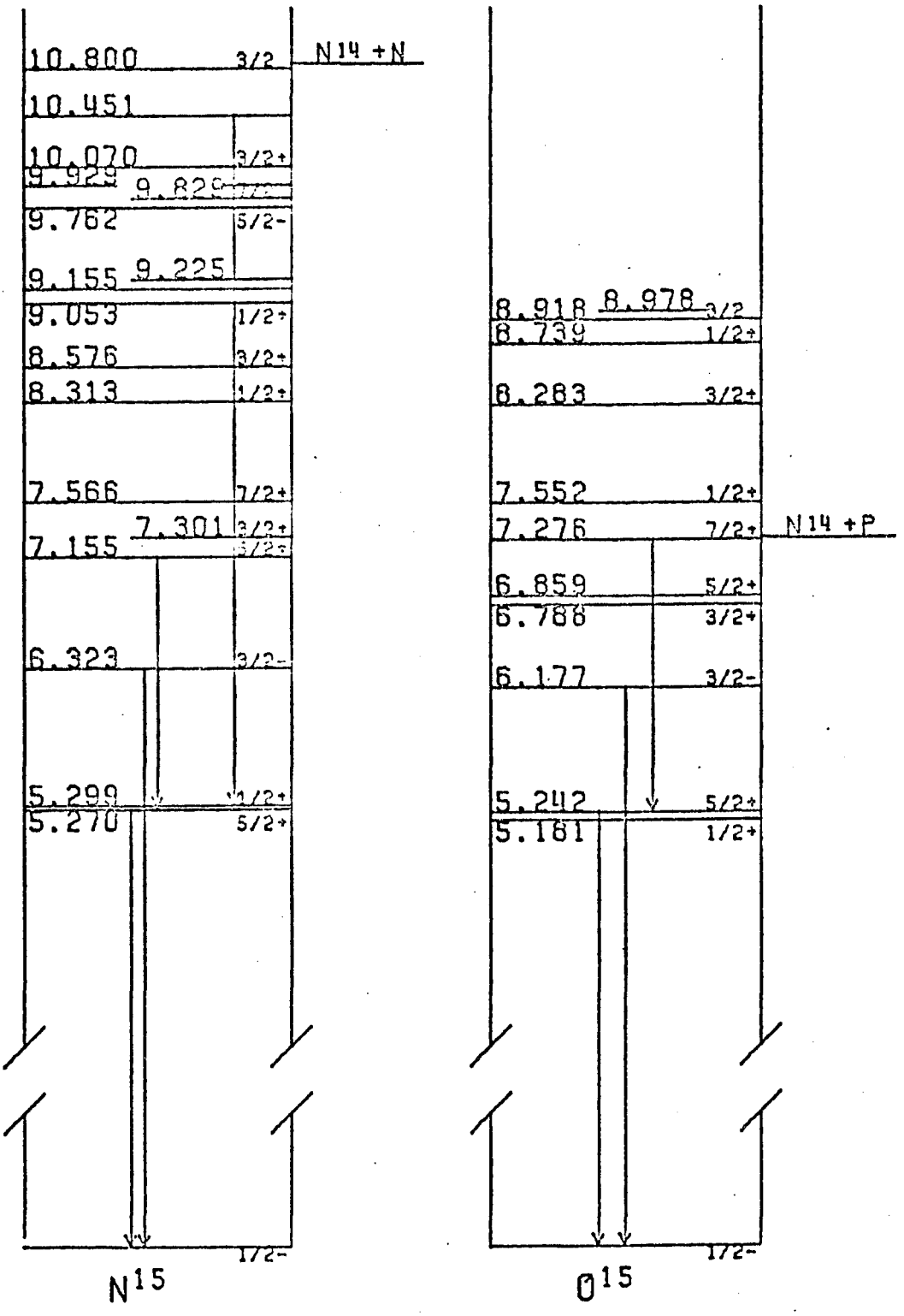
10.800
3/2
N14 +N
10.451
10.070
3/2+
9.929
9.762
5/2-
9.155
9.225
9.053
1/2+
8.576
3/2+
8.313
1/2+
7.566
7/2+
7.301
7.155
6.323
3/2-
5.299
1/2+
5.270
5/2+
1/2-
N15
8.918
8.978
3/2
8.739
1/2+
8.283
3/2+
7.552
1/2+
7.276
7/2+
N14 +P
6.859
5/2+
6.788
3/2+
6.177
3/2-
5.242
5/2+
5.181
1/2+
1/2-
O15

FIG. 10

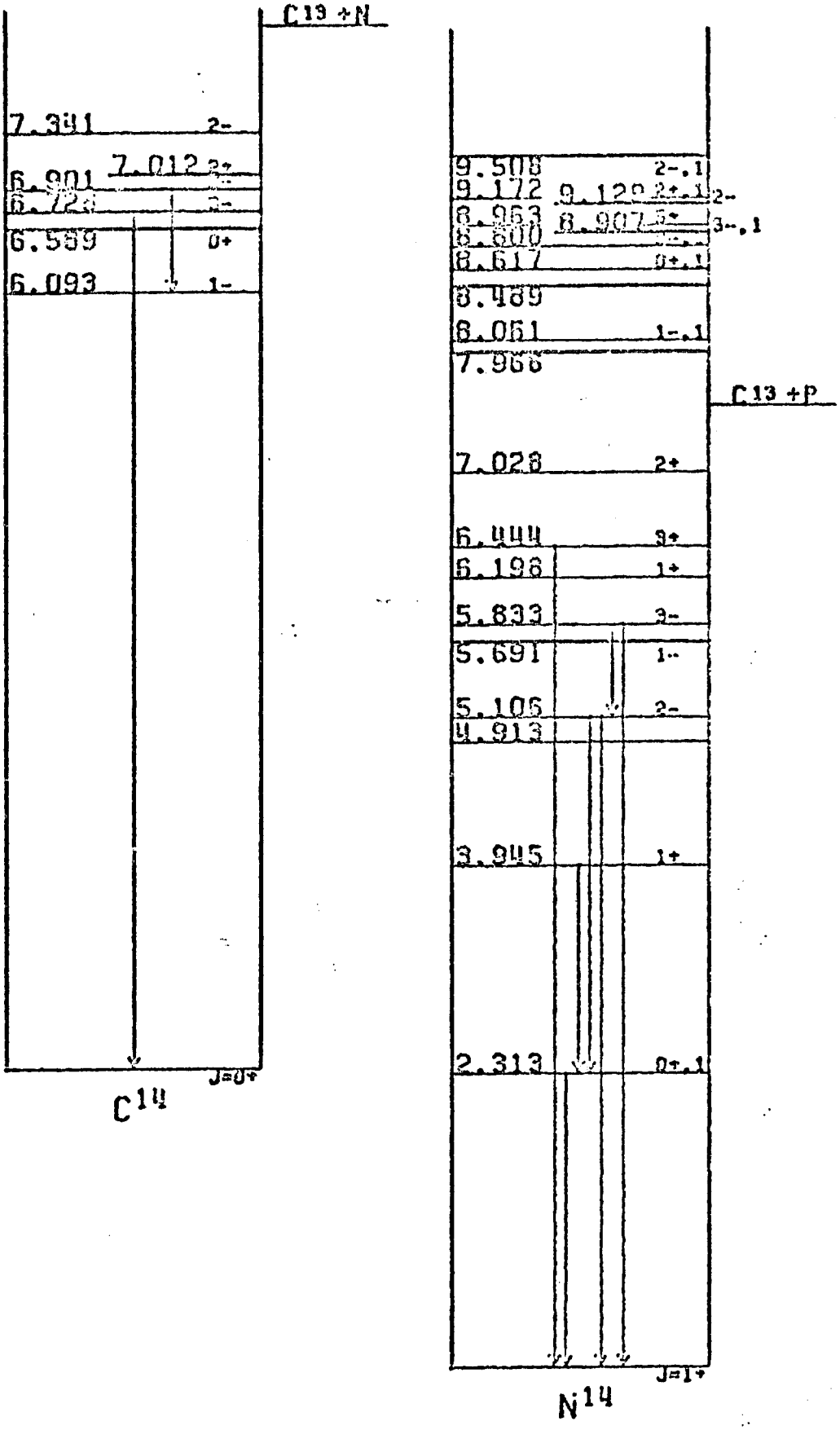
C13 +N
7.381
2-
7.012
3+
6.901
6.728
3-
6.589
0+
6.093
1-
J=0+
C14
9.508
2-,1
9.172
9.129
2+,1
2-
8.963
8.907
3+
3-,1
8.600
8.617
0+,1
8.489
8.061
1-,1
7.966
C13 +P
7.028
2+
6.444
3+
6.196
1+
5.833
3-
5.691
1-
5.106
2-
4.913
3.945
1+
2.313
0+,1
J=1+
N14

FIG. 11

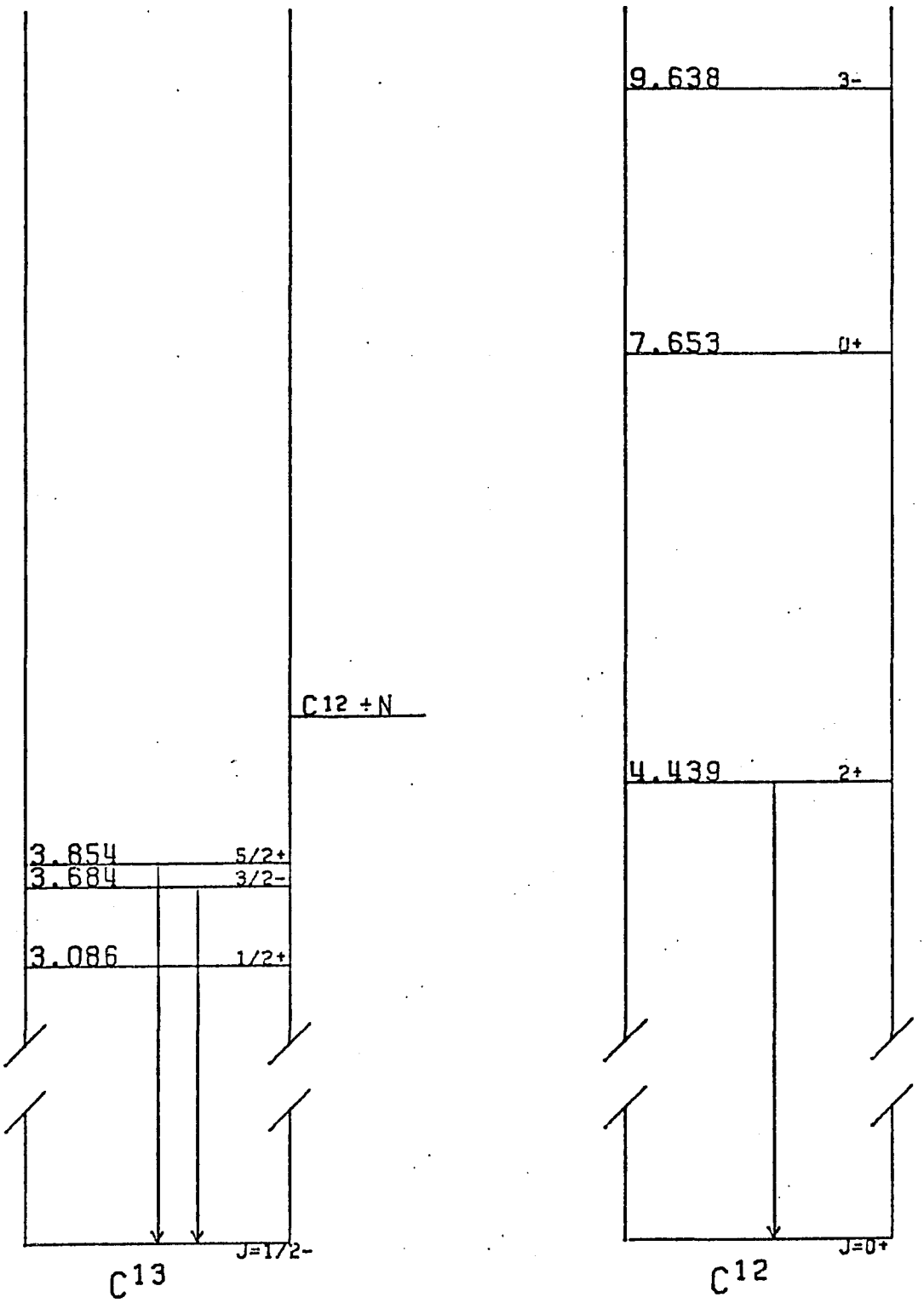

FIG. 12

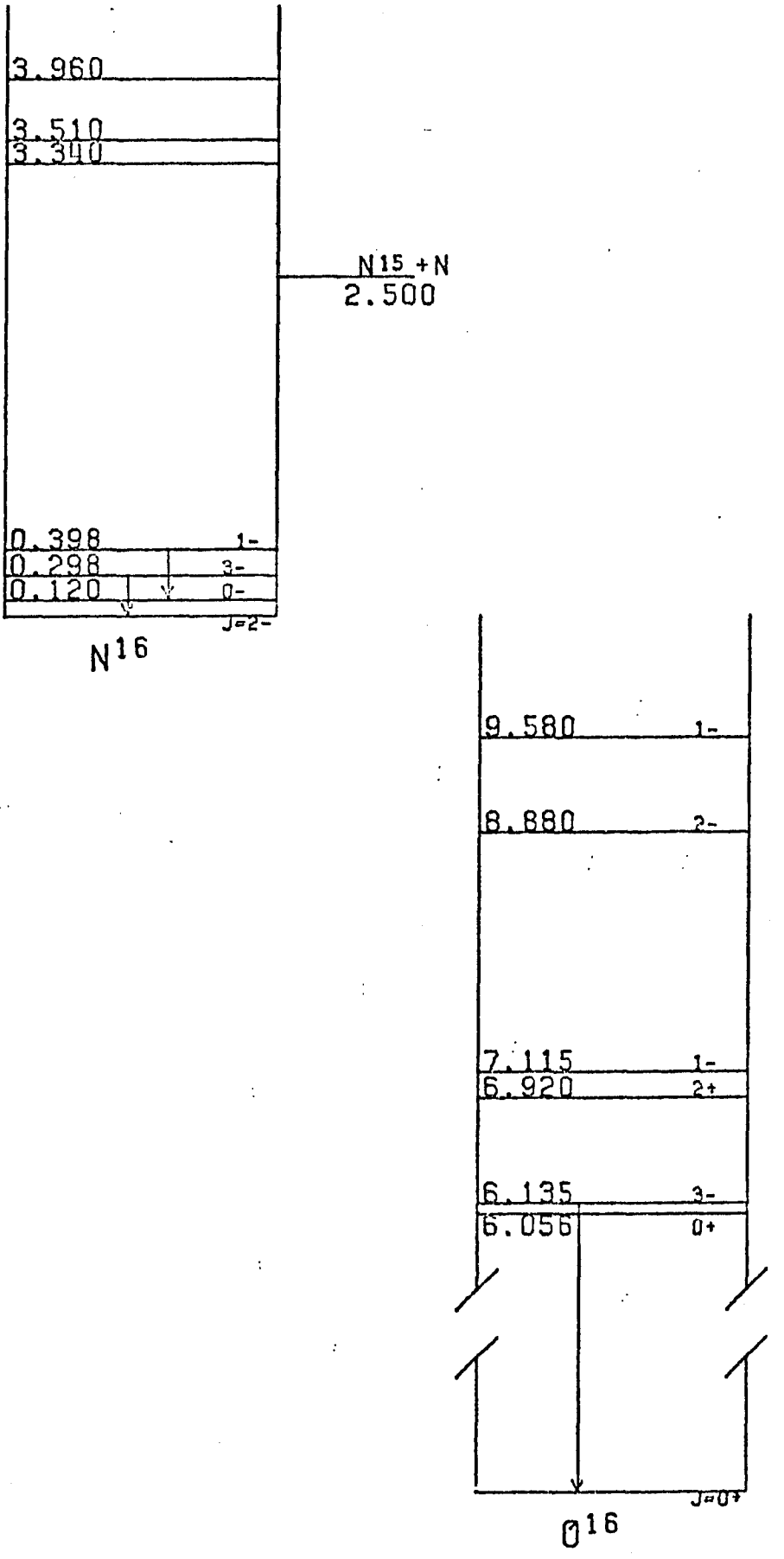
3.960
3.510
3.340
N15 + N
2.500
0.398 1-
0.298 3-
0.120 0-
J=2-
N16
9.580 1-
8.880 2-
7.115 1-
6.920 2+
6.135 3-
6.056 0+
J=0+
016

FIG. 13

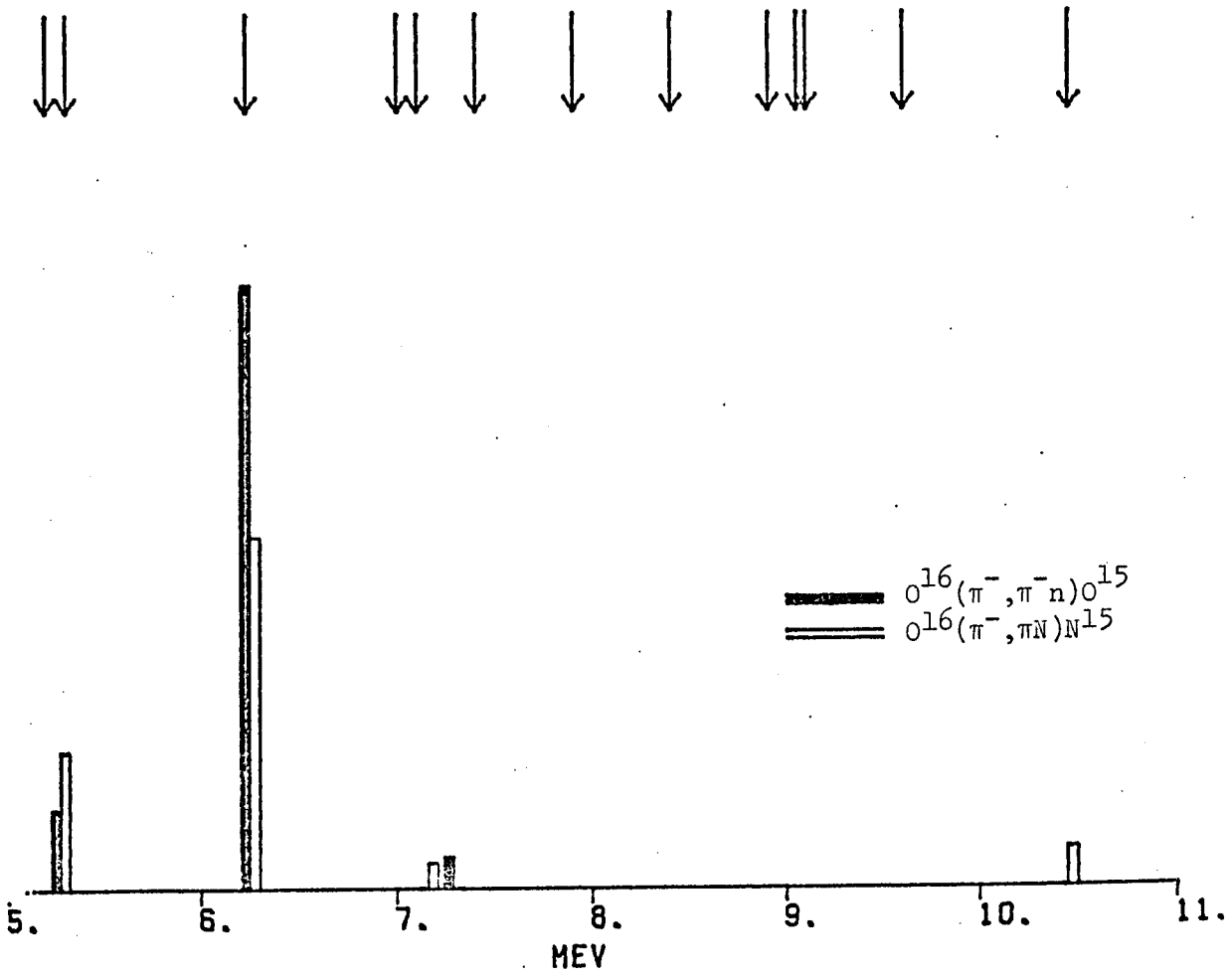

FIG. 14

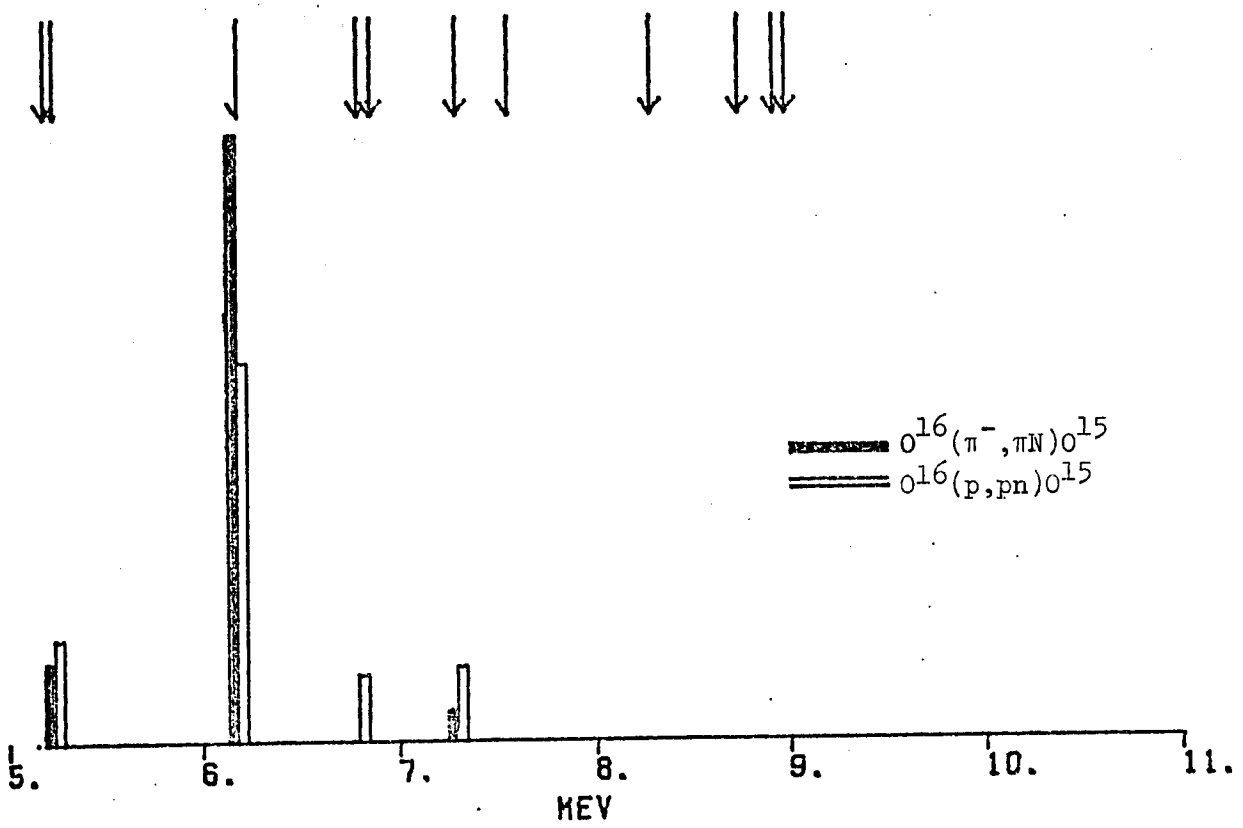
$O^{16}(\pi^-,\pi N)O^{15}$
$O^{16}(p,pn)O^{15}$
5.
6.
7.
8.
9.
10.
11.
MEV

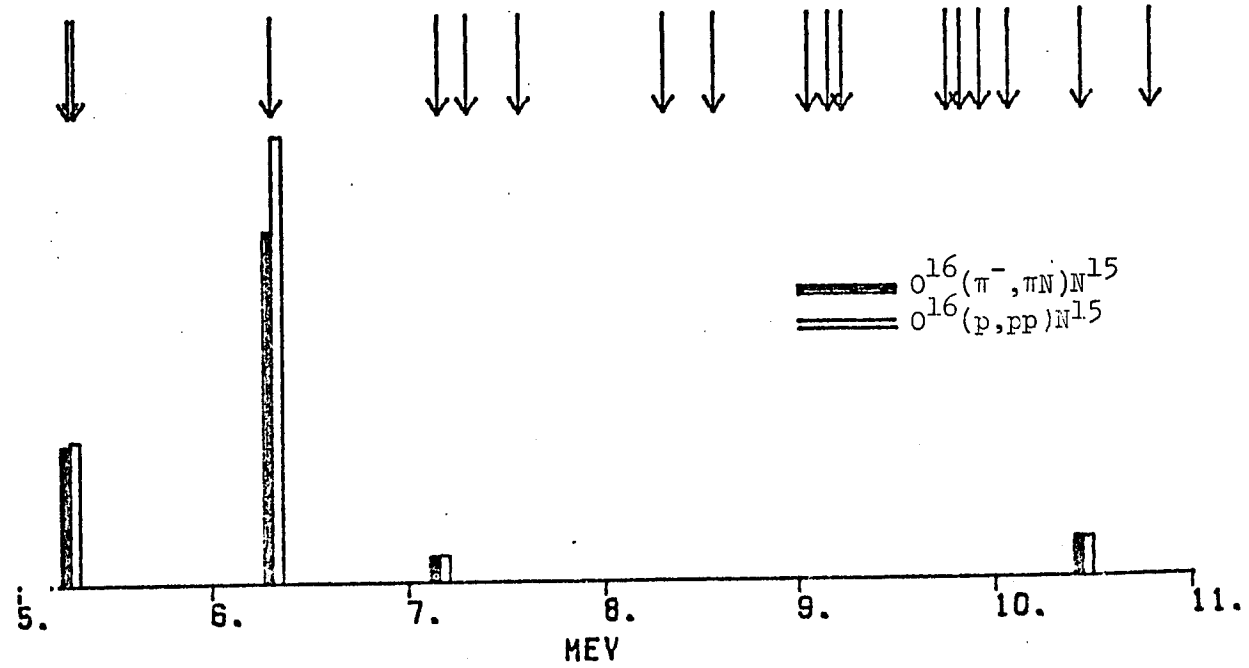
$O^{16}(\pi^-,\pi N)N^{15}$
$O^{16}(p,pp)N^{15}$
5.
6.
7.
8.
9.
10.
11.
MEV

FIG. 15

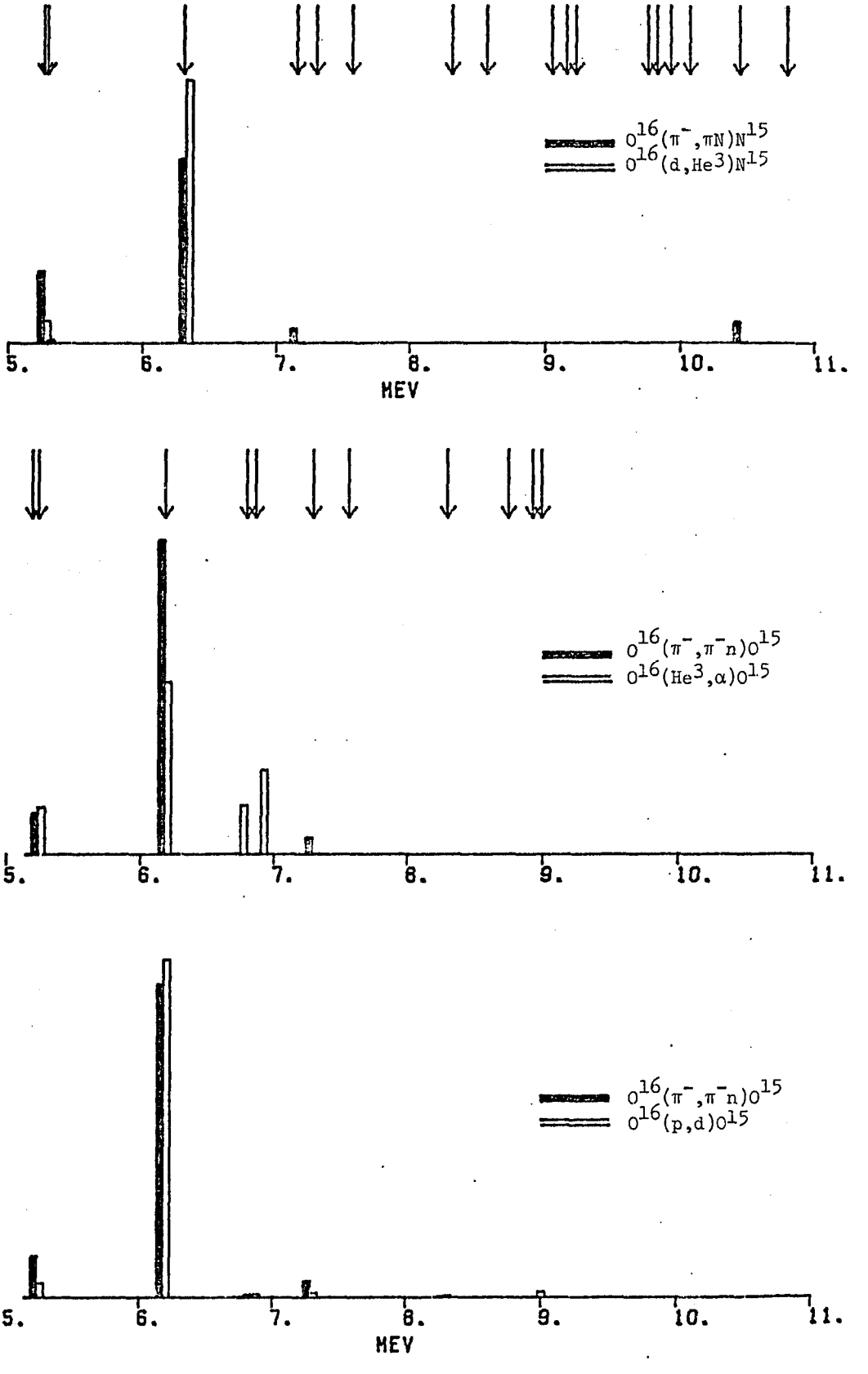
$O^{16}(\pi^-,\pi N)N^{15}$
$O^{16}(d,He^3)N^{15}$
5.
6.
7.
8.
9.
10.
11.
MEV
$O^{16}(\pi^-,\pi^- n)O^{15}$
$O^{16}(He^3,\alpha)O^{15}$
5.
6.
7.
8.
9.
10.
11.
$O^{16}(\pi^-,\pi^- n)O^{15}$
$O^{16}(p,d)O^{15}$
5.
6.
7.
8.
9.
10.
11.
MEV

FIG. 16

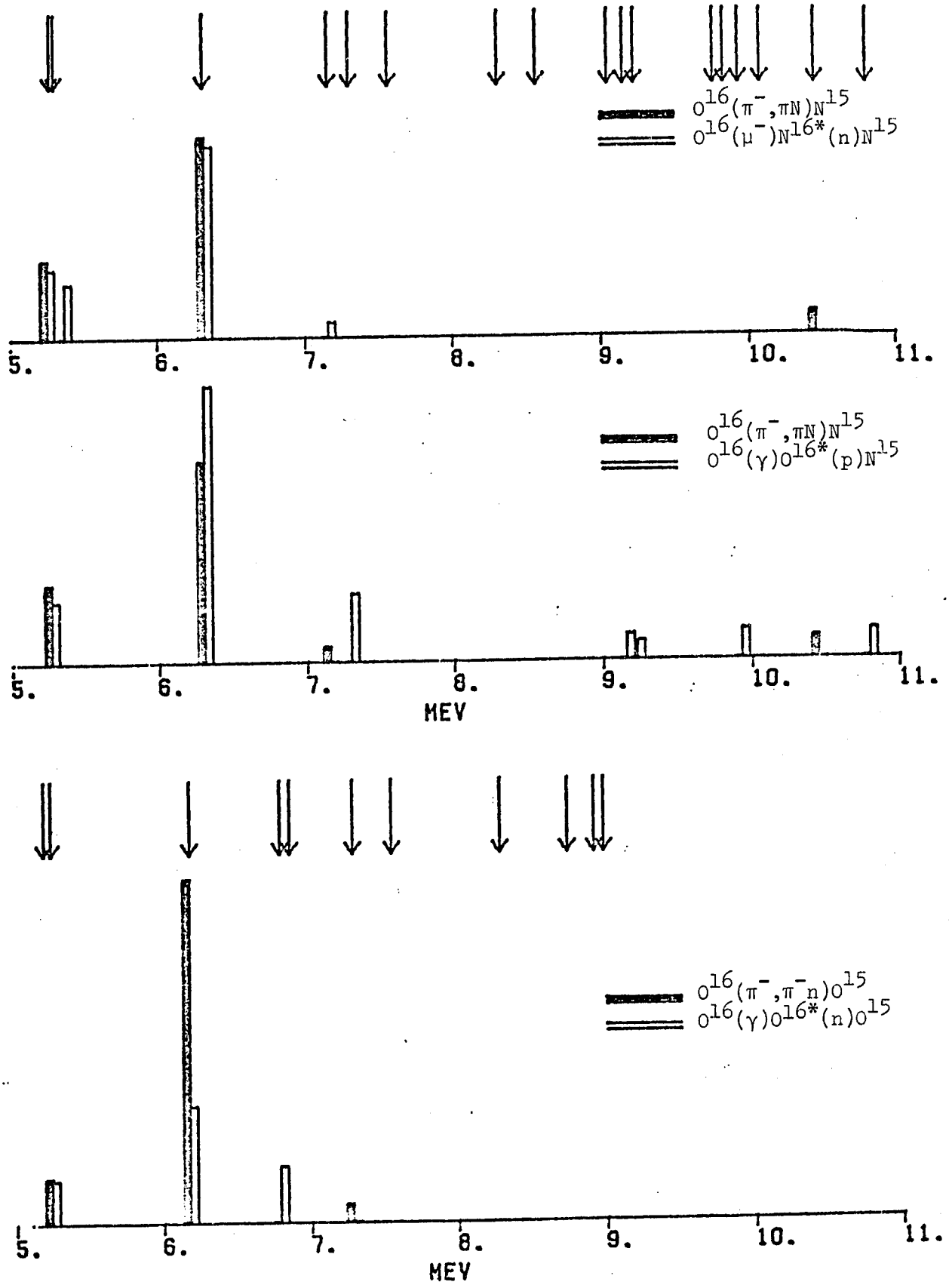
$O^{16}(\pi^-,\pi N)N^{15}$
$O^{16}(\mu^-)N^{16*}(n)N^{15}$
5.
6.
7.
8.
9.
10.
11.
$O^{16}(\pi^-,\pi N)N^{15}$
$O^{16}(\gamma)O^{16*}(p)N^{15}$
5.
6.
7.
8.
9.
10.
11.
MEV
$O^{16}(\pi^-,\pi^-n)O^{15}$
$O^{16}(\gamma)O^{16*}(n)O^{15}$
5.
6.
7.
8.
9.
10.
11.
MEV

FIG. 17

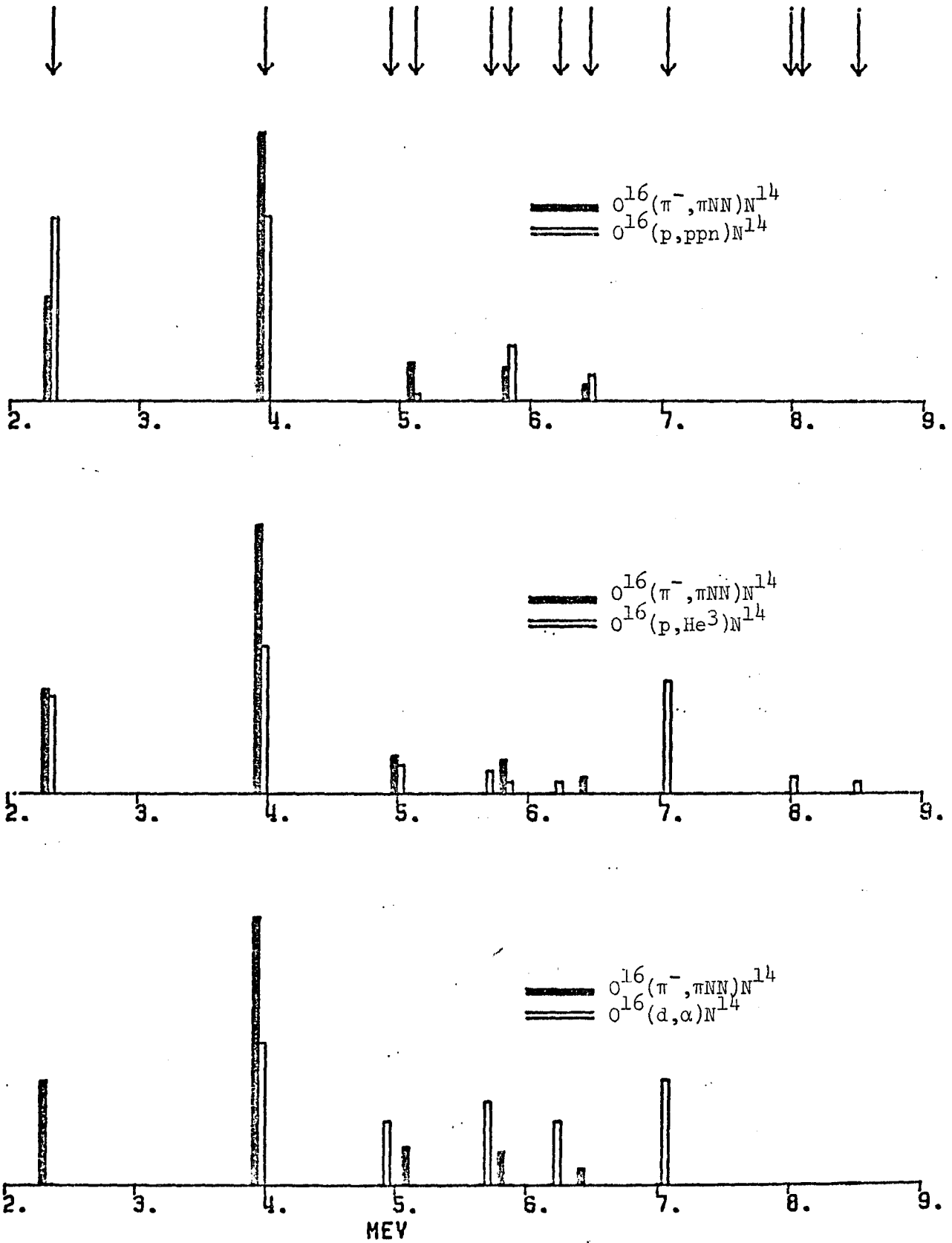
$O^{16}(\pi^-,\pi NN)N^{14}$
$O^{16}(p,ppn)N^{14}$
$O^{16}(\pi^-,\pi NN)N^{14}$
$O^{16}(p,He^3)N^{14}$
$O^{16}(\pi^-,\pi NN)N^{14}$
$O^{16}(d,\alpha)N^{14}$
2. 3. 4. 5. 6. 7. 8. 9.
MEV

FIG. 18